University of Nottingham



School of Mathematical Sciences

Fermions from time-dependent boundaries: stress-energy versus clicks of a particle detector

Wan Mohamad Husni Wan Mokhtar, MSc

A thesis submitted to the University of Nottingham

for the degree of Doctor of Philosophy

October 2018

Abstract

In this thesis, we analyse massless fermion creation by time-dependent boundaries in $(1+1)$-dimensional flat spacetimes. We consider two distinct senses in which the boundaries are said to be time-dependent. On one hand, we study a boundary which remains at rest with respect to a family of inertial observers but imposes a time-dependent boundary condition. On the other hand, we study a boundary that moves along a timelike trajectory while imposing a time-independent boundary condition, that is the MIT bag boundary condition. In both cases, we calculate the stress-energy tensor of the spinor field describing the fermions, renormalised via the point-splitting method, and the response of an inertial Unruh-DeWitt detector coupled linearly to the scalar density of the field. Throughout our analysis, we compare our results to those readily available in the literature for a massless scalar field in similar settings.

In the motionless evolving wall analysis, we first consider a wall that imposes a generic boundary condition parametrised by four arbitrary time-dependent functions. Some of the boundary conditions may be interpreted as arising from a combination of idealised scalar and electric potentials. We find that the wall generates an energy burst of finite magnitude when the evolution is smooth. The response of an inertial detector passing through the generated energy burst is also finite. We then analyse an evolving wall that simulates the creation or demolition of a wall that imposes a double-sided MIT bag boundary condition. In the limit of rapid MIT wall creation or demolition, the energy burst displays a delta function squared divergence but, within first order perturbation theory, the detector response diverges only logarithmically in the duration of wall evolution. The results add to the evidence that a localised matter system may not be as

sensitive to the divergence in local expectation values of field observables such as the stress-energy tensor.

In the moving wall analysis, we first consider a wall that moves along an arbitrary timelike trajectory. We find that the stress-energy tensor of the field is identical to that of a massless scalar field in the moving mirror spacetime. By contrast, we find that the transition rate of an inertial Unruh-DeWitt detector coupled linearly to the scalar density of the spinor field is generically different from that of a detector coupled linearly to a scalar field or its derivative. Hence, an observer examining just the stress-energy tensor sees no difference between a fermion and a boson, neither at late times nor early, while an observer equipped with an Unruh-DeWitt detector will generically be able to distinguish fermions from bosons. We then analyse a wall trajectory for which a mirror scattering a scalar field following the same trajectory is known to emit thermal radiation in the far future. We find that the late time transition rate of the fermionic detector is proportional to the Helmholtz free energy density of a fermionic thermal bath, hence showing a clear sign of Fermi-Dirac statistics, with no counterpart in the response of a scalar detector.

To my mother and my late father.

Acknowledgements

In the name of Allah, the Most Gracious, the Most Merciful.

All praise be to Allah for granting my prayer to pursue my study in the field of mathematical/theoretical physics at the PhD level.

I would like to express my utmost gratitude to my supervisor, Dr. Jorma Louko, for his advice, encouragement and guidance throughout my time here as his student. Many thanks for suggesting the topics, pointing out errors and mistakes that I have made in my calculations and providing assistance whenever I needed them. Thanks also for reading the draft version of this thesis and suggesting numerous improvements.

I thank Dr. Silke Weinfurtner and Prof. Kirill Krasnov, who were my annual reviewers, for their comments and constructive feedback on my research progress. Thanks also to the staff in the School of Mathematical Sciences for their behind-the-scene work that has made my student life here a smooth one.

I thank Prof. Christopher Fewster and Prof. Kirill Krasnov, who were my examiners, for reading the thesis, pointing out technical and typographical errors and providing suggestions for improvement.

I thank Sangchul Lee for responding to a question that I have posted on Mathematics Stack Exchange regarding the order of divergence in the square of Dirac delta distribution. The discussion on the site has helped me establish the lower bound for the total energy transmitted into the field by a wall creation or demolition process.

I thank the Ministry of Education Malaysia (Higher Education) for sponsoring my study under the MyBrainSc scholarship programme. Thanks also to

Universiti Sains Malaysia for accepting me as a fellow and providing an additional funding under the Academic Staff Training Scheme.

I take this opportunity to convey my deepest appreciation to my family, especially my mother, for their endless encouragement, love and support. I thank all my friends who have made my stay in Nottingham a joyful one. Thanks to Vladimir Toussaint and Robert Benkel, both of whom were also Dr. Louko's students. Thanks to all my friends and fellow archers from the University of Nottingham Archery Club and thanks to all my housemates.

Contents

1 Introduction **1**

2 Fermions and Particle Detector **10**

2.1 Fermions in Minkowski Spacetime 10

2.1.1 Quantum Spinor Field 10

2.1.2 Field Propagators 12

2.1.3 Stress-Energy Tensor 13

2.2 Particle Detector 16

2.2.1 The Response Function 16

2.2.2 The Transition Rate 20

2.2.3 Normally-Ordered Coupling 21

3 Fermions from An Evolving Wall **23**

3.1 The Evolving Wall 24

3.1.1 Generalised Boundary Condition 24

3.1.2 Appearance and Disappearance of an MIT Wall 25

3.1.3 Correspondence to Delta Potential 27

3.2 Radiation from An Evolving Wall 30

3.2.1 Mode Solutions and Quantisation 30

3.2.2 Field Propagators 31

3.2.3 Energy Burst from A General Evolving Wall 33

3.2.4 Energy Burst during Wall Creation and Demolition 35

3.3 Unruh-DeWitt Detector Response 37

3.3.1 Static MIT Wall 38
3.3.2 General Evolving Wall 41
3.3.3 Wall Appearance 42
3.3.4 Wall Disappearance 47

4 Fermions From A Moving Wall **49**
4.1 Quantum Spinor Field with A Moving Wall 49
4.1.1 The Moving MIT Wall 49
4.1.2 Mode Solutions, Quantisation and Propagators 51
4.1.3 Stress-Energy Tensor 52
4.2 Unruh-DeWitt Detector Response 54
4.2.1 The Response Function 54
4.2.2 The Transition Rate 56
4.2.3 Collapsing Star Model 59

5 Conclusions **62**

A Supplement for Evolving Wall Analysis **67**
A.1 Self-adjoint Extensions of the Dirac Operator on Disjoint Half-Lines 67
A.2 Correspondence to δ-potential 70
A.3 Total Energy of Creation and Demolition Process 73
A.4 Static MIT Wall Response Function 74
A.5 General Evolving Wall Response Function 77
A.6 Wall Creation Response Function 80
A.6.1 Large Energy Gap Limit for Smooth Wall Creation 80
A.6.2 Rapid Creation Limit at Finite Energy Gap 82

B Supplement for Moving Wall Analysis **86**
B.1 Finite Switch-On Time (H_{int} or $H_{\text{int}}^{\text{no}}$) 86
B.2 Asymptotically Early Switch-On Time ($H_{\text{int}}^{\text{no}}$) 92

List of Figures

3.1 An MIT wall creation at $z = 0$. 35

4.1 A receding wall in Minkowski spacetime. 60

Chapter 1

Introduction

At the fundamental level, our current understanding of the physical world is based on two disunited theories: *quantum field theory* and *general relativity*. The former describes known elementary particles, such as electrons and quarks, and three out of four known fundamental forces in the universe, namely the electromagnetic force, the weak nuclear force and the strong nuclear force. The latter, on the other hand, describes spacetime itself and encodes gravity as the spacetime curvature.

Despite much effort that has been put into quantising gravity over the last century, no satisfactory complete theory of quantum gravity has been found to date. A major reason for this lack of success is the lack of verifiable prediction. Quantum gravity effects are expected to be significant on the Planck scale characterised by the Planck energy $(\hbar c^5/G)^{\frac{1}{2}} \approx 1.221 \times 10^{19}$ GeV, the Planck time $(\hbar G/c^5)^{\frac{1}{2}} \approx 5.391 \times 10^{-44}$ s and the Planck length $(\hbar G/c^3)^{\frac{1}{2}} \approx 1.616 \times 10^{-33}$ cm. Needless to say, designing an experiment to probe such a scale is not an easy task. Even the Large Hadron Collider, which collides protons on an energy scale of TeV, is nowhere near the regime of interest.

Taking a step back, the framework of *quantum field theory in curved spacetime* [1–6] explores the behaviour of matter and non-gravitational forces, modelled as quantum fields, in a curved spacetime, modelled by general relativity. It is

expected that this framework is applicable in the regime where classical aspects of gravity play an important role but its quantum nature is negligible. The early universe, sufficiently long after the big bang so that quantum gravity effects may be ignored, and the vicinity of a black hole whose Schwarzschild radius is bigger than the Planck length are examples of such a regime.

In the 1960's, Parker adopted this point of view and found that particles were created out of the vacuum in an expanding universe [7–9]. The effect, although predicted to be too small to be measured with present technologies, provides a mechanism that could explain the origin of the large scale structure of the universe. Later, in 1975, Hawking considered a spacetime describing a star undergoing gravitational collapse to form a black hole [10]. He discovered that an observer far away from the star will see, in the far future, thermal radiation of particles with temperature $T_{\rm BH} = \hbar\kappa/(2\pi c k_{\rm B})$, where $\hbar$ is the reduced Planck constant, κ is the surface gravity of the black hole, c is the speed of light and $k_{\rm B}$ is the Boltzmann constant. Since this is a late time phenomenon, Hawking interpreted that the radiation originates from the black hole. This led to the conclusion that black holes radiate, lose mass and shrink when quantum effects are taken into account, contradicting the common wisdom of the time that black holes do not radiate.

On one hand, the discovery that black holes emit thermal particles complements Bekenstein's earlier proposals that black holes should have physical entropy and temperature [11] and that a universe with black holes obey a generalised second law of thermodynamics [12]. On the other hand, the discovery that black holes lose mass and shrink leads to a new puzzle. While the elusive full theory of quantum gravity is required to explain the endpoint of such an evaporation, one may proceed by assuming that black holes evaporate completely and study the consequences of such an assumption. Indeed, this is exactly what Hawking did in [13], where his analysis led to the much debated information loss paradox [14].

An issue that curved spacetime quantum field theory put under the spotlight is the ambiguity in determining the particle content of a state using the conventional definition of a particle, which relies on plane wave mode decomposition of the field. One way to address the issue is by focusing instead on expectation values of local covariant quantities such as the stress-energy tensor. In this way, any discrepancy should only be an artefact and can be resolved by an appropriate coordinate transformation. Alternatively, one could resolve the issue by defining the notion of a particle operationally by means of a particle detector. In this approach, a localised quantum system — that is, the detector — interacting with the field in a certain way is what an observer observes. After interacting with the field for a period of time, the detector will undergo an excitation or a de-excitation. In the case of an excitation, the field state is said to contain a certain amount of particle. This pragmatic approach was initiated by Unruh [15] to clarify Hawking's result and then later simplified by DeWitt [16].

Recently, there has been an interest in a particle detector that interacts with fermions [17,18], specifically via a quadratic coupling introduced by Takagi [19]. Of particular interest to us is a result discovered in [18]. For massless fields, it was found that the response of a detector coupled linearly to the scalar density of a Dirac field in Minkowski spacetime with $d \geq 1$ spatial dimension(s) is proportional to that of a detector coupled linearly to a real bosonic field in a Minkowski spacetime with $2d + 1$ spatial dimensions. It was also shown, in particular, that a uniformly accelerating detector registers a Planckian distribution of particles. These results raise a question on the ability of such a detector to probe features of a fermionic field and distinguish fermions from bosons.

In this thesis, we study massless fermion creation by time-dependent boundaries in $1 + 1$ dimensional flat spacetimes. We consider two distinct senses in which the boundaries are said to be time-dependent. On one hand, we examine a boundary which is at rest with respect to a family of inertial observers but imposes a set of time-dependent boundary conditions. On the other hand, we

examine a moving boundary that imposes a time-independent boundary condition. We will refer to the former type of boundary as an evolving wall while to the latter type as a moving wall. In both cases, we are interested in particle creation from the vacuum. Therefore, in Heisenberg picture, we assume that the spinor field describing the fermions is in a state corresponding to the early time vacuum. We first calculate the renormalised expectation value of the field's stress-energy tensor to clarify the flow of energy in the system considered. Then, we analyse the response of an Unruh-DeWitt detector coupled to the scalar density of the field. For simplicity and to isolate the time-dependent effects of the boundary, we focus only on a static detector.

Before proceeding, let us review some motivations for studying time-dependent boundaries in flat spacetime quantum field theory. On one hand, this area of study is interesting in its own right. In 1948, Casimir considered a situation where two neutral conducting plates are placed in parallel to each other, separated by a distance d, in the presence of a quantised electromagnetic field in the vacuum state [20]. The plates put a constraint on the allowed quantum modes within the cavity, inducing a finite shift in the vacuum energy of the system as compared to the situation without any plate. As a consequence of the finite shift in energy, Casimir predicted that each plate will experience an attractive force per unit area with a magnitude proportional to d^{-4} towards each other. After an inconclusive early experiment by Sparnaay in 1958 [21], experiments carried out in later years confirmed Casimir's prediction with increasing precision [22–24]. The situation gets more interesting when the boundary condition is allowed to vary in time. Specifically, when the two plates above are set in motion, Moore predicted, in 1970, that photons can be created from the vacuum [25]. Termed the dynamical Casimir effect, this phenomenon was experimentally verified for the first time in 2011 using a superconducting circuit that simulates mechanical motion by an electrically-modulated boundary condition [26].

On the other hand, time-dependent boundaries in flat spacetime quantum field theory provide simple models that have been used time and again to gain insights on complicated phenomena in curved spacetime quantum field theory. The Davies-Fulling moving mirror model [27, 28] is a well-known example. Two years after Hawking's discovery of black hole radiation, Davies and Fulling showed that a moving mirror in $1+1$ Minkowski spacetime can produce similar thermal radiation provided the mirror follows a trajectory satisfying certain characteristic behaviour at late times. The similarity provides a strong motivation to study the simple Davies-Fulling model to gain insights on various aspects of black hole physics. For selected references, see [29–38]. A mirror trajectory where the Bogoliubov coefficients describing particle production are in exact correspondence with those of a null shell collapse, for instance, is given in [39].

Another example in the context of Hawking radiation is the wall creation model [40]. In the paper, Brown and Louko revisited the problem of mirror creation, previously considered by Obadia and Parentani in the context of perturbation theory [41], and solved it nonperturbatively for a massless scalar field. The motivation behind the study was to provide an exactly solvable model of dynamical quantum correlation breaking which is the main ingredient in the black hole firewall argument [42]. In addition to calculation of local energy density, which was found to be infrared divergent on future lightcones of the creation process, Brown and Louko also considered the response of an inertial Unruh-DeWitt detector passing through the energy burst. Subject to an infrared ambiguity, it was found that the response remains finite in the sharp creation limit. The result adds to the evidence that an actual detector coupled to the field may be less sensitive to divergences in the local energy density [43, 44].

Closely related to [40] is the work by Harada, Kinoshita and Miyamoto [45]. In addition to a sudden appearance of a two-sided Dirichlet mirror, the authors also considered a sudden disappearance of an existing mirror. The two situations are proposed to mimic a splitting and a merger of spacetime respectively. Even

though it was found that both a sudden appearance and a sudden disappearance of a two-sided Dirichlet mirror highly excites the vacuum, resulting in an infinitely strong flux of outgoing energy, the former seems to be more singular due to the existence of a term proportional to the delta distribution squared.

In Chapter 2, we begin with a review of fermions in 1+1 Minkowski spacetime. Then, we introduce and review the notion of Unruh-DeWitt particle detector. We discuss, in particular, the technical difficulties that arise in dealing with a detector that couples quadratically to the field.

In Chapter 3, we consider a non-moving time-dependent four-parameter wall that imposes a particular self-adjointness boundary condition at any instance of time for a massless spinor field. Some of the boundary conditions can be interpreted as arising from idealised non-local separable potential [46] with time-dependent strength. Our main results concern the local energy flow due to the wall's time evolution and the response of an inertial Unruh-DeWitt detector coupled linearly to the scalar density of the field [17–19].

We find that the renormalised stress-energy tensor of the field contains at most first derivatives of the parameters characterising the wall. Thus, if the wall evolves smoothly, the energy burst is finite and non-vanishing. For the detector response, we find that all four parameters simply redefine the switching function of the detector. Roughly speaking, the response to a general time-dependent four-parameter wall can be expressed as a sum of the response to a static impermeable wall. In each term of the sum, the switching function is substituted by a specific modified switching function involving some of the wall parameters. As a result, consistent with the local energy flow, the probability of the detector to be excited as it passes through the energy burst emitted by the wall is also finite (within first order perturbation theory).

For concreteness and to allow comparison with the scalar field analysis [40,45], we consider the appearance and disappearance, both rapidly and smoothly, of an impermeable wall that imposes MIT bag boundary conditions [47] on each

side. We find that the results display striking differences from those for a scalar field, particularly in the stress-energy tensor, but share common features in the response of a particle detector.

The energy burst from the wall is finite for any smoothly appearing and disappearing wall without any infrared ambiguity. The expression of the local energy density takes the same form in the two situations. In particular, there is no extra term that arises only in one of the situations. In the rapid process limit, the local energy density displays a delta distribution squared divergence. However, since there is no additional infrared divergent pre-factor, the energy density divergence can be said to be weaker than that of a wall creation for a scalar field. The total energy injected into the field diverges at least as fast as δ^{-1} where δ is the duration of wall evolution. The exact rate of divergence depends on how the limit $\delta \to 0$ is taken. In some cases, we show that the divergence is as fast as $K\delta^{-1}$ for some constant K.

The response of a particle detector for either a scalar or a spinor field is finite when the wall is created smoothly. In the limit of rapid creation, the response function diverges only logarithmically in the duration of wall evolution, similar to that observed in [40]. This further adds to the evidence that an actual local detector coupled to the field may be less sensitive to divergences in the local energy density. For either field, the divergent term comes solely from the moment at which the particle detector crosses the pulse of energy emitted by the suddenly appearing wall. For a spinor field, all the results mentioned also hold for a wall demolition.

In Chapter 4, we analyse the moving wall model for a massless spinor field. Our aim is to discern what a local observer would observe, particularly when the wall follows a trajectory that would produce thermal radiation at late times. To this end, we focus on two local observables, namely the renormalised stress-energy tensor of the field, which encodes the flow of energy, and the transition rate of an Unruh-DeWitt detector coupled linearly to the scalar density of the field [17,18].

The latter is of special interest following Louko and Toussaint's aforementioned result [18], which shows that the response of such a detector contains a Planck factor instead of a Fermi-Dirac factor when undergoing a uniform acceleration in Minkowski spacetime.

When the field is in the early time vacuum state, we find that the renormalised stress-energy tensor for an arbitrary smooth timelike wall trajectory is identical to that of a massless scalar field at all times [1, 28, 48]. This implies that an observer will not be able to distinguish fermions from bosons by examining only the flow of energy. On the contrary, an observer using an Unruh-DeWitt detector will generically be able to distinguish fermions from bosons. For concreteness, we consider a trajectory for which a mirror reflecting a scalar field is known to emit thermal radiation in the far future [49,50]. For the wall reflecting a fermion field, we find that the detector's late time transition rate is proportional to the Helmholtz free energy density of fermions in a thermal bath, hence showing a clear sign of Fermi-Dirac statistics.

In Chapter 5, we summarise our results and discuss the limitations of our analysis that could be a source of ideas for future projects.

We emphasise here that we are analysing a massless fermionic field. As such, one should have in mind massless neutrinos instead of photons. This means, in particular, that the totally reflecting, impermeable boundary that we consider in this thesis is not a conventional real-world mirror that reflects photons while being virtually invisible to a stream of neutrinos. To keep the readers reminded, we use the phrase "wall" instead of "mirror" to describe the physical boundary. We also note here that, aside from the no-wall boundary condition, almost all other boundary conditions that appear in this thesis are purely mathematical. The only other physical boundary condition is the MIT bag boundary condition [47] used to model the totally reflecting, impermeable wall. It has its origin in the study of hadrons and quark confinement at the phenomenological level.

However, we are not aware of any laboratory setting that could emulate the boundary condition.

We use an asterisk * for complex conjugation. $O(x)$ denotes a quantity such that $O(x)/x$ remains bounded as $x \to 0$, $O^\infty(x)$ denotes a quantity that goes to zero faster than any positive power of x as $x \to 0$ and $o(1)$ indicates a quantity that vanishes in the limit considered. Our metric signature is $(+,-)$ and we adopt units in which $\hbar = c = k_{\rm B} = 1$ throughout the analysis. We also adopt the Einstein summation convention where repeated indices are summed over.

Chapter 2

Fermions and Particle Detector

In this chapter, we review some aspects of a massless spinor field in $1+1$ Minkowski spacetime and the response of an Unruh-DeWitt particle detector [15, 16] which interacts with the field via a coupling to the field's scalar density [17–19]. We discuss, in particular, the technical difficulties that arise with the chosen coupling.

2.1 Fermions in Minkowski Spacetime

2.1.1 Quantum Spinor Field

Consider a $(1+1)$-dimensional Minkowski spacetime, in the standard global coordinates $x^\mu = (t, z)$ and the metric $\eta_{\mu\nu} = \text{diag}(1, -1)$. Null coordinates $u := t - z$ and $v := t + z$ are defined as per usual. Massless fermions in this spacetime are described by a two-component spinor field $\psi(t, z)$, obeying the Dirac equation

$$i\gamma^\mu \partial_\mu \psi = 0, \tag{2.1.1}$$

where γ^μ are the Dirac gamma matrices satisfying $\{\gamma^\mu, \gamma^\nu\} = 2\eta^{\mu\nu} I$, where I is the identity matrix. In what follows, note that we will use $\psi(u, v)$ as a shorthand

for $\psi(t(u,v),z(u,v))$. The Dirac inner product (ψ_1,ψ_2) between any two solutions ψ_1 and ψ_2 of the Dirac equation (2.1.1), evaluated on a constant t hypersurface, is given by

$$(\psi_1,\psi_2)=\int_{-\infty}^{\infty}[\psi_1(t,z)]^\dagger\psi_2(t,z)\,\mathrm{d}z\,. \tag{2.1.2}$$

Following the convention of [51, 52], we introduce a spinor basis $\{U_+,U_-\}$ that is orthonormal, in the sense that $U_+^\dagger U_-=U_-^\dagger U_+=0$ and $U_+^\dagger U_+=U_-^\dagger U_-=1$, and satisfies

$$\gamma^0\gamma^1U_\pm=\pm U_\pm,\qquad \gamma^0U_\pm=U_\mp. \tag{2.1.3}$$

We denote the coefficients of U_+ and U_- in $\psi(t,z)$ with $\psi_+(t,z)$ and $\psi_-(t,z)$ respectively so that $\psi(t,z)=\psi_+(t,z)U_++\psi_-(t,z)U_-$.

The Dirac equation (2.1.1) implies that $\psi_+(t,z)$ is an arbitrary function of u while $\psi_-(t,z)$ is an arbitrary function of v. Hence, $\psi_+(t,z)U_+$ and $\psi_-(t,z)U_-$ are the right-moving and left-moving components of $\psi(t,z)$ respectively. A complete set of plane wave mode solutions, normalised so that $(\psi_{\sigma,k},\psi_{\sigma',k'})=\delta_{\sigma\sigma'}\delta(k-k')$, is given by

$$\psi_{\mathrm{r},k}=\frac{1}{\sqrt{2\pi}}e^{-iku}U_+, \tag{2.1.4}$$

$$\psi_{\mathrm{l},k}=\frac{1}{\sqrt{2\pi}}e^{-ikv}U_-, \tag{2.1.5}$$

where $k\in\mathbb{R}\setminus\{0\}$. The subscript r or l reminds us whether the solution is a right-mover or a left-mover. The field $\psi(t,z)$ can then be expanded as

$$\psi(t,z)=\int_0^\infty\left(a_{\mathrm{r},k}\psi_{\mathrm{r},k}+a_{\mathrm{l},k}\psi_{\mathrm{l},k}+b_{\mathrm{r},k}^\dagger\psi_{\mathrm{r},-k}+b_{\mathrm{l},k}^\dagger\psi_{\mathrm{l},-k}\right)\mathrm{d}k\,. \tag{2.1.6}$$

To quantise the field, we promote $\psi(t,z)$ to an operator and impose the equal-time anticommutation relations

$$\{\psi_a(t,z),\psi_b(t,z')\} = \{\psi_a^\dagger(t,z),\psi_b^\dagger(t,z')\} = 0, \tag{2.1.7}$$

$$\{\psi_a(t,z),\psi_b^\dagger(t,z')\} = \delta_{ab}\delta(z-z'). \tag{2.1.8}$$

This is equivalent to promoting the coefficients $a_{\mathrm{r},k}, a_{\mathrm{l},k}, b_{\mathrm{r},k}, b_{\mathrm{l},k}$ and their hermitian conjugates, respectively, to a set of annihilation and creation operators, with non-vanishing anti-commutators

$$\{a_{\sigma,k}, a^\dagger_{\sigma',k'}\} = \{b_{\sigma,k}, b^\dagger_{\sigma',k'}\} = \delta_{\sigma\sigma'}\delta(k-k'), \tag{2.1.9}$$

where $k,k' > 0$. The annihilation operators define the standard Minkowski vacuum state $|0_{\mathrm{M}}\rangle$, which satisfies

$$a_{\mathrm{r},k}\,|0_{\mathrm{M}}\rangle = a_{\mathrm{l},k}\,|0_{\mathrm{M}}\rangle = b_{\mathrm{r},k}\,|0_{\mathrm{M}}\rangle = b_{\mathrm{l},k}\,|0_{\mathrm{M}}\rangle = 0 \qquad \text{for } k>0, \tag{2.1.10}$$

and is normalised to $\langle 0_{\mathrm{M}}|0_{\mathrm{M}}\rangle = 1$.

2.1.2 Field Propagators

In the convention of [18, 19], the positive and negative frequency propagators of $\psi(t,z)$ are defined as

$$S^+_{ab}(u,v;u',v') := \langle 0_{\mathrm{M}}|\,\psi_a(u,v)\overline{\psi}_b(u',v')\,|0_{\mathrm{M}}\rangle\,, \tag{2.1.11}$$

$$S^-_{ab}(u,v;u',v') := \langle 0_{\mathrm{M}}|\,\overline{\psi}_b(u',v')\psi_a(u,v)\,|0_{\mathrm{M}}\rangle\,, \tag{2.1.12}$$

respectively, where $\overline{\psi} = \psi^\dagger\gamma^0$ is the Dirac conjugate of ψ. Substituting the general solution (2.1.6) and using (2.1.4) – (2.1.5) as well as (2.1.10), we obtain

that

$$S^+_{ab}(u,v;u',v') = \int_0^\infty \frac{\mathrm{d}k}{2\pi}\left(e^{-ik(u-u')}U_{+,a}U^\dagger_{+,c} + e^{-ik(v-v')}U_{-,a}U^\dagger_{-,c}\right)\gamma^0_{cb}, \quad (2.1.13)$$

$$S^-_{ab}(u,v;u',v') = \int_0^\infty \frac{\mathrm{d}k}{2\pi}\left(e^{ik(u-u')}U_{+,a}U^\dagger_{+,c} + e^{ik(v-v')}U_{-,a}U^\dagger_{-,c}\right)\gamma^0_{cb}, \quad (2.1.14)$$

where $U_{\pm,i}$ is the i-th component of a 2×1 matrix representation of $U_\pm$, $U^\dagger_{\pm,j}$ is the j-th component of a 1×2 matrix representation of $U^\dagger_\pm$ and γ^0_{ij} is the (i,j) entry of a 2×2 matrix representation of γ^0. We interpret S^+_{ab} and S^-_{ab} as distributions in the sense of $\epsilon \to 0_+$ via the prescription

$$\int_0^\infty \mathrm{d}p\, e^{\pm ipz} \to \lim_{\epsilon\to 0_+}\int_0^\infty \mathrm{d}p\, e^{\pm ipz - p\epsilon} = \lim_{\epsilon\to 0_+}\frac{\pm i}{z \pm i\epsilon}. \quad (2.1.15)$$

This gives us

$$S^+_{ab}(u,v;u',v') = -\frac{i}{2\pi}\frac{1}{u-u'-i\epsilon}U_{+,a}U^\dagger_{+,c}\gamma^0_{cb} - \frac{i}{2\pi}\frac{1}{v-v'-i\epsilon}U_{-,a}U^\dagger_{-,c}\gamma^0_{cb}, \quad (2.1.16)$$

$$S^-_{ab}(u,v;u',v') = \frac{i}{2\pi}\frac{1}{u-u'+i\epsilon}U_{+,a}U^\dagger_{+,c}\gamma^0_{cb} + \frac{i}{2\pi}\frac{1}{v-v'+i\epsilon}U_{-,a}U^\dagger_{-,c}\gamma^0_{cb}, \quad (2.1.17)$$

where the limit $\epsilon \to 0_+$ is implicitly implied. Note that in the case of a spacetime without boundary here, the prescription (2.1.15) is equivalent to the commonly used regularisation $t - t' \to t - t' - i\epsilon$.

2.1.3 Stress-Energy Tensor

The stress-energy tensor of a Dirac field is given by [1]

$$T_{\mu\nu} = \frac{i}{2}\left[\overline{\psi}\gamma_{(\mu}\partial_{\nu)}\psi - (\partial_{(\mu}\overline{\psi})\gamma_{\nu)}\psi\right], \quad (2.1.18)$$

where $\gamma_\mu := \eta_{\mu\nu}\gamma^\nu$ and $A_{(\mu\nu)} := (A_{\mu\nu} + A_{\nu\mu})/2$ denotes the symmetric part of a tensor $A_{\mu\nu}$. Using (2.1.4), (2.1.5), (2.1.6) and (2.1.10), we obtain the components of the vacuum expectation value $\langle T_{\mu\nu}\rangle_{\rm M} \equiv \langle 0_{\rm M}| T_{\mu\nu} |0_{\rm M}\rangle$, which are given by

$$\langle T_{tt}\rangle_{\rm M} = \langle T_{zz}\rangle_{\rm M} = -2\int_0^\infty \frac{k}{2\pi}\,{\rm d}k\,, \tag{2.1.19}$$

$$\langle T_{tz}\rangle_{\rm M} = \langle T_{zt}\rangle_{\rm M} = 0. \tag{2.1.20}$$

Clearly, some of the components are divergent. This is the well-known divergence attributed to the fact that each mode, particularly the ultraviolet modes, has a non-vanishing contribution to the vacuum expectation value $\langle T_{\mu\nu}\rangle_{\rm M}$. In non-gravitational settings, however, only energy differences can be measured. Hence, this infinite vacuum energy density is subtracted away to obtain a renormalised expectation value of the stress-energy tensor.

We shall adopt the point-split renormalisation method [1]. In this method, one starts by point-splitting the stress-energy tensor $T_{\mu\nu}$ so that

$$T_{\mu\nu}(t,z) = \lim_{t',z'\to t,z} \frac{i}{2}\left[\overline{\psi}(t,z)\gamma_{(\mu}\partial'_{\nu)}\psi(t',z') - (\partial_{(\mu}\overline{\psi}(t,z))\gamma_{\nu)}\psi(t',z')\right], \tag{2.1.21}$$

where the prime in ∂'_ν indicates a derivative with respect to t' and z', as opposed to t and z. Using (2.1.6), (2.1.9), (2.1.10) and (2.1.12), we can formally express the components of $\langle T_{\mu\nu}\rangle_{\rm M}$ as

$$\langle T_{tt}\rangle_{\rm M} = \lim_{u',v'\to u,v} \frac{i}{2}\Big[\partial_u F(u,v;u',v') + \partial_v F(u,v;u',v')\Big], \tag{2.1.22}$$

$$\langle T_{zz}\rangle_{\rm M} = \lim_{u',v'\to u,v} \frac{i}{2}\Big[\partial_u G(u,v;u',v') - \partial_v G(u,v;u',v')\Big], \tag{2.1.23}$$

$$\begin{aligned}\langle T_{tz}\rangle_{\rm M} = \langle T_{zt}\rangle_{\rm M} = \lim_{u',v'\to u,v} \frac{i}{4}\Big[&- \partial_u F(u,v;u',v') + \partial_v F(u,v;u',v') \\ &- \partial_u G(u,v;u',v') - \partial_v G(u,v;u',v')\Big],\end{aligned} \tag{2.1.24}$$

where

$$F(u,v;u',v') := \mathrm{Tr}\big\{S^-(u,v;u',v')\gamma^0\big\} - \mathrm{Tr}\big\{S^-(u',v';u,v)\gamma^0\big\}, \tag{2.1.25}$$

$$G(u,v;u',v') := \mathrm{Tr}\big\{S^-(u,v;u',v')\gamma^1\big\} - \mathrm{Tr}\big\{S^-(u',v';u,v)\gamma^1\big\}. \tag{2.1.26}$$

Substituting (2.1.17) into (2.1.25) and (2.1.26), we obtain

$$\begin{aligned}\langle T_{tt}\rangle_{\mathrm{M}} = \langle T_{zz}\rangle_{\mathrm{M}} = \lim_{u',v'\to u,v} \frac{1}{4\pi}\bigg[&\frac{1}{(u-u'+i\epsilon)^2} + \frac{1}{(u-u'-i\epsilon)^2} \\ &+ \frac{1}{(v-v'+i\epsilon)^2} + \frac{1}{(v-v'-i\epsilon)^2}\bigg],\end{aligned} \tag{2.1.27}$$

$$\begin{aligned}\langle T_{tz}\rangle_{\mathrm{M}} = \langle T_{zt}\rangle_{\mathrm{M}} = \lim_{u',v'\to u,v} \frac{1}{4\pi}\bigg[&-\frac{1}{(u-u'+i\epsilon)^2} - \frac{1}{(u-u'-i\epsilon)^2} \\ &+ \frac{1}{(v-v'+i\epsilon)^2} + \frac{1}{(v-v'-i\epsilon)^2}\bigg],\end{aligned} \tag{2.1.28}$$

where the limit $\epsilon \to 0_+$ is again implicitly implied.

Suppose that we are interested in the renormalised expectation value of the stress-energy tensor when the field is in the state $|\Psi\rangle$, that is $\langle\Psi|\, T_{\mu\nu}\, |\Psi\rangle_{\mathrm{ren}}$. Its components are defined by subtracting the corresponding Minkowski vacuum component, (2.1.27) or (2.1.28), and taking the limit $\epsilon \to 0_+$ before taking the coincidence limit $u', v' \to u, v$. The necessity to set $\epsilon = 0$ before taking the coincidence limit will be exemplified in Chapter 4 where we would otherwise get a divergent result.

We note that it is not sufficient to simply identify from an integral expression of $\langle\Psi|\, T_{\mu\nu}\, |\Psi\rangle$, the term equal to the right-hand side of (2.1.19) and subtract it away under the integral. We will see in Chapter 3, where $|\Psi\rangle$ corresponds to the early time vacuum, that this simple subtraction would give a result that contradicts the result from point-split renormalisation.

2.2 Particle Detector

We now turn our attention to the notion of a particle detector. Specifically, we consider a point-like Unruh-DeWitt detector [1,15,16] with two energy levels $|0_{\mathrm{D}}\rangle$ and $|\omega\rangle$, associated to energies 0 and ω respectively, following a smooth timelike trajectory $(u(\tau), v(\tau))$ where τ is the detector's proper time. When $\omega > 0$, the state $|0_{\mathrm{D}}\rangle$ corresponds to the detector's ground state while $|\omega\rangle$ corresponds to the excited state. When $\omega < 0$, the roles are exchanged.

We couple our detector to the spinor field via the interaction Hamiltonian [17–19]

$$H_{\mathrm{int}} = c\mu(\tau)\chi(\tau)\overline{\psi}(u(\tau), v(\tau))\psi(u(\tau), v(\tau)), \tag{2.2.1}$$

where c is the coupling constant, $\mu(\tau)$ is the detector's monopole moment and $\chi(\tau)$ is a switching function that specifies how the interaction is switched on and off [53]. We assume that χ takes non-negative real values and is smooth with compact support. Note the absence of normal ordering in the interaction Hamiltonian above. This choice of coupling, unsurprisingly, introduces a divergence in the response of the detector. In Section 2.2.1, we present a technical prescription to handle the divergence and then, in Section 2.2.3, comment on an alternative interaction Hamiltonian that involves normal ordering .

2.2.1 The Response Function

Suppose that the detector is prepared in the state $|0_{\mathrm{D}}\rangle$ and the field is in an arbitrary state $|\Psi\rangle$ before the interaction is turned on. Working within first order perturbation theory, the probability $P(\omega)$ for the detector to have made a transition to the state $|\omega\rangle$ and the field to any state after the interaction has

ceased factorises as [1]

$$P(\omega) = c^2 |\langle 0_{\rm D}| \, \mu(0) \, |\omega\rangle|^2 F(\omega). \tag{2.2.2}$$

The pre-factor $|\langle 0_{\rm D}| \, \mu(0) \, |\omega\rangle|^2$ depends only on the internal structure of the detector. All dependence on the field's initial state, the detector's trajectory and the switching function are encoded in the response function $F(\omega)$, which reads

$$F(\omega) = \int_{-\infty}^{\infty} {\rm d}\tau \int_{-\infty}^{\infty} {\rm d}\tau' \, e^{-i\omega(\tau-\tau')} \chi(\tau)\chi(\tau') W^{(2,\bar{2})}(\tau,\tau'), \tag{2.2.3}$$

where $W^{(2,\bar{2})}(\tau,\tau') \equiv W^{(2,\bar{2})}(u(\tau),v(\tau);u(\tau'),v(\tau'))$ is the pull-back of the two-point correlation function

$$W^{(2,\bar{2})}(u,v;u',v') := \langle \Psi| \, \overline{\psi}(u,v)\psi(u,v)\overline{\psi}(u',v')\psi(u',v') \, |\Psi\rangle \tag{2.2.4}$$

onto the detector's worldline. In an abuse of terminology, we will drop the pre-factor and refer to $F(\omega)$ as the transition probability.

Using the properties $W^{(2,\bar{2})}(\tau,\tau') = [W^{(2,\bar{2})}(\tau',\tau)]^*$, the response function (2.2.3) can be expressed as [53, 54]

$$F(\omega) = 2 \int_{-\infty}^{\infty} {\rm d}r \, \chi(r) \int_{0}^{\infty} {\rm d}s \, \chi(r-s) \, {\rm Re}\Big\{ e^{-i\omega s} W^{(2,\bar{2})}(r, r-s) \Big\}. \tag{2.2.5}$$

The main advantage of expressing $F(\omega)$ in the form of (2.2.5) is that the following causality structure of the detector's response can be extracted. The transition probability of the detector after all interaction has ceased is given by the sum of contributions from every time r where χ is non-vanishing, that is, when the detector interacts with ψ. The contribution at each time r in turn is given by the sum of correlations between $\overline{\psi}\psi$ at the time r and $\overline{\psi}\psi$ in the past, back until when the detector-field interaction is switched on.

We are particularly interested in the detector's response when the field is initially in the vacuum state, that is when $|\Psi\rangle = |0\rangle_{\rm M}$ for this chapter. By virtue of (2.1.10), we can formally write the two-point function (2.2.4) in terms of the positive and negative frequency propagators as [18]

$$W^{(2,\bar{2})}(u,v;u',v') = \mathrm{Tr}\big\{S^+(u,v;u',v')S^-(u',v';u,v)\big\} + \mathrm{Tr}\big\{S^-(u,v;u,v)\big\}\,\mathrm{Tr}\big\{S^-(u',v';u',v')\big\}, \tag{2.2.6}$$

where the trace is over spinor indices. As S^+ and S^- are distributions, (2.2.6) needs to be understood in a distributional sense. The response function $F(\omega)$ in turn, be it in the form of (2.2.3) or (2.2.5), should be evaluated as follows: make the replacement $W^{(2,\bar{2})} \to W_\epsilon^{(2,\bar{2})}$, where $W_\epsilon^{(2,\bar{2})}$ is the appropriate smooth function whose $\epsilon \to 0_+$ limit is the distribution $W^{(2,\bar{2})}$, then perform the double integral and finally take the limit $\epsilon \to 0_+$. However, there are two technical difficulties that need to be addressed in defining the appropriate $W_\epsilon^{(2,\bar{2})}$. These difficulties are related to the fact that, as can be seen from (2.2.6), $W^{(2,\bar{2})}$ contains a product of two distributions and, in the second term of (2.2.6), each of the two propagators is "evaluated" at coincident spacetime points. The latter, in particular, is the source of the divergence mentioned at the beginning of this section.

Let us start with the first term in (2.2.6). Viewed as distributions, S^+ and S^- are well-defined individually as the $\epsilon \to 0_+$ limits of (2.1.16) and (2.1.17) respectively. Upon multiplication, each factor should *a priori* come with its own ϵ parameter, say ϵ_+ and ϵ_-, which need not be equal or even related to each other. This gives us

$$\mathrm{Tr}\big\{S^+(u,v;u',v')S^-(u',v';u,v)\big\} = -\frac{1}{4\pi^2}\left[\frac{1}{(u-u'-i\epsilon_+)(v-v'-i\epsilon_-)} + \frac{1}{(u-u'-i\epsilon_-)(v-v'-i\epsilon_+)}\right], \tag{2.2.7}$$

where the limits $\epsilon_\pm \to 0_+$ are implied. When pulled back onto the detector's wordline to evaluate the corresponding detector response contribution, the order in which the limits are taken could be expected to matter since such limits need not, in general, commute. However, notice that each term in (2.2.7) is a product of two distributions with different sets of variables. Since each factor in each term may be evaluated, after a suitable change of variables, using the Sokhotsky formula

$$\lim_{\epsilon\to 0_+} \frac{1}{x - i\epsilon} = \mathcal{P}\left(\frac{1}{x}\right) + i\pi\delta(x), \tag{2.2.8}$$

where $\mathcal{P}(1/x)$ denotes the Cauchy principal value, (2.2.7) does define the same distribution on $\mathbb{R}^4$ regardless of the order in which the two limits are taken. Hence, we may set $\epsilon_+ = \epsilon_-$ before pulling them back onto the detector's worldline. This way of defining a product of two distributions is implicit in [18].

Now consider the second term in (2.2.6). Due to the coincidence limit, S^- in this term is not well-defined. However, we see from (2.1.14) and (2.1.17) that the trace of S^- is proportional to $U_\pm^\dagger \gamma^0 U_\pm$, which vanishes by virtue of (2.1.3) and the orthogonality of the spinor basis. Hence, if we take the spinorial trace in $\mathrm{Tr}\{S^-(u,v;u,v)\}$ before performing any other operations, that is by defining $\mathrm{Tr}\{S^-(u,v;u,v)\}$ as the coincidence limit of $\mathrm{Tr}\{S^-(u,v;u',v')\}$, then each factor in the second term of (2.2.6) vanishes. Accepting this definition, we shall drop the second term in (2.2.6).

With the technical prescriptions above, the regularised two-point function $W_\epsilon^{(2,\bar{2})}$ in the absence of a boundary is given by

$$W_{\epsilon,\mathrm{NW}}^{(2,\bar{2})}(u,v;u',v') = -\frac{1}{2\pi^2}\frac{1}{(u-u'-i\epsilon)(v-v'-i\epsilon)}, \tag{2.2.9}$$

in agreement with [18]. Note that we have added the subscript "NW" in (2.2.9) as a reference to "no-wall" in order to distinguish the two-point functions in various situations that we will consider later. Theorem 1 of [18] states that the

corresponding response function (2.2.3), which we will also add the subscript "NW", is twice the response function of an Unruh-DeWitt detector, coupled linearly to a scalar field in $3+1$ Minkowski spacetime. Hence, from (3.8) of [53], and accounting for the difference in the sign convention, it follows that

$$F_{\text{NW}}(\omega) = -\frac{\omega}{2\pi}\int_{-\infty}^{\infty} \mathrm{d}r\,[\chi(r)]^2 + \frac{1}{\pi^2}\int_0^{\infty}\frac{\mathrm{d}s}{s^2}\int_{-\infty}^{\infty}\mathrm{d}r\,\chi(r)[\chi(r)-\chi(r-s)] + \frac{1}{\pi^2}\int_{-\infty}^{\infty}\mathrm{d}r\,\chi(r)\int_0^{\infty}\mathrm{d}s\,\chi(r-s)\left(\frac{1}{s^2}-\frac{\cos(\omega s)}{(\Delta x)^2}\right), \tag{2.2.10}$$

where $\Delta x = x(r) - x(r-s)$ is the geodesic distance between the detector's spacetime coordinate at proper time r and $r-s$, and $(\Delta x)^2$ is a shorthand for $\eta_{\mu\nu}\Delta x^\mu \Delta x^\nu$.

2.2.2 The Transition Rate

In analysing time-dependent situations, one often wants to know not just the transition probability but how it changes over time. The notion of instantaneous transition rate introduced in [53], which we will now review, is one way to do so.

Suppose that the switching function takes the form

$$\chi(r) = h_{\text{on}}\left(\frac{r-\tau_0+\delta}{\delta}\right)\times h_{\text{off}}\left(\frac{-r+\tau+\delta}{\delta}\right), \tag{2.2.11}$$

where τ and τ_0 are real parameters satisfying $\tau > \tau_0$, δ is a small positive parameter, and h_{on} and h_{off} are smooth non-negative functions such that $h_{\text{on}}(x) = h_{\text{off}}(x) = 0$ for $x \leq 0$ and $h_{\text{on}}(x) = h_{\text{off}}(x) = 1$ for $x \geq 1$. Then, the detector-field interaction is smoothly switched on during the interval $(\tau_0-\delta, \tau_0)$ according to the function h_{on}, stays at a constant coupling strength c for the interval $\Delta\tau = \tau - \tau_0$ and is smoothly switched off during the interval $(\tau, \tau+\delta)$ according to the function h_{off}.

The instantaneous transition rate $\dot{F}(\omega,\tau)$ of the detector is defined as $\partial_\tau F(\omega)$. Operationally, $\dot{F}(\omega,\tau)$ cannot be measured by a single or even an ensemble of

particle detectors since a measurement would change the initial condition for the dynamics of the detector. Instead, we need an ensemble of ensembles of particle detectors to measure $\dot{F}(\omega,\tau)$ [55,56]. While this means that $\dot{F}(\omega,\tau)$ is difficult to be measured in practice, it has a very useful intuitive physical interpretation that makes it suitable for theoretical investigation. It quantifies how the transition probability would change if the detector continues to interact with the field, at constant coupling c, for an infinitesimal extra time. Taking the limit $\delta \to 0$ to eliminate any switching effect, the result for a detector in Minkowski spacetime without a wall is readily available from (4.11) of [53], that is

$$\dot{F}_{\rm NW}(\omega,\tau) = -\frac{\omega}{2\pi} + \frac{1}{\pi^2}\int_0^{\Delta\tau}\left(\frac{1}{s^2} - \frac{\cos(\omega s)}{(\Delta x)^2}\right) + \frac{1}{\pi^2\Delta\tau}. \tag{2.2.12}$$

We note that the sharp switching limit $\delta \to 0$ should be taken after differentiating $F(\omega)$ with respect to τ. This is due to the second term in (2.2.10) which diverges as $\delta \to 0$. For details of the issue, see [53].

2.2.3 Normally-Ordered Coupling

Instead of (2.2.1), one may also consider the interaction Hamiltonian [17]

$$H_{\rm int}^{\rm no} = c\mu(\tau)\chi(\tau) : \overline{\psi}(u(\tau),v(\tau))\psi(u(\tau),v(\tau)) :, \tag{2.2.13}$$

where $: \overline{\psi}\psi :$ denotes normally-ordered scalar density. In this case, only the first term of (2.2.6) contributes to the two-point function $W^{(2,\bar{2})}(u,v;u',v')$ [18]. The divergence issue due to the second term of (2.2.6) hence does not arise. Indeed, the normally-ordered interaction Hamiltonian (2.2.13) is proposed in [17] precisely to address the divergence issue.

In Minkowski spacetime without a wall, the end result is the same whether one discards the divergence by means of operation ordering, as we did above, or by working with (2.2.13). However, in the presence of a boundary, the second term of

(2.2.6) contains a term which gives a finite contribution to the detector response. Hence, a detector interacting via the non-normally-ordered Hamiltonian (2.2.1) will have an additional term in its response function when compared to a detector interacting via the normally-ordered Hamiltonian (2.2.13). To make it easily identifiable, we will denote the additional term with a superscript "(2)" — for instance, $F^{(2)}_{\mathrm{MIT}}(\omega)$ in (3.3.6).

In what follows, we will focus primarily on a detector interacting via (2.2.1) and make occasional comments about one interacting via (2.2.13). In particular, we will regularly remind the readers whether a given formula is valid for both interactions or not. In the latter case, we will remind the readers which term is the additional term that arise due to the use of the non-normally-ordered Hamiltonian (2.2.1).

Chapter 3

Fermions from An Evolving Wall

In this chapter, we consider an evolving wall that remains at rest with respect to the spatial coordinate z but imposes time-dependent boundary conditions. We begin in Section 3.1 by introducing at the wall a boundary condition with four independent parameters, all of which may depend on time. We then identify a discrete set of time-dependent boundary conditions, each of which interpolates smoothly between no wall and a wall with the two-sided MIT bag boundary condition [47], henceforth referred to as an MIT wall. We consider both the case when the MIT wall is created and the case when the MIT wall is demolished. We end the section with a discussion on possible correspondence between the presented boundary conditions and an idealised delta potential. In Section 3.2, we quantise the field and analyse the energy burst coming from the evolving wall. We calculate, in particular, the amount of energy transmitted into the field by the creation and demolition process of the MIT wall. In Section 3.3, we focus our attention to the response of an inertial Unruh-DeWitt particle detector which remains at rest with respect to the evolving wall. After considering a static MIT wall, we analyse the response to a general evolving wall. Finally, we consider the response when an MIT wall is created or demolished, both in a finite amount of time and instantaneously.

3.1 The Evolving Wall

3.1.1 Generalised Boundary Condition

The Dirac equation (2.1.1) can alternatively be written as

$$i\partial_t\psi = -i\alpha\partial_z\psi, \tag{3.1.1}$$

where $\alpha = \gamma^0\gamma^1$. In this form, the operator $D := -i\alpha\partial_z$ on the right-hand-side of the equation is also known as the Dirac operator [57]. To introduce an evolving wall at $z = 0$, we replace (3.1.1) with

$$i\partial_t\psi = D_{U(t)}\psi, \tag{3.1.2}$$

where D_U is a four-parameter family of self-adjoint extensions of the Dirac operator D on disjoint half-lines.

In Appendix A.1, we show that each self-adjoint extension D_U is characterised by a 2×2 unitary matrix U, hence by four independent parameters. We have allowed U to depend on t in (3.1.2) to impose, in the spinor basis $\{U_+, U_-\}$, the time-dependent boundary condition

$$\begin{pmatrix} \psi_+(t, 0_+) \\ \psi_-(t, 0_-) \end{pmatrix} = U(t) \begin{pmatrix} \psi_+(t, 0_-) \\ \psi_-(t, 0_+) \end{pmatrix}, \tag{3.1.3}$$

where

$$U(t) := e^{i\varphi(t)} \begin{pmatrix} e^{i\varphi_1(t)} \cos\theta(t) & ie^{i\varphi_2(t)} \sin\theta(t) \\ ie^{-i\varphi_2(t)} \sin\theta(t) & e^{-i\varphi_1(t)} \cos\theta(t) \end{pmatrix}. \tag{3.1.4}$$

With the parametrisation (3.1.4), note that different sets of φ, φ_1, φ_2 and θ need not imply distinct boundary conditions. For a given φ_1, φ_2 and θ, the cases of

$\varphi = 0$ and $\varphi = 2\pi$, for instance, obviously correspond to the same U, hence the same boundary condition.

To assist the standard definition of an early time vacuum when we quantise the field, we require that $U(t)$ depends on t only over a finite interval of time. Additionally, looking ahead to a detector response calculation, we require that all four parameter functions, $\varphi(t)$, $\varphi_1(t)$, $\varphi_2(t)$ and $\theta(t)$, are smooth functions of time.

3.1.2 Appearance and Disappearance of an MIT Wall

In [47], Chodos and collaborators consider confining fermions in a region whose position of boundary is not determined *a priori*. By matching the field at the boundary and then taking the field mass to infinity in the exterior region, they obtain the boundary conditions[1]

$$in_\mu \gamma^\mu \psi\big|_{\text{boundary}} = \psi\big|_{\text{boundary}}, \tag{3.1.5}$$

$$-n_\mu \partial^\mu (\overline{\psi}\psi)\big|_{\text{boundary}} = 2B, \tag{3.1.6}$$

where n_μ is the inward-directed unit normal to the boundary and $B > 0$ is a real constant. The linear boundary condition (3.1.5) is responsible for confining the fermions in the region while the non-linear boundary condition (3.1.6) allows for the position of the boundary to be determined dynamically [58]. Since we have fixed the position of our wall to be at $z = 0$, (3.1.6) plays no role in our analysis and only (3.1.5) is relevant.

A confinement to the right portion ($z > 0$) of the spacetime corresponds to $n_\mu = (0, 1)$ whereas a confinement to the left portion ($z < 0$) of the spacetime corresponds to $n_\mu = (0, -1)$. The two-sided MIT bag boundary condition

[1] Note that (3.1.6) is (5.3b) of [47]. The minus pre-factor on the left-hand side of (3.1.6) accounts for the difference in sign convention.

imposed by the MIT wall hence reads

$$(1 \mp i\gamma^1)\psi(t, 0_\pm) = 0. \tag{3.1.7}$$

In the spinor basis $\{U_+, U_-\}$, the boundary condition (3.1.7) reduces to

$$\psi_\pm(t, 0_\pm) = -i\psi_\mp(t, 0_\pm). \tag{3.1.8}$$

Recall that $\psi_+ U_+$ and $\psi_- U_-$ are respectively the right-moving and left-moving component of the massless field ψ. The boundary condition (3.1.8) implies that, up to some constant, the right-moving component of the field for $z > 0$ is determined only by the left-moving component that hits the wall from the same side and not by anything from the left portion of the spacetime. Similarly, the left-moving component of the field for $z < 0$ is determined only by the right-moving component from the left portion of the spacetime. So, we see that the MIT wall is totally reflective on both sides.

From (3.1.3), we see that the absence of a wall is described by $U(t) = I$, which translates (3.1.3) to a continuity condition across $z = 0$ for each field component. The presence of an MIT wall, on the other hand, is given by

$$U(t) = U_{\text{MIT}} \equiv \begin{pmatrix} 0 & -i \\ -i & 0 \end{pmatrix}. \tag{3.1.9}$$

Among all possible ways of smoothly changing the boundary condition from $U(t) = I$ to $U(t) = U_{\text{MIT}}$, we shall pay particular attention to the ones described by the following discrete family of one-parameter subgroups of boundary conditions,

$$U_n(t) = e^{2in\theta(t)} \begin{pmatrix} \cos\theta(t) & (-1)^{n+1} i \sin\theta(t) \\ (-1)^{n+1} i \sin\theta(t) & \cos\theta(t) \end{pmatrix}, \tag{3.1.10}$$

where the integer n indexes the subgroups. This amounts to setting $\varphi(t) = 2n\theta(t)$, $\varphi_1(t) = 0$ and $\varphi_2(t) = (n+1)\pi$.

The appearance of an MIT wall is described by

$$\theta(t) = \theta_1(t) := \begin{cases} 0 & \text{for } t \leq t_0, \\ h_1(t) & \text{for } t_0 < t < t_0 + \delta, \\ \frac{\pi}{2} & \text{for } t \geq t_0 + \delta, \end{cases} \tag{3.1.11}$$

where $h_1(t)$ is some smooth function interpolating the initial and final conditions. The disappearance of an MIT wall is described by

$$\theta(t) = \theta_2(t) := \begin{cases} \frac{\pi}{2} & \text{for } t \leq t_0, \\ h_2(t) & \text{for } t_0 < t < t_0 + \delta, \\ 0 & \text{for } t \geq t_0 + \delta, \end{cases} \tag{3.1.12}$$

where $h_2(t)$ is another smooth interpolating function. In both cases, $\delta > 0$ is the amount of time taken for the process the complete. The limit $\delta \to 0$ thus corresponds to sudden appearance and disappearance of an MIT wall.

3.1.3 Correspondence to Delta Potential

In physics, the presence of a point source or a thin wall is often described by a delta potential in the equation of motion. If we suppose that the wall in Section 3.1.1 and 3.1.2 can be represented by a combination of time-dependent point-like real scalar and electric potentials, this amounts to replacing (3.1.1) with

$$i\partial_t\psi = -i\alpha\partial_z\psi + (S(t)\beta + V(t))\delta(z)\psi, \tag{3.1.13}$$

where $\beta = \gamma^0$. The strengths of the scalar and electric potentials are given by the real functions $S(t)$ and $V(t)$ respectively. The corresponding boundary condition

imposed by the delta potential is then usually derived by taking the limit $\epsilon \to 0$ after integrating both sides of the equation of motion over a small interval $[-\epsilon, \epsilon]$, where $\epsilon > 0$.

Unlike the Klein-Gordon or the Schrödinger equations, however, the Dirac equation is first order in spatial derivative. The addition of a delta potential into the equation, like in (3.1.13), implies that ψ is discontinuous at $z = 0$. This makes the expression such as

$$\int_{-\epsilon}^{\epsilon} \delta(z)\psi(z)\,\mathrm{d}z\,, \tag{3.1.14}$$

which appears in the derivation of boundary condition imposed by (3.1.13), ill-defined. Hence, without an additional information or a prescription to define (3.1.14), it is not clear what sort of boundary condition the equation (3.1.13) imposes. In [59, 60], it was pointed out that the definition

$$\lim_{\epsilon\to 0_+} \int_{-\epsilon}^{\epsilon} \delta(z)\psi(z)\,\mathrm{d}z := \frac{1}{2}(\psi(0_-) + \psi(0_+)) \tag{3.1.15}$$

is not appropriate when the δ-potential is considered as the limit of a family of local potentials. However, if the δ-potential is considered as the limit of a family of non-local separable potentials, then (3.1.15) is indeed correct [46].

In Appendix A.2, we show that if the boundary condition (3.1.3) is taken to arise from (3.1.13) with the prescription (3.1.15), then the following relations must hold (suppressing dependence on t),

$$(-1)^{c_1}[(V^2 - S^2 - 4)\cos\varphi + 4V\sin\varphi]\cos\theta = S^2 - V^2 - 4, \tag{3.1.16}$$

$$(-1)^{c_2}[(V^2 - S^2 - 4)\cos\varphi + 4V\sin\varphi]\sin\theta = 4S, \tag{3.1.17}$$

$$4V\cos\varphi - (V^2 - S^2 - 4)\sin\varphi = 0, \tag{3.1.18}$$

where c_1 and c_2 are integers. For the wall appearance and disappearance described by (3.1.10) - (3.1.12), in particular, the strengths of the scalar and electric

potentials are given by (restoring dependence on t)

$$S(t) = \frac{2(-1)^n \sin\theta(t)}{\cos\theta(t) + \cos 2n\theta(t)}, \tag{3.1.19}$$

$$V(t) = -\frac{2\sin 2n\theta(t)}{\cos\theta(t) + \cos 2n\theta(t)}. \tag{3.1.20}$$

Notice that, unless $n = 0$, both $S(t)$ and $V(t)$ necessarily diverge at some point of time along the evolution. This may hint that only $n = 0$ models a physically realisable process.

We note that [46] actually only considered a time-independent potential. So, in deriving the correspondence above, we have implicitly assumed that the definition (3.1.15) remains valid when the strength of our family of non-local separable potentials is time-dependent. To put the correspondence on a solid foundation, it is necessary to first solve the equation (3.1.13) with the δ-potential replaced by a class of non-local potentials, take the δ-function limit and show that the solutions coincide with that obtain in the next section where we use the self-adjoint extension method. Since we have not verified this is the case, we would like to stress that the rest of our calculations are based on the well-defined self-adjointness boundary conditions introduced in Section 3.1.1 rather than the δ-potential framework described in this section. The latter is meant to provide some physical insights to possible interpretation of the wall parameters, that is as scalar and electric potentials.

3.2 Radiation from An Evolving Wall

3.2.1 Mode Solutions and Quantisation

Recall that ψ_+ and ψ_- are functions of u and v respectively for a massless field. Hence, we consider the mode solution ansatz

$$\psi^{\text{in}}_{\text{r},k}(u,v) = \begin{cases} \frac{1}{\sqrt{2\pi}} e^{-iku} U_+ + E_{\text{r},k}(v) U_- & \text{for } z < 0, \\ F_{\text{r},k}(u) U_+ & \text{for } z > 0, \end{cases} \tag{3.2.1}$$

$$\psi^{\text{in}}_{\text{l},k}(u,v) = \begin{cases} E_{\text{l},k}(v) U_- & \text{for } z < 0, \\ F_{\text{l},k}(u) U_+ + \frac{1}{\sqrt{2\pi}} e^{-ikv} U_- & \text{for } z > 0, \end{cases} \tag{3.2.2}$$

where $E_{\text{r},k}(v), F_{\text{r},k}(u), E_{\text{l},k}(v), F_{\text{l},k}(u)$ are functions to be determined. The right-moving part of $\psi^{\text{in}}_{\text{r},k}(u,v)$ is a multiple of $e^{-iku}U_+$ for $z < 0$ to indicate the fact that this part has no knowledge of the wall, since this part originates from left past null infinity. For similar reason, the left-moving part of $\psi^{\text{in}}_{\text{l},k}(u,v)$ is a multiple of $e^{-ikv}U_-$ for $z > 0$. The superscript "in" indicates that this ansatz reduces to an appropriate set of stationary mode solutions at early times. The subscripts r and l, on the other hand, indicate that the solutions reduce to (2.1.4) and (2.1.5) respectively in the absence of a wall.

Substitution of (3.2.1) – (3.2.2) into (3.1.3) with the general boundary condition (3.1.4) then gives

$$\psi^{\text{in}}_{\text{r},k}(u,v) = \begin{cases} \frac{1}{\sqrt{2\pi}} e^{-iku} U_+ + \frac{i}{\sqrt{2\pi}} e^{-ikv + i\varphi(v) - i\varphi_2(v)} \sin\theta(v) U_- & \text{for } z < 0, \\ \frac{1}{\sqrt{2\pi}} e^{-iku + i\varphi(u) + i\varphi_1(u)} \cos\theta(u) U_+ & \text{for } z > 0, \end{cases} \tag{3.2.3}$$

$$\psi^{\text{in}}_{\text{l},k}(u,v) = \begin{cases} \frac{1}{\sqrt{2\pi}} e^{-ikv + i\varphi(v) - i\varphi_1(v)} \cos\theta(v) U_- & \text{for } z < 0, \\ \frac{i}{\sqrt{2\pi}} e^{-iku + i\varphi(u) + i\varphi_2(u)} \sin\theta(u) U_+ + \frac{1}{\sqrt{2\pi}} e^{-ikv} U_- & \text{for } z > 0. \end{cases} \tag{3.2.4}$$

The mode solutions above are normalised in the Dirac inner product (2.1.2) so that they satisfy $(\psi^{\rm in}_{\sigma,k}, \psi^{\rm in}_{\sigma',k'}) = \delta_{\sigma\sigma'}\delta(k-k')$ for $k, k' \in \mathbb{R}\setminus\{0\}$.

Given the mode solutions (3.2.3) and (3.2.4), a general solution to the Dirac equation (3.1.2) can then be expanded as

$$\psi(u,v) = \int_0^\infty \mathrm{d}q \left(a^{\rm in}_{{\rm r},q}\psi^{\rm in}_{{\rm r},q} + a^{\rm in}_{{\rm l},q}\psi^{\rm in}_{{\rm l},q} + b^{{\rm in}\dagger}_{{\rm r},q}\psi^{\rm in}_{{\rm r},-q} + b^{{\rm in}\dagger}_{{\rm l},q}\psi^{\rm in}_{{\rm l},-q}\right). \tag{3.2.5}$$

Since the modes reduce to early time stationary modes, it is reasonable that, upon quantisation, we promote $a^{\rm in}_{{\rm r},q}$, $a^{\rm in}_{{\rm l},q}$, $b^{\rm in}_{{\rm r},q}$ and $b^{\rm in}_{{\rm l},q}$ to be annihilation operators associated with excitations of the field before the wall starts to exhibit time dependence. The hermitian conjugates $a^{{\rm in}\dagger}_{{\rm r},q}$, $a^{{\rm in}\dagger}_{{\rm l},q}$, $b^{{\rm in}\dagger}_{{\rm r},q}$ and $b^{{\rm in}\dagger}_{{\rm l},q}$, on the other hand, are promoted to be creation operators. The non-vanishing canonical anticommutators are

$$\{a^{\rm in}_{\sigma,p}, a^{{\rm in}\dagger}_{\sigma',q}\} = \{b^{\rm in}_{\sigma,p}, b^{{\rm in}\dagger}_{\sigma',q}\} = \delta_{\sigma\sigma'}\delta(p-q), \tag{3.2.6}$$

where $p, q > 0$. The in-vacuum state $|0_{\rm in}\rangle$ is normalised so that $\langle 0_{\rm in}|0_{\rm in}\rangle = 1$ and satisfies

$$a^{\rm in}_{{\rm r},k}\,|0_{\rm in}\rangle = a^{\rm in}_{{\rm l},k}\,|0_{\rm in}\rangle = b^{\rm in}_{{\rm r},k}\,|0_{\rm in}\rangle = b^{\rm in}_{{\rm l},k}\,|0_{\rm in}\rangle = 0 \qquad \text{for } k>0. \tag{3.2.7}$$

3.2.2 Field Propagators

The positive and negative frequency propagators are defined similar to (2.1.11) and (2.1.12). The only difference is that the Minkowski vacuum is replaced by the in-vacuum, so that now

$$S^+_{ab}(u,v;u',v') := \langle 0_{\rm in}|\,\psi_a(u,v)\overline{\psi}_b(u',v')\,|0_{\rm in}\rangle\,, \tag{3.2.8}$$

$$S^-_{ab}(u,v;u',v') := \langle 0_{\rm in}|\,\overline{\psi}_b(u',v')\psi_a(u,v)\,|0_{\rm in}\rangle\,, \tag{3.2.9}$$

respectively. For our purposes, we only need to know the expressions for (3.2.8) and (3.2.9) when (u, v) and (u', v') are both on the same side. Using (3.2.3) – (3.2.7), followed by the prescription (2.1.15), we obtain

$$\begin{aligned}
&S^+_{ab}(u,v;u',v') \\
&\quad= -\frac{i}{2\pi}\frac{1}{u-u'-i\epsilon}U_{+,a}U^\dagger_{+,c}\gamma^0_{cb} + \frac{1}{2\pi}\frac{e^{i\varphi(v)-i\varphi_2(v)}\sin\theta(v)}{v-u'-i\epsilon}U_{-,a}U^\dagger_{+,c}\gamma^0_{cb} \\
&\qquad - \frac{1}{2\pi}\frac{e^{-i\varphi(v')+i\varphi_2(v')}\sin\theta(v')}{u-v'-i\epsilon}U_{+,a}U^\dagger_{-,c}\gamma^0_{cb} \\
&\qquad - \frac{i}{2\pi}\frac{e^{i[\varphi(v)-\varphi(v')]-i[\varphi_2(v)-\varphi_2(v')]}\sin\theta(v)\sin\theta(v')}{v-v'-i\epsilon}U_{-,a}U^\dagger_{-,c}\gamma^0_{cb} \\
&\qquad - \frac{i}{2\pi}\frac{e^{i[\varphi(v)-\varphi(v')]-i[\varphi_1(v)-\varphi_1(v')]}\cos\theta(v)\cos\theta(v')}{v-v'-i\epsilon}U_{-,a}U^\dagger_{-,c}\gamma^0_{cb}, \qquad (3.2.10)
\end{aligned}$$

$$\begin{aligned}
&S^-_{ab}(u,v;u',v') \\
&\quad= \frac{i}{2\pi}\frac{1}{u-u'+i\epsilon}U_{+,a}U^\dagger_{+,c}\gamma^0_{cb} - \frac{1}{2\pi}\frac{e^{i\varphi(v)-i\varphi_2(v)}\sin\theta(v)}{v-u'+i\epsilon}U_{-,a}U^\dagger_{+,c}\gamma^0_{cb} \\
&\qquad + \frac{1}{2\pi}\frac{e^{-i\varphi(v')+i\varphi_2(v')}\sin\theta(v')}{u-v'+i\epsilon}U_{+,a}U^\dagger_{-,c}\gamma^0_{cb} \\
&\qquad + \frac{i}{2\pi}\frac{e^{i[\varphi(v)-\varphi(v')]-i[\varphi_2(v)-\varphi_2(v')]}\sin\theta(v)\sin\theta(v')}{v-v'+i\epsilon}U_{-,a}U^\dagger_{-,c}\gamma^0_{cb} \\
&\qquad + \frac{i}{2\pi}\frac{e^{i[\varphi(v)-\varphi(v')]-i[\varphi_1(v)-\varphi_1(v')]}\cos\theta(v)\cos\theta(v')}{v-v'+i\epsilon}U_{-,a}U^\dagger_{-,c}\gamma^0_{cb}, \qquad (3.2.11)
\end{aligned}$$

when $z, z' < 0$, and

$$\begin{aligned}
&S^+_{ab}(u,v;u',v') \\
&\quad= -\frac{i}{2\pi}\frac{1}{v-v'-i\epsilon}U_{-,a}U^\dagger_{-,c}\gamma^0_{cb} + \frac{1}{2\pi}\frac{e^{i\varphi(u)+i\varphi_2(u)}\sin\theta(u)}{u-v'-i\epsilon}U_{+,a}U^\dagger_{-,c}\gamma^0_{cb} \\
&\qquad - \frac{1}{2\pi}\frac{e^{-i\varphi(u')-i\varphi_2(u')}\sin\theta(u')}{v-u'-i\epsilon}U_{-,a}U^\dagger_{+,c}\gamma^0_{cb} \\
&\qquad - \frac{i}{2\pi}\frac{e^{i[\varphi(u)-\varphi(u')]+i[\varphi_2(u)-\varphi_2(u')]}\sin\theta(u)\sin\theta(u')}{u-u'-i\epsilon}U_{+,a}U^\dagger_{+,c}\gamma^0_{cb} \\
&\qquad - \frac{i}{2\pi}\frac{e^{i[\varphi(u)-\varphi(u')]+i[\varphi_1(u)-\varphi_1(u')]}\cos\theta(u)\cos\theta(u')}{u-u'-i\epsilon}U_{+,a}U^\dagger_{+,c}\gamma^0_{cb}, \qquad (3.2.12)
\end{aligned}$$

$$
\begin{aligned}
&S^{-}_{ab}(u,v;u',v') \\
&\quad= \frac{i}{2\pi}\frac{1}{v-v'+i\epsilon}U_{-,a}U^{\dagger}_{-,c}\gamma^{0}_{cb} - \frac{1}{2\pi}\frac{e^{i\varphi(u)+i\varphi_2(u)}\sin\theta(u)}{u-v'+i\epsilon}U_{+,a}U^{\dagger}_{-,c}\gamma^{0}_{cb} \\
&\qquad+ \frac{1}{2\pi}\frac{e^{-i\varphi(u')-i\varphi_2(u')}\sin\theta(u')}{v-u'+i\epsilon}U_{-,a}U^{\dagger}_{+,c}\gamma^{0}_{cb} \\
&\qquad+ \frac{i}{2\pi}\frac{e^{i[\varphi(u)-\varphi(u')]+i[\varphi_2(u)-\varphi_2(u')]}\sin\theta(u)\sin\theta(u')}{u-u'+i\epsilon}U_{+,a}U^{\dagger}_{+,c}\gamma^{0}_{cb} \\
&\qquad+ \frac{i}{2\pi}\frac{e^{i[\varphi(u)-\varphi(u')]+i[\varphi_1(u)-\varphi_1(u')]}\cos\theta(u)\cos\theta(u')}{u-u'+i\epsilon}U_{+,a}U^{\dagger}_{+,c}\gamma^{0}_{cb}, \quad (3.2.13)
\end{aligned}
$$

when $z, z' > 0$. In all four expressions above, the limit $\epsilon \to 0_+$ is implied.

3.2.3 Energy Burst from A General Evolving Wall

We are interested in the energy transmitted into the field by the evolving wall. To obtain the renormalised expectation value of $T_{\mu\nu}$ in the in-vacuum state, that is $\langle T_{\mu\nu}\rangle^{\rm in}_{\rm ren} \equiv \langle 0_{\rm in}|\, T_{\mu\nu}\, |0_{\rm in}\rangle - \langle T_{\mu\nu}\rangle_{\rm M}$, we employ the point-split renormalisation procedure outlined in Chapter 2. Using (3.2.5), (3.2.6), (3.2.7) and (3.2.9), we obtain a set of expressions analogous to (2.1.22) – (2.1.24) for the components of $\langle 0_{\rm in}|\, T_{\mu\nu}\, |0_{\rm in}\rangle$. The negative frequency propagator that appears in the corresponding expressions of $F(u,v;u',v')$ and $G(u,v;u',v')$ in this case is, of course, (3.2.9) instead of (2.1.12). This allows us to use (3.2.11) and (3.2.13) in our calculation of $\langle T_{\mu\nu}\rangle^{\rm in}_{\rm ren}$.

Performing the subtraction of $\langle T_{\mu\nu}\rangle_{\rm M}$ before taking the coincidence limit, we obtain, for $z < 0$,

$$
\langle T_{tt}\rangle^{\rm in}_{\rm ren} = \langle T_{zz}\rangle^{\rm in}_{\rm ren} = \langle T_{tz}\rangle^{\rm in}_{\rm ren} = \langle T_{zt}\rangle^{\rm in}_{\rm ren} = \frac{1}{4\pi}f_{\rm L}(v), \quad (3.2.14)
$$

where

$$
\begin{aligned}
f_{\rm L}(v) &= (\partial_v\varphi(v))^2 + (\partial_v\varphi_1(v))^2\cos^2\theta(v) + (\partial_v\varphi_2(v))^2\sin^2\theta(v) + (\partial_v\theta(v))^2 \\
&\quad - 2\,\partial_v\varphi(v)\Big[\partial_v\varphi_1(v)\cos^2\theta(v) + \partial_v\varphi_2(v)\sin^2\theta(v)\Big]. \quad (3.2.15)
\end{aligned}
$$

Meanwhile, for $z > 0$,

$$\langle T_{tt}\rangle^{\rm in}_{\rm ren} = \langle T_{zz}\rangle^{\rm in}_{\rm ren} = -\langle T_{tz}\rangle^{\rm in}_{\rm ren} = -\langle T_{zt}\rangle^{\rm in}_{\rm ren} = \frac{1}{4\pi} f_{\rm R}(u), \tag{3.2.16}$$

where

$$\begin{aligned} f_{\rm R}(u) = {} & (\partial_u\varphi(u))^2 + (\partial_u\varphi_1(u))^2\cos^2\theta(u) + (\partial_u\varphi_2(u))^2\sin^2\theta(u) + (\partial_u\theta(u))^2 \\ & + 2\,\partial_u\varphi(u)\Big[\partial_u\varphi_1(u)\cos^2\theta(u) + \partial_u\varphi_2(u)\sin^2\theta(u)\Big]. \end{aligned} \tag{3.2.17}$$

From (3.2.14) – (3.2.17), we see that there will always be a finite pulse of energy on, and only on, the future lightcones of a smoothly evolving wall. This is illustrated in Figure 3.1 for an MIT wall creation.

Before we proceed, let us return to the remark made in Chapter 2 regarding renormalisation. Suppose that we had calculated $\langle T_{\mu\nu}\rangle_{\rm in} \equiv \langle 0_{\rm in}|\, T_{\mu\nu}\, |0_{\rm in}\rangle$ by substituting (3.2.3) – (3.2.5) directly into $\langle T_{\mu\nu}\rangle_{\rm in}$. Then, we would have obtained, for $z < 0$,

$$\langle T_{tt}\rangle_{\rm in} = \langle T_{zz}\rangle_{\rm in} = -2\int_0^\infty \frac{p}{2\pi}\,{\rm d}p + g_{\rm L}(v), \tag{3.2.18}$$

$$\langle T_{tz}\rangle_{\rm in} = \langle T_{zt}\rangle_{\rm in} = g_{\rm L}(v), \tag{3.2.19}$$

where

$$g_{\rm L}(v) = \int_0^\infty \frac{{\rm d}p}{2\pi}\left(-\partial_v\varphi(v) + \partial_v\varphi_1(v)\cos^2\theta(v) + \partial_v\varphi_2(v)\sin^2\theta(v)\right), \tag{3.2.20}$$

and for $z > 0$,

$$\langle T_{tt}\rangle_{\rm in} = \langle T_{zz}\rangle_{\rm in} = -2\int_0^\infty \frac{p}{2\pi}\,{\rm d}p + g_{\rm R}(u), \tag{3.2.21}$$

$$\langle T_{tz}\rangle_{\rm in} = \langle T_{zt}\rangle_{\rm in} = -g_{\rm R}(u), \tag{3.2.22}$$

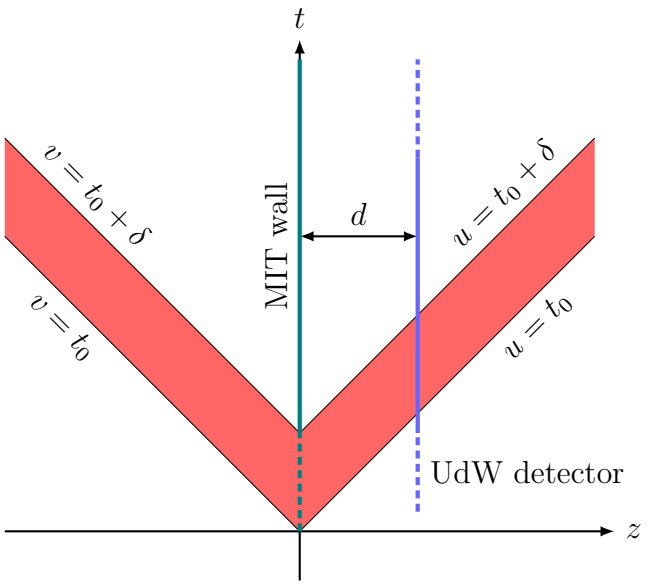


Figure 3.1: An MIT wall creation at $z = 0$. The process of wall creation begins at $t = t_0$ and completes after δ unit of time. The wall emits non-vanishing energy pulse while being created. The figure also shows an Unruh-DeWitt (UdW) detector at $z = d > 0$.

where

$$g_{\mathrm{R}}(u) = \int_0^\infty \frac{\mathrm{d}p}{2\pi} \left(-\partial_u\varphi(u) - \partial_u\varphi_1(u)\cos^2\theta(u) - \partial_u\varphi_2(u)\sin^2\theta(u)\right). \quad (3.2.23)$$

Comparing (3.2.18) – (3.2.23) to (2.1.19) – (2.1.20), we would then have identified the first terms of (3.2.18) and (3.2.21) as the vacuum contribution in the absence of wall, and interpreted the remaining terms as coming from the wall. Since these remaining terms are independent of p, we would have concluded that the renormalised stress-energy tensor is, in general, ultraviolet divergent. Furthermore, we would have concluded that there is no energy burst if φ, φ_1 and φ_2 are held constant and only θ evolves. These conclusions would have been incorrect, as the expressions (3.2.14) – (3.2.17) obtained by point-splitting show.

3.2.4 Energy Burst during Wall Creation and Demolition

Keeping in mind the relations (3.2.14) and (3.2.16), we focus here only on $\langle T_{tt}\rangle^{\mathrm{in}}_{\mathrm{ren}}$. Substituting $\varphi(t) = 2n\theta(t)$, $\varphi_1(t) = 0$ and $\varphi_2(t) = (n+1)\pi$ into (3.2.15) and

(3.2.17), we obtain the corresponding renormalised energy density expectation value for the wall appearance and disappearance scenarios described by (3.1.10) – (3.1.12), that is

$$\langle T_{tt}\rangle^{\text{in}}_{\text{ren}} = \frac{1+4n^2}{4\pi} \times \begin{cases} [\partial_v \theta(v)]^2 & \text{for } z<0, \\ [\partial_u \theta(u)]^2 & \text{for } z>0. \end{cases} \tag{3.2.24}$$

A few remarks are in order. First, contrary to the scalar field case [40, 45], which displays an infrared divergence, the energy pulse emitted by our wall is always finite for smooth wall creation and demolition. Second, we can see that $\langle T_{tt}\rangle^{\text{in}}_{\text{ren}}$ takes the same form for both wall appearance and disappearance, again in contrast to the scalar field [45]. Third, in the rapid process limit, we have $\partial_v\theta(v) \to \delta(v-t_0)$ and $\partial_u\theta(u) \to \delta(u-t_0)$ where $\delta(x)$ is the Dirac delta distribution. It follows that $\langle T_{tt}\rangle^{\text{in}}_{\text{ren}}$ is proportional to the square of the delta distribution on either side for both rapid wall creation and demolition. However, the square of the delta distribution is non-existent. Hence, $\langle T_{tt}\rangle^{\text{in}}_{\text{ren}}$ is ill-defined in the rapid process limit.

The total energy transmitted into the field during the creation or demolition process is given by

$$\langle E\rangle = \int_{-\infty}^{\infty} \langle T_{tt}\rangle^{\text{in}}_{\text{ren}}\, \mathrm{d}z\,, \tag{3.2.25}$$

where the integral may be evaluated on any constant t hypersurface in the region $t > t_0 + \delta$. Substituting (3.2.24) into (3.2.25) and using (3.1.11) – (3.1.12), we find that

$$\begin{aligned} \langle E\rangle &= \frac{1+4n^2}{4\pi}\left(\int_{t_0-t}^{t_0+\delta-t} [h_j'(t+z)]^2\,\mathrm{d}z - \int_{t-t_0}^{t-(t_0+\delta)} [h_j'(t-z)]^2\,\mathrm{d}z\right) \\ &= \frac{1+4n^2}{2\pi}\int_0^{\delta} [h_j'(t_0+x)]^2\,\mathrm{d}x\,, \end{aligned} \tag{3.2.26}$$

where $j = 1$ and $j = 2$ correspond to wall creation and demolition respectively. To obtain the second line of (3.2.25), we first change the integration variable $z \to -z$ in the second integral so that it becomes identical to the first integral. Then, after adding the two integrals, we perform another change of variable $z \to x = z - t_0 + t$.

To establish the lower bound of $\langle E \rangle$, start by noting that

$$\left| \int_0^\delta h_j'(t_0 + x)\, \mathrm{d}x \right|^2 = |h_j(t_0 + \delta) - h_j(t_0)|^2 = \frac{\pi^2}{4}, \tag{3.2.27}$$

where we have used (3.1.11) for a wall creation or (3.1.12) for a wall demolition. The Cauchy-Schwarz inequality then implies that[2]

$$\frac{\pi^2}{4} = \left| \int_0^\delta h_j'(t_0 + x) \cdot 1\, \mathrm{d}x \right|^2 \leq \int_0^\delta \left| h_j'(t_0 + x) \right|^2 \mathrm{d}x \cdot \int_0^\delta |1|^2\, \mathrm{d}x\,, \tag{3.2.28}$$

from which we obtain the lower bound of the integral in (3.2.26),

$$\int_0^\delta [h_j'(t_0 + x)]^2\, \mathrm{d}x \geq \frac{\pi^2}{4\delta}. \tag{3.2.29}$$

It follows then that $\langle E \rangle \geq K\delta^{-1}$ for some real δ-independent constant K. The total energy transmitted into field by the creation or demolition process hence diverges as $\delta \to 0$. The exact rate of divergence depends on how the limit $\delta \to 0$ is taken. In Appendix A.3, we illustrate a class of constructions where the equality in $\langle E \rangle \geq K\delta^{-1}$ holds for a wall creation.

3.3 Unruh-DeWitt Detector Response

Let us now turn our attention to the response of an Unruh-DeWitt particle detector. Specifically, we consider a detector which is at rest with respect to the

[2]Thanks to Sangchul Lee for responding to the question posted on Mathematics Stack Exchange (https://math.stackexchange.com/questions/2305650) and showing how the Cauchy-Schwarz inequality implies the lower bound (3.2.29).

wall. Supposing that the detector's position is $z = d > 0$, we parametrise its trajectory as

$$(t(\tau), z(\tau)) = (\tau + d, d). \tag{3.3.1}$$

This parametrisation is such that information about an event at the spatial origin $z = 0$ on $t = t_{\text{event}}$ hypersurface will be received by the detector when it crosses the event's future lightcone at $\tau = t_{\text{event}}$.

Recall that the two-point function $W^{(2,\bar{2})}(u, v; u', v')$ is defined by (2.2.4). When $|\Psi\rangle = |0_{\text{in}}\rangle$, by the properties (3.2.7) of the in-vacuum $|0_{\text{in}}\rangle$, $W^{(2,\bar{2})}$ is again given by the formula (2.2.6), which we reproduce here for convenience:

$$\begin{aligned} W^{(2,\bar{2})}(u, v; u', v') = \text{Tr}\big\{S^+(u, v; u', v')S^-(u', v'; u, v)\big\} \\ + \text{Tr}\big\{S^-(u, v; u, v)\big\}\,\text{Tr}\big\{S^-(u', v'; u', v')\big\}. \end{aligned} \tag{3.3.2}$$

The positive and negative frequency propagators in (3.3.2), of course, are given by (3.2.8) and (3.2.9) respectively, instead of (2.1.11) and (2.1.12). In Section 2.2.3, we have stated that the second term of (3.3.2), in the presence of a wall, contains a term that gives a finite contribution to the detector response. To demonstrate this point, we begin by considering in Section 3.3.1 the static MIT wall. As it turns out, the results from this time-independent analysis will also be useful later, when we analyse the general time-dependent wall.

3.3.1 Static MIT Wall

Comparing (3.1.4) and (3.1.9), we see that a static MIT wall can be represented by the set of parameters $\varphi(t) = 0$, $\varphi_2(t) = \pi$ and $\theta(t) = \pi/2$. The parameter $\varphi_1(t)$ may be left arbitrary. Substituting this choice into (3.2.12) – (3.2.13), we

obtain that for $z, z' > 0$,

$$\begin{aligned} &S^{+}_{ab}(u,v;u',v') \\ &\quad = -\frac{i}{2\pi}\frac{1}{u-u'-i\epsilon}U_{+,a}U^{\dagger}_{+,c}\gamma^{0}_{cb} - \frac{1}{2\pi}\frac{1}{u-v'-i\epsilon}U_{+,a}U^{\dagger}_{-,c}\gamma^{0}_{cb} \\ &\qquad + \frac{1}{2\pi}\frac{1}{v-u'-i\epsilon}U_{-,a}U^{\dagger}_{+,c}\gamma^{0}_{cb} - \frac{i}{2\pi}\frac{1}{v-v'-i\epsilon}U_{-,a}U^{\dagger}_{-,c}\gamma^{0}_{cb}, \end{aligned} \tag{3.3.3}$$

$$\begin{aligned} &S^{-}_{ab}(u,v;u',v') \\ &\quad = \frac{i}{2\pi}\frac{1}{u-u'+i\epsilon}U_{+,a}U^{\dagger}_{+,c}\gamma^{0}_{cb} + \frac{1}{2\pi}\frac{1}{u-v'+i\epsilon}U_{+,a}U^{\dagger}_{-,c}\gamma^{0}_{cb} \\ &\qquad - \frac{1}{2\pi}\frac{1}{v-u'+i\epsilon}U_{-,a}U^{\dagger}_{+,c}\gamma^{0}_{cb} + \frac{i}{2\pi}\frac{1}{v-v'+i\epsilon}U_{-,a}U^{\dagger}_{-,c}\gamma^{0}_{cb}. \end{aligned} \tag{3.3.4}$$

Implementing the procedure that leads to (2.2.9), but now using (3.3.3) and (3.3.4), gives us

$$\begin{aligned} &W^{(2,\bar{2})}_{\epsilon,\mathrm{MIT}}(u,v;u',v') \\ &\quad = -\frac{1}{2\pi^2}\Bigg[\frac{1}{(u-u'-i\epsilon)(v-v'-i\epsilon)} - \frac{1}{(u-v'-i\epsilon)(v-u'-i\epsilon)} \\ &\qquad - 2\frac{u-v}{((u-v)^2+\epsilon^2)}\frac{u'-v'}{((u'-v')^2+\epsilon^2)}\Bigg], \end{aligned} \tag{3.3.5}$$

where the subscript "MIT" indicates that (3.3.5) is associated to the static MIT wall. The first two terms in (3.3.5) come from the first term in (3.3.2) after we set both epsilons in the product to be equal to each other. Note that the first term of (3.3.5) is none other than the no-wall two point function (2.2.9). The last term in (3.3.5) comes from the second term in (3.3.2) as follows. Unlike in the no-wall case, we see from (3.3.4) that not every term is ill-defined at the coincidence limit. After dropping those ill-defined terms by operation ordering, each factor in the second term of (3.3.2) becomes a well-defined distribution. Since each factor is defined on a different $\mathbb{R}^2$, the product is also a well-defined distribution regardless of whether the two ϵ parameters associated with each factor are distinct or otherwise. Choosing to work with a single ϵ then gives the last term in (3.3.5).

In Appendix A.4, we show that the response of a detector at $z = d$ in the presence of a static MIT wall at the origin is given by

$$F_{\text{MIT}}(\omega) = F_{\text{NW}}(\omega) + F^{(1)}_{\text{MIT}}(\omega) + F^{(2)}_{\text{MIT}}(\omega), \tag{3.3.6}$$

where

$$\begin{aligned} F_{\text{NW}}(\omega) = &-\frac{\omega}{2\pi}\int_{-\infty}^{\infty} \mathrm{d}r\,[\chi(r)]^2 + \frac{1}{\pi^2}\int_0^{\infty}\frac{\mathrm{d}s}{s^2}\int_{-\infty}^{\infty}\mathrm{d}r\,\chi(r)[\chi(r)-\chi(r-s)] \\ &+ \frac{1}{\pi^2}\int_{-\infty}^{\infty}\mathrm{d}r\,\chi(r)\int_0^{\infty}\mathrm{d}s\,\chi(r-s)\left(\frac{1}{s^2}-\frac{\cos(\omega s)}{s^2}\right), \end{aligned} \tag{3.3.7}$$

$$\begin{aligned} F^{(1)}_{\text{MIT}}(\omega) = &\frac{1}{4\pi^2 d}\text{Re}\Bigg\{e^{-2i\omega d}\Bigg[i\pi G(2d) \\ &+ \int_0^{\infty}\mathrm{d}r\,\frac{G(2d+r)e^{-i\omega r} - G(2d-r)e^{i\omega r}}{r}\Bigg]\Bigg\}, \end{aligned} \tag{3.3.8}$$

$$F^{(2)}_{\text{MIT}}(\omega) = \frac{1}{2\pi^2 d^2}\int_{-\infty}^{\infty}\mathrm{d}u\,\chi(u)\int_0^{\infty}\mathrm{d}s\,\chi(u-s)\cos(\omega s), \tag{3.3.9}$$

$$G(y) := \int_{-\infty}^{\infty}\mathrm{d}u\,\chi(u)\chi(u-y). \tag{3.3.10}$$

The first term in (3.3.6) corresponds to the first term in (3.3.5), which, as noted above, is none other than the no-wall two point function (2.2.9). It is no surprise then that (3.3.7) is none other than (2.2.10) with $(\Delta x)^2 = s^2$. The second and third terms in (3.3.6) correspond respectively to the second and third terms in (3.3.5). Thus, for a detector interacting with the field via the normally-ordered Hamiltonian (2.2.13), the last term in (3.3.6) does not contribute.

We also show in Appendix A.4 that, in the large energy gap limit $|\omega| \to \infty$,

$$\begin{aligned} F_{\text{MIT}}(\omega) = &-\frac{\omega\Theta(-\omega)}{\pi}\int_{-\infty}^{\infty}\mathrm{d}u\,[\chi(u)]^2 + \frac{\Theta(-\omega)}{2\pi d}\sin(2\omega d)G(2d) \\ &+ O^{\infty}\big(|\omega|^{-1}\big), \end{aligned} \tag{3.3.11}$$

which applies to both types of interaction (2.2.1) and (2.2.13). The non-vanishing first and second terms in (3.3.11) originate from $F_{\text{NW}}(\omega)$ and $F^{(1)}_{\text{MIT}}(\omega)$ respectively.

For a detector interacting with the field via the non-normally-ordered Hamiltonian (2.2.1), the vanishing term $O^{\infty}(|\omega|^{-1})$ includes $F^{(2)}_{\rm MIT}(\omega)$.

3.3.2 General Evolving Wall

Now, let us consider a general evolving wall. We show in Appendix A.5 that the detector response can be written, roughly speaking, as a sum of the response to a static MIT wall but with the switching function of each term modified by the wall parameters. After some rearrangement, we show in Appendix A.5 that the regulator-free expression can be written as

$$F_{\rm GEW}(\omega) = F^{(0)}_{\rm GEW}(\omega) + F^{(1)}_{\rm GEW}(\omega) + F^{(2)}_{\rm GEW}(\omega) \tag{3.3.12}$$

where the subscript "GEW" indicates a general evolving wall,

$$F^{(0)}_{\rm GEW}(\omega) = -\frac{\omega\Theta(-\omega)}{\pi}\int_{-\infty}^{\infty} {\rm d}u\,[\chi(u)]^2 + \Delta F^{(0)}_{\rm GEW}(\omega), \tag{3.3.13}$$

$$F^{(1)}_{\rm GEW}(\omega) = \frac{\Theta(-\omega)}{2\pi d}\sin(2\omega d)[G_3(2d) - G_4(2d)] + \Delta F^{(1)}_{\rm GEW}(\omega), \tag{3.3.14}$$

$$F^{(2)}_{\rm GEW}(\omega) = \frac{1}{2\pi^2 d^2}\int_0^{\infty} {\rm d}s\cos(\omega s)G_3(s), \tag{3.3.15}$$

$$\Delta F^{(0)}_{\rm GEW}(\omega) = \frac{1}{\pi^2}\sum_{j=1}^{4}\int_0^{\infty}{\rm d}s\,\frac{\cos\omega s}{s^2}\int_{-\infty}^{\infty}{\rm d}u\,\chi_j(u)[\chi_j(u) - \chi_j(u-s)], \tag{3.3.16}$$

$$\begin{aligned}\Delta F^{(1)}_{\rm GEW}(\omega) = \frac{1}{4\pi^2 d}\Bigg[&\cos(2\omega d)\int_0^{\infty}{\rm d}r\cos\omega r\frac{G_3(2d+r) - G_3(2d-r)}{r}\\ &- \cos(2\omega d)\int_0^{\infty}{\rm d}r\cos\omega r\frac{G_4(2d+r) - G_4(2d-r)}{r}\\ &- \sin(2\omega d)\int_0^{\infty}{\rm d}r\sin\omega r\frac{G_3(2d+r) + G_3(2d-r) - 2G_3(2d)}{r}\\ &+ \sin(2\omega d)\int_0^{\infty}{\rm d}r\sin\omega r\frac{G_4(2d+r) + G_4(2d-r) - 2G_4(2d)}{r}\Bigg],\end{aligned} \tag{3.3.17}$$

$$G_j(y) = \int_{-\infty}^{\infty}{\rm d}u\,\chi_j(u)\chi_j(u-y), \tag{3.3.18}$$

and the modified switching functions χ_j, for $j = 1, 2, 3, 4$, are given by

$$\chi_1(\tau) = \cos(\varphi(\tau) + \varphi_1(\tau)) \cos\theta(\tau)\chi(\tau), \tag{3.3.19}$$

$$\chi_2(\tau) = \sin(\varphi(\tau) + \varphi_1(\tau)) \cos\theta(\tau)\chi(\tau), \tag{3.3.20}$$

$$\chi_3(\tau) = \cos(\varphi(\tau) + \varphi_2(\tau)) \sin\theta(\tau)\chi(\tau), \tag{3.3.21}$$

$$\chi_4(\tau) = \sin(\varphi(\tau) + \varphi_2(\tau)) \sin\theta(\tau)\chi(\tau). \tag{3.3.22}$$

The last term in (3.3.12), that is $F^{(2)}_{\text{GEW}}(\omega)$, is the additional term that arises due to the use of a non-normally-ordered Hamiltonian (2.2.1).

The large energy gap limit of $F_{\text{GEW}}(\omega)$ is given by

$$\begin{aligned} F_{\text{GEW}}(\omega) = &-\frac{\omega\Theta(-\omega)}{\pi}\int_{-\infty}^{\infty} \mathrm{d}u\,[\chi(u)]^2 + \frac{\Theta(-\omega)}{2\pi d}\sin(2\omega d)\int_{-\infty}^{\infty}\mathrm{d}u\,\chi_3(u)\chi_3(u-2d) \\ &- \frac{\Theta(-\omega)}{2\pi d}\sin(2\omega d)\int_{-\infty}^{\infty}\mathrm{d}u\,\chi_4(u)\chi_4(u-2d) + O^{\infty}\big(|\omega|^{-1}\big). \end{aligned} \tag{3.3.23}$$

The asymptotic result (3.3.23) above is immediate once one notices that all four modified switching functions (3.3.19) – (3.3.22) are smooth functions with compact support and the large energy gap limit calculations in Appendix A.4 for a static MIT wall depend precisely on the fact that χ is a smooth function with compact support. As with (3.3.11), note that (3.3.23) is valid for both interaction Hamiltonians (2.2.1) and (2.2.13).

3.3.3 Wall Appearance

To obtain a clearer understanding on how the detector responds when the wall suddenly changes, we now turn our attention to the scenario of wall appearance described in Section 3.1.2. In this situation, the modified switching functions

(3.3.19) - (3.3.22) read

$$\chi_1(\tau) = \cos(2n\theta(\tau))\cos\theta(\tau)\chi(\tau), \tag{3.3.24}$$

$$\chi_2(\tau) = \sin(2n\theta(\tau))\cos\theta(\tau)\chi(\tau), \tag{3.3.25}$$

$$\chi_3(\tau) = (-1)^{n+1}\cos(2n\theta(\tau))\sin\theta(\tau)\chi(\tau), \tag{3.3.26}$$

$$\chi_4(\tau) = \sin(2n\theta(\tau))\sin\theta(\tau)\chi(\tau). \tag{3.3.27}$$

Upon substitution of the condition (3.1.11), we obtain

$$\chi_1(\tau) = \begin{cases} \chi(\tau) & \text{for } \tau \leq t_0, \\ \cos(2nh_1(\tau))\cos h_1(\tau)\chi(\tau) & \text{for } t_0 < \tau < t_0 + \delta, \\ 0 & \text{for } \tau \geq t_0 + \delta, \end{cases} \tag{3.3.28}$$

$$\chi_2(\tau) = \begin{cases} 0 & \text{for } \tau \leq t_0, \\ \sin(2nh_1(\tau))\cos h_1(\tau)\chi(\tau) & \text{for } t_0 < \tau < t_0 + \delta, \\ 0 & \text{for } \tau \geq t_0 + \delta, \end{cases} \tag{3.3.29}$$

$$\chi_3(\tau) = \begin{cases} 0 & \text{for } \tau \leq t_0, \\ (-1)^{n+1}\cos(2nh_1(\tau))\sin h_1(\tau)\chi(\tau) & \text{for } t_0 < \tau < t_0 + \delta, \\ -\chi(\tau) & \text{for } \tau \geq t_0 + \delta, \end{cases} \tag{3.3.30}$$

$$\chi_4(\tau) = \begin{cases} 0 & \text{for } \tau \leq t_0, \\ \sin(2nh_1(\tau))\sin h_1(\tau)\chi(\tau) & \text{for } t_0 < \tau < t_0 + \delta, \\ 0 & \text{for } \tau \geq t_0 + \delta. \end{cases} \tag{3.3.31}$$

Due to the factor $\sin(2n\theta(\tau))$, χ_2 and χ_4 effectively switch on only during the interval $t_0 < \tau < t_0 + \delta$ and thus only give rise to some sort of transient effect. The factors $\cos\theta(\tau)$ and $\sin\theta(\tau)$ effectively determine when the modified switching functions χ_1 and χ_3 switch off and on respectively. The value of n,

roughly speaking, determines how often χ_j switches on and off *within the interval* $t_0 < \tau < t_0 + \delta$ before settling down.

The response of the detector to wall appearance can obtained straightforwardly by substituting $\varphi(t) = 2n\theta(t)$, $\varphi_1(t) = 0$ and $\varphi_2(t) = (n+1)\pi$ into (3.3.12) - (3.3.23). Notation-wise, we replace the subscript "GEW" with "WC" in this setting to indicate wall creation. From (3.3.28) - (3.3.31), we see that if the detector operates only within the future lightcone of the fully developed wall (so that $\chi(\tau) = 0$ for $\tau \leq t_0 + \delta$), we have $\chi_1(\tau) = \chi_2(\tau) = \chi_4(\tau) = 0$ and may replace all $\chi_3(\tau)$ in $F_{\rm WC}(\omega)$ with $\chi(\tau)$. It follows that the response in this situation is identical to that in Section 3.3.1 where we have a static MIT wall.

Now, let us return to the general situation where the detector may start to operate at arbitrarily early time. When δ is finite, we show in Appendix A.6.1 that in the large $|\omega|$ limit, the response function is given by

$$F_{\rm WC}(\omega) = -\frac{\omega\Theta(-\omega)}{\pi}\int_{-\infty}^{\infty} \mathrm{d}u\,[\chi(u)]^2 + \frac{\Theta(-\omega)}{2\pi d}\sin(2\omega d)\int_{t_0+2d}^{\infty} \mathrm{d}u\,\chi(u)\chi(u-2d) + \frac{\Theta(-\omega)}{2\pi d}\sin(2\omega d)\Delta F_{\rm WC}(\omega) + O^{\infty}\big(|\omega|^{-1}\big). \tag{3.3.32}$$

The first term is simply the response in absence of a wall while the second term is the response due to the *existence* of the wall. The contribution from the wall appearance *process* itself is given by the third term which is only $O(\delta)$ — see Appendix A.6.1 for an explicit expression of $\Delta F_{\rm WC}(\omega)$. Note that, since (3.3.32) follows directly from (3.3.23), it is valid for both types of interaction Hamiltonians (2.2.1) and (2.2.13).

In order to compare the response of our detector to that in [40], we shall consider the rapid wall creation limit. If we first take the limit of large $|\omega|$, we need to consider two distinct cases separately. If $\omega < 0$, then it does not make sense to take the limit $\delta \to 0$ because the limit of large $|\omega|$ does not yield a finite result to begin with. If, on the other hand, $\omega > 0$, then $F_{\rm WC}(\omega)$ vanishes already in the limit of large $|\omega|$, implying that the detector does not give any

response to a rapid wall creation. While this may seem contradictory to the energy (density) analysis results in Section 3.2.4 at first, one should remember that we have ignored any dependence on δ in the $O^{\infty}(|\omega|^{-1})$ term since we are taking the large $|\omega|$ limit first. As δ becomes comparable to $|\omega|^{-1}$, the expression (3.3.32) may no longer be valid. This brings us to our next result.

In [40], the authors keep the energy gap ω finite and take the rapid process limit $\delta \to 0$ first. So, it is only fair that we consider a similar analysis for comparison. We will see that the result is different from that obtained above, as anticipated. This shows that the two limits do not commute. As argued in Appendix A.6.2, for finite ω, the limit $\delta \to 0$ gives

$$\begin{aligned} F_{\text{WC}}(\omega) = &-\frac{[\chi(t_0)]^2}{\pi^2}\ln(|\omega|\delta) + F_{\text{NW}}(\omega) + F^{(0)}_{\text{RWC}}(\omega) \\ &+ F^{(1)}_{\text{RWC}}(\omega) + F^{(2)}_{\text{RWC}}(\omega) + O(\delta) \end{aligned} \tag{3.3.33}$$

where

$$\begin{aligned} F^{(0)}_{\text{RWC}}(\omega) = &-\frac{[\chi(t_0)]^2}{\pi^2}\gamma + \frac{1}{\pi^2}\int_0^\infty \mathrm{d}s\cos(\omega s)\frac{f(s) - sf'(0)}{s^2} \\ &- \frac{1}{\pi^2}\int_0^\infty \mathrm{d}s\,\frac{f(s) - sf'(s)}{s^2}\ln s - \frac{\chi(t_0)}{\pi^2}\int_{t_0}^\infty \mathrm{d}u\,\chi'(u)\ln(u - t_0) \\ &- \frac{1}{\pi^2}\int_{t_0}^\infty \mathrm{d}u\,\chi(u)\int_{u-t_0}^\infty \mathrm{d}s\,\frac{\chi'(u-s)}{s}, \end{aligned} \tag{3.3.34}$$

$$\begin{aligned} F^{(1)}_{\text{RWC}}(\omega) = &\frac{\Theta(-\omega)}{2\pi d}\sin(2\omega d)H_1(2d) \\ &+ \frac{1}{4\pi^2 d}\cos(2\omega d)\int_0^\infty \mathrm{d}r\cos\omega r\frac{H_1(2d+r) - H_1(2d-r)}{r} \\ &- \frac{1}{4\pi^2 d}\sin(2\omega d)\int_0^\infty \mathrm{d}r\sin\omega r\frac{H_1(2d+r) + H_1(2d-r) - 2H_1(2d)}{r} \\ &+ \frac{1}{4\pi^2 d}\cos(2\omega d)\int_{2d}^\infty \mathrm{d}r\,\frac{\cos\omega r}{r}f(r-2d) \\ &+ \frac{1}{4\pi^2 d}\sin(2\omega d)\int_{2d}^\infty \mathrm{d}r\,\frac{\sin\omega r}{r}f(r-2d), \end{aligned} \tag{3.3.35}$$

$$F^{(2)}_{\text{RWC}}(\omega) = \frac{1}{2\pi^2 d^2}\int_0^\infty \mathrm{d}s\cos(\omega s)H_1(s), \tag{3.3.36}$$

γ is the Euler-Mascheroni constant and

$$f(s) = \int_{t_0-\frac{s}{2}}^{t_0+\frac{s}{2}} \mathrm{d}v\, \chi(v+\frac{s}{2})\chi(v-\frac{s}{2}) \tag{3.3.37}$$

$$H_1(y) = \int_{t_0+y}^{\infty} \mathrm{d}u\, \chi(u)\chi(u-y). \tag{3.3.38}$$

The second last term in (3.3.33), that is $F^{(2)}_{\mathrm{RWC}}(\omega)$, does not contribute if the detector interacts with the field via the normally-ordered Hamiltonian (2.2.13).

Two observations can be made. First, for any finite energy gap $|\omega|$, the response diverges logarithmically in the duration of wall evolution δ as $\delta \to 0$ unless the detector does not operate at the moment it crosses the lightcone of the wall creation event. A similar behaviour is shown by the detector considered in [40].[3] Recalling that the total energy transmitted into the field is $\langle E\rangle \geq K\delta^{-1}$, we observed once again that a local matter system being less sensitive to a divergence in energy (density) [40, 43, 44]. Second, all dependence on n is hidden in $O(\delta)$. Given that n only gives rise to transient effect while the wall is being created, this is not very surprising. Nevertheless, this is not entirely consistent with the result in Section 3.2.4 where n plays a role in determining how fast $\langle E\rangle$ diverges as $\delta \to 0$.

Due to divergence of the term $\ln\delta$ as $\delta \to 0$, the large $|\omega|$ limit of rapid wall creation is not well-defined for any sign of ω. Nevertheless, we can still look at the large $|\omega|$ limit of terms that remain finite as $\delta \to 0$. Ignoring any dependence

[3] To make the comparison, it is important to note that we did not introduce any cutoff in this paper. The detector response in [40] diverges logarithmically as we take the infrared cutoff $\mu \to 0$ unless the detector does not operate at the moment of crossing.

on ω in $O(\delta)$, repeated integration by parts gives

$$\begin{aligned} F^{(0)}_{\text{RWC}}(\omega) = &-\frac{[\chi(t_0)]^2}{\pi^2}\gamma - \frac{1}{\pi^2}\int_0^\infty \mathrm{d}s\, \frac{f(s) - sf'(s)}{s^2}\ln s \\ &- \frac{\chi(t_0)}{\pi^2}\int_{t_0}^\infty \mathrm{d}u\, \chi'(u)\ln(u-t_0) \\ &- \frac{1}{\pi^2}\int_{t_0}^\infty \mathrm{d}u\, \chi(u)\int_{u-t_0}^\infty \mathrm{d}s\, \frac{\chi'(u-s)}{s} + O\big(|\omega|^{-2}\big), \end{aligned} \tag{3.3.39}$$

$$F^{(1)}_{\text{RWC}}(\omega) = \frac{\Theta(-\omega)}{2\pi d}\sin(2\omega d)H_1(2d) + O\big(|\omega|^{-2}\big), \tag{3.3.40}$$

$$F^{(2)}_{\text{RWC}}(\omega) = O\big(|\omega|^{-2}\big) \tag{3.3.41}$$

as $|\omega| \to \infty$. The non-vanishing terms in $F_{\text{NW}}(\omega)$ and $F^{(1)}_{\text{RWC}}(\omega)$ are expected from (3.3.11). Unlike in [40], the remaining terms do not come strictly from the moment of crossing the lightcone of the wall creation event. Some of them arise from the fact that the wall was created at some *finite* point in the past. Although this phenomenon of remnant response seems to mimic one that arises in [61], the result here should not be taken seriously since we have ignored the divergence associated with $\ln\delta$. In any case, we see that the two limits $\delta \to 0$ and $|\omega| \to \infty$ do not commute.

Perhaps, a more appropriate way would be to take the limit $\delta \to 0$ and $|\omega| \to \infty$ simultaneously. This can be done if we first let $\delta = a/|\omega|$, where a is an arbitrary constant, and then take the limit $|\omega| \to \infty$. In this way, $O(\delta)$ turns into $O(|\omega|^{-1})$ and (3.3.39) - (3.3.41) are still valid. However, we now have a term proportional to $\ln a$ which is arbitrary.

3.3.4 Wall Disappearance

Similar analysis as Section 3.3.3 and Appendix A.6 can also be done for wall disappearance. Since most properties of the result are similar to previous case, we only note here the differences.

First, the large $|\omega|$ limit of the response function when the disappearance process takes place over a finite interval is now

$$F_{\rm WD}(\omega) = -\frac{\omega\Theta(-\omega)}{\pi}\int_{-\infty}^{\infty} \mathrm{d}u\,[\chi(u)]^2 + \frac{\Theta(-\omega)}{2\pi d}\sin(2\omega d)\int_{-\infty}^{t_0}\mathrm{d}u\,\chi(u)\chi(u-2d) + \frac{\Theta(-\omega)}{2\pi d}\sin(2\omega d)\Delta F_{\rm WD}(\omega) + O^{\infty}\big(|\omega|^{-1}\big) \tag{3.3.42}$$

where the subscript "WD" stands for "wall demolition". When $2d < \delta$,

$$\begin{aligned}\Delta F_{\rm WD}(\omega) = (-1)^n &\int_{t_0}^{t_0+2d}\mathrm{d}u\cos(2nh_2(u))\sin h_2(u)\chi(u)\chi(u-2d)\\ &+\int_{t_0+2d}^{t_0+\delta}\mathrm{d}u\cos(2nh_2(u))\sin h_2(u)\chi(u)\\ &\qquad\times\cos(2nh_2(u-2d))\sin h_2(u-2d)\chi(u-2d)\\ &-\int_{t_0+2d}^{t_0+\delta}\mathrm{d}u\sin(2nh_2(u))\sin h_2(u)\chi(u)\\ &\qquad\times\sin(2nh_2(u-2d))\sin h_2(u-2d)\chi(u-2d),\end{aligned} \tag{3.3.43}$$

whereas when $2d \geq \delta$,

$$\Delta F_{\rm WD}(\omega) = (-1)^n\int_{t_0}^{t_0+\delta}\mathrm{d}u\cos(2nh_2(u))\sin h_2(u)\chi(u)\chi(u-2d). \tag{3.3.44}$$

Similar to the wall creation case, the last term in (3.3.43) vanishes when $n = 0$. Compared to (3.3.32), there are only two differences. One, the second term now integrates from $-\infty$ to t_0 to account for the fact that the wall is pre-existing. Two, $\Delta F_{\rm WD}(\omega)$ is slightly different from $\Delta F_{\rm WC}(\omega)$. Nevertheless, the response function displays the same discrepancy as for wall creation when compared to the energy density (3.2.24).

Second, for finite ω, the rapid wall disappearance limit only replaces H_1 in wall creation case (3.3.38) with

$$H_2(y) := \int_{-\infty}^{t_0}\mathrm{d}u\,\chi(u)\chi(u-y). \tag{3.3.45}$$

Chapter 4

Fermions From A Moving Wall

In this chapter, we turn our attention to an MIT wall that moves along a non-stationary timelike trajectory. We begin in Section 4.1 with a discussion of the boundary condition. After solving the equation of motion and quantising the field, we calculate its renormalised stress-energy tensor. We consider the response of an Unruh-DeWitt detector in Section 4.2. Keeping the detector and wall trajectories arbitrary, we discuss some general features of the detector response. Specialising to a static detector, we then calculate the transition rate for a wall moving on an arbitrary trajectory. Finally, we consider a wall that moves along a trajectory that models a collapsing star and discuss the significance of the late time transition rate.

4.1 Quantum Spinor Field with A Moving Wall

4.1.1 The Moving MIT Wall

Consider an MIT wall that follows a prescribed timelike trajectory defined by $W(u,v) = 0$ where $W(u,v) := v - w(u)$ for some smooth function $w(u)$. We denote the position z of the wall at any given time t with $z_{\mathrm{w}}(t)$. In order to ensure that the early time state is well-defined, we restrict ourselves to wall trajectories which are asymptotically inertial in the far past. At late times, the condition

need not hold. We allow for wall trajectories which are asymptotically null in the far future.

We consider a two-component spinor field ψ that lives in the spacetime portion to the right of the wall, that is the region given by $v \geq w(u)$. The Dirac inner product (ψ_1, ψ_2) between any two solutions ψ_1 and ψ_2 of Dirac equation (2.1.1) in this portion of spacetime reads

$$(\psi_1, \psi_2) = \int_{z_{\rm w}(t)}^{\infty} [\psi_1(t,z)]^\dagger \psi_2(t,z)\, \mathrm{d}z\,. \tag{4.1.1}$$

The boundary condition on the surface of the wall is given by (3.1.5). Due to the way we parametrise $W(u,v)$, the inward-directed unit normal n_μ in the moving wall case here is given by

$$n_\mu = \frac{\partial_\mu W}{\sqrt{|\eta^{\alpha\beta}\partial_\alpha W \partial_\beta W|}} = \frac{1}{2\sqrt{w'(u)}}(1 - w'(u), 1 + w'(u)). \tag{4.1.2}$$

The direction of n_μ as given in (4.1.2) may be verified by considering, for instance, a wall which is static at the origin in the far past. During the early time of such a scenario, $w(u) = u$, so we have $n_\mu = (0,1)$, in agreement with n_μ used in Section 3.1.2 for a static MIT wall that confines the field to the spacetime region $z > 0$. Should we parametrise $W(u,v)$ as $w(u) - v$, then n_μ as defined by the first equality in (4.1.2) would be leftward, hence outward, directed.

Substituting (4.1.2) into the boundary condition (3.1.5) and using the fact that a massless field propagates on null geodesics, we have

$$\psi_+(u) = -i\sqrt{w'(u)}\psi_-(w(u)) \tag{4.1.3}$$

everywhere to the right of the wall. Note that the reflected field is not only sensitive to the existence of the wall but also to the instantaneous motion of the wall through $w'(u)$. In particular, $w'(u)$ directly influences the reflected field's amplitude. This phenomenon, which is not observed in the scalar field case, plays

an important role in ensuring, for instance, the convergence of the renormalised stress-energy tensor below.

4.1.2 Mode Solutions, Quantisation and Propagators

For a wall that moves inertially in the far past, we only need to consider an in-mode ansatz ψ_k^{in} whose left moving part is proportional to $e^{-ikv}U_-$. The boundary condition on the wall's surface then implies that

$$\psi_k^{\text{in}}(u,v) = -i\sqrt{\frac{w'(u)}{2\pi}}e^{-ikw(u)}U_+ + \frac{1}{\sqrt{2\pi}}e^{-ikv}U_-, \tag{4.1.4}$$

where a normalisation choice has been made so that the mode function is normalised in the Dirac inner product such that $(\psi_k^{\text{in}}, \psi_{k'}^{\text{in}}) = \delta(k-k')$ for any $k, k' \in \mathbb{R}\setminus\{0\}$.

A general solution to the Dirac equation in the moving wall spacetime can then be expanded as

$$\psi(u,v) = \int_0^\infty \mathrm{d}k \left(a_k^{\text{in}}\psi_k^{\text{in}}(u,v) + b_k^{\text{in}\dagger}\psi_{-k}^{\text{in}}(u,v)\right), \tag{4.1.5}$$

where $a_k^{\text{in}}, b_k^{\text{in}}$ and $a_k^{\text{in}\dagger}, b_k^{\text{in}\dagger}$ are the set of annihilation and creation operators respectively with non-vanishing anticommutators $\{a_k^{\text{in}}, a_{k'}^{\text{in}\dagger}\} = \{b_k^{\text{in}}, b_{k'}^{\text{in}\dagger}\} = \delta(k-k')$ for $k, k' > 0$. As in Chapter 3, these operators define a normalised in-vacuum state $|0_{\text{in}}\rangle$ satisfying $\langle 0_{\text{in}}|0_{\text{in}}\rangle = 1$ and

$$a_k^{\text{in}}|0_{\text{in}}\rangle = b_k^{\text{in}}|0_{\text{in}}\rangle = 0 \qquad \text{for } k > 0. \tag{4.1.6}$$

The positive and negative frequency propagators are defined similarly to (3.2.8) and (3.2.9) respectively, that is

$$S^{+}_{ab}(u,v;u',v') := \langle 0_{\rm in}| \, \psi_a(u,v)\overline{\psi}_b(u',v') \, |0_{\rm in}\rangle \, , \tag{4.1.7}$$

$$S^{-}_{ab}(u,v;u',v') := \langle 0_{\rm in}| \, \overline{\psi}_b(u',v')\psi_a(u,v) \, |0_{\rm in}\rangle \, . \tag{4.1.8}$$

The in-vacuum state in (4.1.7) and (4.1.8) now refers to that defined in (4.1.6) instead of (3.2.7). Using (4.1.4) – (4.1.6) followed by the prescription (2.1.15), we obtain that the positive and negative frequency propagators are given by

$$\begin{aligned} &S^{+}_{ab}(u,v;u',v') \\ &\quad = -\frac{i}{2\pi}\frac{\sqrt{w'(u)w'(u')}}{w(u)-w(u')-i\epsilon}U_{+,a}U^{\dagger}_{+,c}\beta_{cb} - \frac{1}{2\pi}\frac{\sqrt{w'(u)}}{w(u)-v'-i\epsilon}U_{+,a}U^{\dagger}_{-,c}\beta_{cb} \\ &\qquad + \frac{1}{2\pi}\frac{\sqrt{w'(u')}}{v-w(u')-i\epsilon}U_{-,a}U^{\dagger}_{+,c}\beta_{cb} - \frac{i}{2\pi}\frac{1}{v-v'-i\epsilon}U_{-,a}U^{\dagger}_{-,c}\beta_{cb}, \end{aligned} \tag{4.1.9}$$

$$\begin{aligned} &S^{-}_{ab}(u,v;u',v') \\ &\quad = \frac{i}{2\pi}\frac{\sqrt{w'(u)w'(u')}}{w(u)-w(u')+i\epsilon}U_{+,a}U^{\dagger}_{+,c}\beta_{cb} + \frac{1}{2\pi}\frac{\sqrt{w'(u)}}{w(u)-v'+i\epsilon}U_{+,a}U^{\dagger}_{-,c}\beta_{cb} \\ &\qquad - \frac{1}{2\pi}\frac{\sqrt{w'(u')}}{v-w(u')+i\epsilon}U_{-,a}U^{\dagger}_{+,c}\beta_{cb} + \frac{i}{2\pi}\frac{1}{v-v'+i\epsilon}U_{-,a}U^{\dagger}_{-,c}\beta_{cb} \end{aligned} \tag{4.1.10}$$

respectively, where the limit $\epsilon \to 0_+$ is, as usual, implied.

4.1.3 Stress-Energy Tensor

Let us now consider the renormalised in-vacuum expectation value of the stress-energy tensor of the field $\langle T_{\mu\nu}\rangle^{\rm in}_{\rm ren} \equiv \langle 0_{\rm in}| \, T_{\mu\nu} \, |0_{\rm in}\rangle - \langle T_{\mu\nu}\rangle_{\rm M}$. Similar to Section 3.2.3, we find a set of expressions analogous to (2.1.22) – (2.1.24) for the components of $\langle 0_{\rm in}| \, T_{\mu\nu} \, |0_{\rm in}\rangle$ after a similar formal manipulation. The only difference is that it is now the moving wall negative frequency propagator that appears in the corresponding expressions of $F(u,v;u',v')$ and $G(u,v;u',v')$.

Using (4.1.10), upon point-splitting and subtraction of the Minkowski vacuum contribution, we obtain

$$\langle T_{tt}\rangle^{\rm in}_{\rm ren} = \langle T_{zz}\rangle^{\rm in}_{\rm ren} = -\langle T_{tz}\rangle^{\rm in}_{\rm ren} = -\langle T_{zt}\rangle^{\rm in}_{\rm ren} = -\frac{1}{24\pi}(Sw)(u), \tag{4.1.11}$$

where

$$(Sw)(u) = \frac{w'''(u)}{w'(u)} - \frac{3}{2}\left(\frac{w''(u)}{w'(u)}\right)^2 \tag{4.1.12}$$

is the Schwarzian derivative of $w(u)$ with respect to u. Upon comparison, we find that every component of the renormalised stress-energy tensor expectation value above is identical to that of a massless scalar field at all times [1, 28, 48]. Hence, an observer examining only the stress-energy tensor will not be able to discern that the radiation is made up of fermions.

Two technical remarks are in order. First, as mentioned in Section 2.1.3, when calculating $\langle T_{\mu\nu}\rangle^{\rm in}_{\rm ren}$ via the point-splitting method, the parameter ϵ should be set to zero before taking the coincidence limit. In the moving wall case here, should we do otherwise, $\langle T_{\mu\nu}\rangle^{\rm in}_{\rm ren}$ will be proportional to $(1-w'(u)^2)\epsilon^{-2}$, which is divergent. Second, the appearance of a third derivative in (4.1.11) can be seen as follows. For concreteness, let us take $\langle T_{tt}\rangle^{\rm in}_{\rm ren}$ as an example. Similar remarks apply to other components of the stress-energy tensor. Also, since all divergent terms eventually cancel out during the calculation, we focus only on how the non-vanishing finite part of $\langle T_{tt}\rangle^{\rm in}_{\rm ren}$ emerges. From the analogue of (2.1.22) for a moving wall, which is

$$\langle 0_{\rm in}|\, T_{tt}\, |0_{\rm in}\rangle = \lim_{u',v'\to u,v} \frac{i}{2}\Big[\partial_u F(u,v;u',v') + \partial_v F(u,v;u',v')\Big], \tag{4.1.13}$$

where

$$F(u,v;u',v') = {\rm Tr}\big\{S^-(u,v;u',v')\gamma^0\big\} - {\rm Tr}\big\{S^-(u',v';u,v)\gamma^0\big\}, \tag{4.1.14}$$

with S^- referring to (4.1.10), we know that $\langle 0_{\text{in}}| T_{tt} |0_{\text{in}}\rangle$ is proportional to the first derivatives of $F(u,v;u',v')$. All non-vanishing finite contributions to $\langle T_{tt}\rangle^{\text{in}}_{\text{ren}}$ comes from the u-derivative part of $\langle 0_{\text{in}}| T_{tt} |0_{\text{in}}\rangle$, which is given by

$$\partial_u F(u,v;u',v') \propto \frac{1}{2}\sqrt{\frac{w'(u')}{w'(u)}}\frac{w''(u)}{w(u)-w(u')} - \frac{w'(u)\sqrt{w'(u)w'(u')}}{(w(u)-w(u'))^2}. \tag{4.1.15}$$

Note that, due to the trace operation in (4.1.14), only the first and fourth terms of (4.1.10) contributes to $F(u,v;u',v')$, hence why $\partial_u F$ takes the form given above. Now, notice that we have written the coincidence limit in (4.1.13) such that u',v' approaches u,v. So, we should think of u as a fixed point and expand $\partial_u F$ around $u'=u$. In particular, observe the second term in (4.1.15). Its denominator is of order $(\Delta u)^2$. So, we have to expand $\sqrt{w'(u')}$ at least up to order $(\Delta u)^2$ to obtain the finite part. The coefficient of $\sqrt{w'(u')}$ at the order $(\Delta u)^2$ involves $w'''(u)$, hence the appearance of a third derivative in (4.1.11).

4.2 Unruh-DeWitt Detector Response

We consider now an observer equipped with a point-like Unruh-DeWitt detector. To ensure that the observer is on the same side as the field ψ and never collides with the wall even in the asymptotic past and future, we require that the condition $v(\tau) - w(u(\tau)) \geq h_{\min}$ holds for all $\tau \in \mathbb{R}$, where $h_{\min}$ is a real positive constant. We will refer to this constraint as the no-collision condition. For a given wall trajectory $w(u)$, the requirement puts a restriction on the detector's trajectory. Conversely, a given detector trajectory limits our choice of wall trajectory $w(u)$.

4.2.1 The Response Function

By the properties (4.1.6) of the in-vacuum $|0_{\text{in}}\rangle$, the two-point function $W^{(2,\bar{2})}$ in the in-vacuum is again given by the formula (2.2.6), with the positive and

negative frequency propagators appropriately replaced by (4.1.9) and (4.1.10) respectively. Implementing the method of handling product of distributions and the coincidence limit discussed in Chapter 2, we obtain

$$\begin{aligned} &W^{(2,\bar{2})}_{\epsilon,\mathrm{MW}}(u,v;u',v') \\ &\quad = -\frac{1}{2\pi^2}\Bigg[\frac{\sqrt{w'(u)w'(u')}}{(w(u)-w(u')-i\epsilon)(v-v'-i\epsilon)} - \frac{\sqrt{w'(u)w'(u')}}{(w(u)-v'-i\epsilon)(v-w(u')-i\epsilon)} \\ &\qquad\qquad - 2\frac{\sqrt{w'(u)}(w(u)-v)}{((w(u)-v)^2+\epsilon^2)}\frac{\sqrt{w'(u')}(w(u')-v')}{((w(u')-v')^2+\epsilon^2)}\Bigg], \end{aligned} \tag{4.2.1}$$

where the subscript "MW" stands for "moving wall". Substituting (4.2.1) into the response function (2.2.5), we have that

$$F_{\mathrm{MW}}(\omega) = F^{(0)}_{\mathrm{MW}}(\omega) + F^{(1)}_{\mathrm{MW}}(\omega) + F^{(2)}_{\mathrm{MW}}(\omega), \tag{4.2.2}$$

where

$$\begin{aligned} F^{(0)}_{\mathrm{MW}}(\omega) = \lim_{\epsilon\to 0_+} -\frac{1}{\pi^2}\int_{-\infty}^{\infty}\mathrm{d}r\,\chi(r)\int_0^{\infty}\mathrm{d}s\,\chi(r-s) \\ \times \mathrm{Re}\Bigg\{\frac{e^{-i\omega s}\sqrt{w'(u(r))w'(u(r-s))}}{(w(u(r))-w(u(r-s))-i\epsilon)(v(r)-v(r-s)-i\epsilon)}\Bigg\}, \end{aligned} \tag{4.2.3}$$

$$\begin{aligned} F^{(1)}_{\mathrm{MW}}(\omega) = \lim_{\epsilon\to 0_+} \frac{1}{\pi^2}\int_{-\infty}^{\infty}\mathrm{d}r\,\chi(r)\int_0^{\infty}\mathrm{d}s\,\chi(r-s) \\ \times \mathrm{Re}\Bigg\{\frac{e^{-i\omega s}\sqrt{w'(u(r))w'(u(r-s))}}{(w(u(r))-v(r-s)-i\epsilon)(v(r)-w(u(r-s))-i\epsilon)}\Bigg\}, \end{aligned} \tag{4.2.4}$$

$$F^{(2)}_{\mathrm{MW}}(\omega) = \frac{2}{\pi^2}\int_{-\infty}^{\infty}\mathrm{d}r\,\frac{\chi(r)\sqrt{w'(u(r))}}{w(u(r))-v(r)}\int_0^{\infty}\mathrm{d}s\,\frac{\chi(r-s)\cos(\omega s)\sqrt{w'(u(r-s))}}{w(u(r-s))-v(r-s)}. \tag{4.2.5}$$

In arriving at (4.2.5), which comes from the last term in (4.2.1), we have used the no-collision condition and the fact that χ has a compact support to show that the integrand has an integrable upper bound. Then, justified by the dominated

convergence theorem, we set $\epsilon = 0$ under the double integral. Note that, $F^{(2)}_{\mathrm{MW}}(\omega)$ arises due to the use of a non-normally-ordered Hamiltonian. For a detector interacting via a normally-ordered Hamiltonian, $F^{(2)}_{\mathrm{MW}}(\omega)$ does not contribute.

Before proceeding with the analysis, we would like to introduce the notion of "return time" and comment on the singularity structure of $F^{(1)}_{\mathrm{MW}}(\omega)$. Consider any right-moving component of ψ that intersects the detector at some proper time τ. When propagated backwards along the null line $u(\tau)$, the right-mover will be reflected by the wall at $v = w(u(\tau))$ and becomes a left-mover which may intersect the detector at some earlier proper time τ_e. This is guaranteed if the detector follows a trajectory which is asymptotically inertial in the far past. In such cases, we define the return time $\Delta t_{\mathrm{ret}}(\tau)$ at proper time τ as the difference $\tau - \tau_e$. To determine the quantity, notice that if we start from τ_e and propagate the left-mover forward in time, it will intersect the wall at $v = v(\tau_e)$. Hence, the return time $\Delta t_{\mathrm{ret}}(\tau)$ satisfy the equation

$$v(\tau - \Delta t_{\mathrm{ret}}(\tau)) = w(u(\tau)) \implies \Delta t_{\mathrm{ret}}(\tau) = \tau - v^{-1}(w(u(\tau))). \tag{4.2.6}$$

Notice that $s = \Delta t_{\mathrm{ret}}(r)$ is precisely where the integrand of $F^{(1)}_{\mathrm{MW}}(\omega)$ is singular when $\epsilon = 0$. Non-existence of $\Delta t_{\mathrm{ret}}(r)$ for a given r then implies that the first factor in the integrand is regular at that r. Note also that the condition $v(r) - w(u(r-s)) \geq v(r) - w(u(r)) \geq h_{\min}$, which is true for any non-intersecting timelike detector and wall trajectories, implies that the second factor of the integrand has no singular points for any $r \in \mathbb{R}$.

4.2.2 The Transition Rate

We now specialise to a detector resting at $z = d$ and parametrise its worldline as (3.3.1). In terms of null coordinates, the parametrisation is

$$(u(\tau), v(\tau)) = (\tau, \tau + 2d). \tag{4.2.7}$$

The no-collision condition now reads $\tau + 2d - w(\tau) \geq h_{\min}$. Since $\Delta t_{\rm ret}(\tau) = \tau + 2d - w(\tau)$ in this case, we incidentally have $\Delta t_{\rm ret}(\tau) \geq h_{\min}$.

Using methods in [49, 53, 62, 63], we evaluate the limit $\epsilon \to 0_+$ of $F^{(0)}_{\rm MW}(\omega)$ explicitly and obtain

$$\begin{aligned} &F^{(0)}_{\rm MW}(\omega) \\ &\quad = -\frac{\omega}{2\pi}\int_{-\infty}^{\infty} \mathrm{d}r\,[\chi(r)]^2 + \frac{1}{\pi^2}\int_0^\infty \frac{\mathrm{d}s}{s^2}\int_{-\infty}^{\infty}\mathrm{d}r\,\chi(r)[\chi(r)-\chi(r-s)] \\ &\qquad + \frac{1}{\pi^2}\int_{-\infty}^{\infty}\mathrm{d}r\,\chi(r)\int_0^\infty \mathrm{d}s\,\chi(r-s)\left(\frac{1}{s^2} - \frac{\cos(\omega s)\sqrt{w'(r)w'(r-s)}}{s(w(r)-w(r-s))}\right). \end{aligned} \tag{4.2.8}$$

For $F^{(1)}_{\rm MW}(\omega)$, setting $\epsilon = 0$ in the second factor introduces an error of order ϵ which hence vanishes as we take the limit $\epsilon \to 0_+$. The remaining term, viewed as an integral over r, has an integrand that is bounded uniformly by an ϵ-independent constant. Together with the fact that χ has a compact support, we may use dominated convergence theorem to justify commuting the limit $\epsilon \to 0_+$ through the outer r-integral and obtain

$$\begin{aligned} &F^{(1)}_{\rm MW}(\omega) \\ &\quad = \frac{1}{\pi^2}\,\mathrm{Re}\left\{\int_{-\infty}^{\infty}\mathrm{d}r\,\chi(r)\lim_{\epsilon\to 0_+}\int_0^\infty \mathrm{d}s\,\frac{e^{-i\omega s}\chi(r-s)\sqrt{w'(r)w'(r-s)}}{(s-\Delta t_{\rm ret}(r)-i\epsilon)(s+\Delta t_{\rm ret}(r-s))}\right\}. \end{aligned} \tag{4.2.9}$$

One may then proceed to evaluate the limit $\epsilon \to 0_+$ using the Sokhotsky formula (2.2.8) if the singularity $s = \Delta t_{\rm ret}(r)$ is within the range of integration. Otherwise, if the singularity is outside the range or on the boundary, one may simply set $\epsilon = 0$ under the integral. The latter is justified by the fact that the singularity is suppressed by the switching function.[1] For our purpose here, however, $F^{(1)}_{\rm MW}(\omega)$ as given by (4.2.9) is sufficient. As for $F^{(2)}_{\rm MW}(\omega)$, substitution of (4.2.7)

[1] This can be seen by evaluating the inner s-integral for arbitrary χ using the Sokhotsky formula, then specialising to one where $\chi(r-s) = 0$ for $s \geq \Delta t_{\rm ret}(r)$.

into (4.2.5) gives

$$F^{(2)}_{\text{MW}}(\omega) = \frac{2}{\pi^2}\int_{-\infty}^{\infty} \mathrm{d}r\, \chi(r)\frac{\sqrt{w'(r)}}{\Delta t_{\text{ret}}(r)}\int_{0}^{\infty} \mathrm{d}s\, \chi(r-s)\cos(\omega s)\frac{\sqrt{w'(r-s)}}{\Delta t_{\text{ret}}(r-s)}. \tag{4.2.10}$$

Now that we have the regulator-free expressions of the response function, we can calculate the detector transition rate. Following the procedure in [53], we first substitute (2.2.11) into (4.2.8) – (4.2.10). Then, we differentiate the response function with respect to τ and take the sharp switching limit $\delta \to 0$ to obtain the transition rate

$$\dot{F}_{\text{MW}}(\omega,\tau) = \dot{F}^{(0)}_{\text{MW}}(\omega,\tau) + \dot{F}^{(1)}_{\text{MW}}(\omega,\tau) + \dot{F}^{(2)}_{\text{MW}}(\omega,\tau), \tag{4.2.11}$$

where

$$\begin{aligned}\dot{F}^{(0)}_{\text{MW}}(\omega,\tau) = &-\frac{\omega}{\pi}\Theta(-\omega) + \frac{1}{\pi^2}\int_0^{\Delta\tau}\mathrm{d}s\cos(\omega s)\left(\frac{1}{s^2} - \frac{\sqrt{w'(\tau)w'(\tau-s)}}{s(w(\tau)-w(\tau-s))}\right)\\ &+ \frac{1}{\pi^2}\int_{\Delta\tau}^{\infty}\mathrm{d}s\,\frac{\cos(\omega s)}{s^2},\end{aligned} \tag{4.2.12}$$

$$\dot{F}^{(1)}_{\text{MW}}(\omega,\tau) = \lim_{\epsilon\to 0_+}\frac{1}{\pi^2}\int_0^{\Delta\tau}\mathrm{d}s\,\mathrm{Re}\left\{\frac{e^{-i\omega s}\sqrt{w'(\tau)w'(\tau-s)}}{(s-\Delta t_{\text{ret}}(\tau)-i\epsilon)(s+\Delta t_{\text{ret}}(\tau-s))}\right\}, \tag{4.2.13}$$

$$\dot{F}^{(2)}_{\text{MW}}(\omega,\tau) = \frac{2\sqrt{w'(\tau)}}{\pi^2\Delta t_{\text{ret}}(\tau)}\int_0^{\Delta\tau}\mathrm{d}s\cos(\omega s)\frac{\sqrt{w'(\tau-s)}}{\Delta t_{\text{ret}}(\tau-s)}. \tag{4.2.14}$$

A few technical remarks are in order. First, similarly to (4.2.9), the evaluation of $\epsilon \to 0_+$ limit in (4.2.13) depends on the relationship between $\Delta\tau$ and $\Delta t_{\text{ret}}(\tau)$. We may simply set $\epsilon = 0$ under the integral when $\Delta\tau < \Delta t_{\text{ret}}(\tau)$ and use the Sokhotsky formula (2.2.8) when $\Delta\tau > \Delta t_{\text{ret}}(\tau)$. However, when $\Delta\tau = \Delta t_{\text{ret}}(\tau)$, the limit is undefined since the singularity occurs at the boundary of integration interval and there is no switching function in (4.2.13) to suppress the divergence. Hence, the expressions above are valid only when $\Delta\tau \neq \Delta t_{\text{ret}}(\tau)$. Second, the

integrand of $\dot{F}^{(2)}_{\rm MW}(\omega,\tau)$ oscillates about a non-zero constant at large s. We thus have to keep the switch-on time τ_0 strictly finite. Third, if one is working with the normally-ordered interaction Hamiltonian (2.2.13), the previous two remarks do not apply. Since $\dot{F}^{(2)}_{\rm MW}(\omega,\tau)$ does not contribute to the transition rate, we may push the switch-on time τ_0 to the asymptotic past. When this is done, the last term in (4.2.12) is $O(1/\Delta\tau)$ and the limit $\epsilon \to 0_+$ in (4.2.13) should only be evaluated using the Sokhotsky formula (2.2.8).

4.2.3 Collapsing Star Model

Of particular interest to us is the detector transition rate at late times when the wall follows a trajectory that produces Hawking-like radiation in the far future. Such a trajectory has the characteristic asymptotic behaviour [1, 28]

$$z_{\rm w}(t) \to -t - Ae^{-2at} + B \qquad \text{as } t \to \infty, \tag{4.2.15}$$

where a, A and B are positive constants. The parameter a, in particular, plays the role of the surface gravity κ in the Bekenstein-Hawking temperature $T_{\rm BH}$ mentioned in Chapter 1. For concreteness, let us consider the trajectory [49, 50]

$$w(u) = -\frac{1}{a}\ln\big(1+e^{-au}\big), \tag{4.2.16}$$

where $a > 0$. Using the formula $\sinh^{-1}(x) = \ln\big(x+\sqrt{x^2+1}\big)$, we obtain that

$$z_{\rm w}(t) = \frac{1}{a}\ln\left(-\frac{e^{at}}{2} + \sqrt{\frac{e^{2at}}{4}+1}\right). \tag{4.2.17}$$

At early times, the wall moves with an inertial motion as required. The trajectory (4.2.16) asymptotes to $z_{\rm w}(t) = 0$ from the left as $t \to -\infty$. At late times, the wall approaches a null trajectory with $v = 0$ as the asymptote and (4.2.17) satisfies (4.2.15) with $A = 1$ and $B = 0$. The worldline of a wall following the trajectory (4.2.16) is illustrated in Figure 4.1.

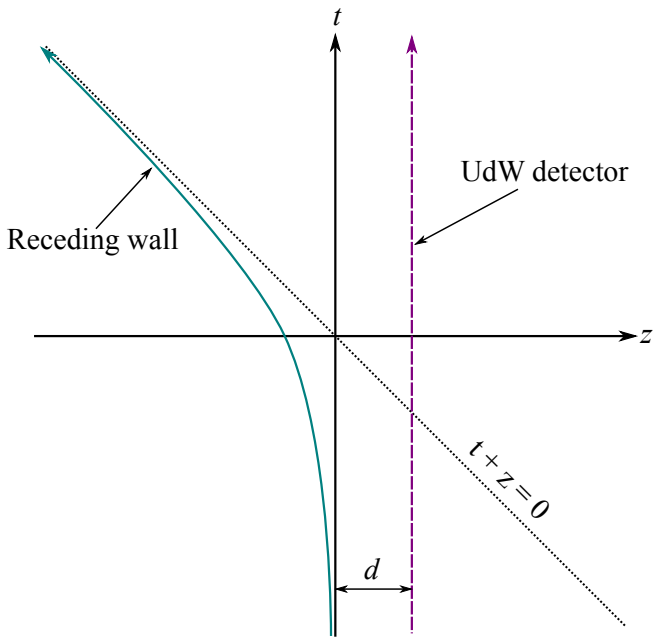


Figure 4.1: A receding wall in Minkowski spacetime and an Unruh-DeWitt (UdW) detector at $z = d > 0$. The dashed line $t + z = 0$ shows the future asymptote of the wall.

From previous particle detector calculations involving a massless scalar field [49, 50], one may expect that the late time transition rate in our case here to contain a term proportional to the Fermi-Dirac statistics, that is

$$\dot{F}(\omega, \tau) = f(\omega, a)\Theta(-\omega) + \frac{g(\omega, a)}{1 + e^{2\pi\omega/a}} + h(\omega, a), \tag{4.2.18}$$

where f, g and h are some functions of ω and a. The first and second terms represent the contributions from undisturbed left-movers and thermal right-movers respectively. However, as shown in Appendix B, this is not the case. The late time transition rate of a static detector at $z = d$, interacting with the field via either interaction Hamiltonian (2.2.1) or (2.2.13) is in fact given by

$$\dot{F}(\omega, \tau) = \frac{a}{2\pi^2} \ln\left(1 + e^{-\frac{2\pi\omega}{a}}\right) + o(1) \tag{4.2.19}$$

when it is switched on at an arbitrary fixed finite τ_0. The same holds when the detector interacts via (2.2.13) and is switched on in the asymptotic past. Comparing (4.2.19) to (4.2.18), two observations can be made.

First, the separation between contributions from undisturbed left-movers and thermal right-movers is not apparent in (4.2.19). This can actually be traced back to the quadratic nature of the detector-field coupling whose general feature is to couple the left-moving and right-moving components of the field in $W^{(2,\bar{2})}$.

Second, (4.2.19) contains no term that is proportional to the number density of fermions with energy ω in a fermionic thermal bath at temperature $a/2\pi$, as suggested in (4.2.18). Our detector hence is not counting the number of fermions with energy ω in usual sense of particle counting. Recall, nevertheless, that the Helmholtz free energy of fermions in length L at temperature $T = a/2\pi$ is given by [64]

$$F = -2L \int_0^\infty \frac{\mathrm{d}\omega}{2\pi} \left[\omega + 2 \times \frac{a}{2\pi} \ln\left(1 + e^{-\frac{2\pi\omega}{a}}\right) \right]. \tag{4.2.20}$$

The first term is the vacuum energy, hence may be ignored. The factor two in the second term accounts for the existence of fermions and anti-fermions. Meanwhile, the overall factor two outside the integral accounts for the existence of a left-mover and a right-mover for each energy. We see that, for $\omega > 0$, the transition rate (4.2.19) is actually proportional to the Helmholtz free energy density of fermions with energy ω in a thermal bath at temperature $a/2\pi$. An observer equipped with a detector will therefore be able to infer that the late time radiation from the wall is made of fermions.

Chapter 5

Conclusions

In this thesis, we have analysed massless fermion creation by time-dependent boundaries in $(1+1)$-dimensional flat spacetimes. We considered two distinct senses in which the boundaries are said to be time-dependent. On one hand, a boundary which remains at rest with respect to a family of inertial observers but imposes a time-dependent boundary condition. On the other hand, a boundary that moves along a timelike trajectory while imposing a time-independent boundary condition, specifically the MIT bag boundary condition. In both cases, we have calculated the stress-energy tensor of the spinor field describing the fermions, renormalised via the point-splitting method, and the response of an inertial Unruh-DeWitt detector coupled linearly to the scalar density of the field. Throughout our analysis, we have compared our results to those readily available in the literature for a massless scalar field in similar settings.

In Chapter 3, we focused our attention to the motionless evolving wall, which was taken to impose a boundary condition parametrised by four arbitrary time-dependent functions. Technically, at any instance of time, the wall imposes a particular self-adjointness condition of the Dirac operator. We argued that some of the boundary conditions may be interpreted as arising from a combination of idealised scalar and electric potentials. In this setting, we have analysed the properties of the energy flux emitted by the wall and also the response of an

inertial Unruh-DeWitt particle detector that passes through the energy burst. Our findings are as follows.

First, when the field is in a state corresponding to early time vacuum, the energy flux is finite for any smoothly evolving wall. This is deduced from the field's renormalised stress energy tensor (3.2.14) – (3.2.17). Second, the response of a detector that passes through the energy burst can be expressed, roughly speaking, as a sum of the response to a static impermeable wall. For each term in the sum, the switching function is multiplied by specific trigonometric functions involving the wall parameters. As such, within first order perturbation theory, the detector's probability of excitation due to the wall's evolution is finite for any smoothly evolving wall.

For concreteness, we considered the creation and demolition of an impermeable wall that imposes MIT bag boundary condition [47] on both sides — the MIT wall for short. We chose discrete one-parameter families of the self-adjointness boundary condition (3.1.10) to describe the process. The discrete parameter $n \in \mathbb{Z}$ can be thought as labelling different ways to carry out the process. We analysed in detail the behaviour of the energy flux, the total energy transmitted into the field by such a process and the response of a particle detector in the rapid process limit, and compared our spinor field results to that of a scalar field analysis carried out in [40, 45]. The results obtained are as follows.

First, for any smooth process of wall creation or demolition, the energy flux emitted by the wall is finite. From (3.2.24), we see that large values of $|n|$ lead to a higher energy flux. Second, in rapid process limit, the burst of energy displays a delta distribution squared divergence. The total energy transmitted into the field diverges at least as fast as the inverse of the wall's evolution duration δ. The exact rate of divergence depends on how the limit $\delta \to 0$ is taken. Third, the detector's response is finite for any smooth MIT wall creation or demolition. Fourth, in the limit of large detector energy gap ω but finite δ, contributions from the wall's evolution itself, as opposed to the wall's existence, is only of

order δ. While this may seem contradictory to the energy density result at first, the conclusion is not expected to hold in the rapid process limit, that is when δ^{-1} is comparable to ω. This suspicion is supported by our subsequent analysis, which brings us to our fifth point. In the limit of rapid process but finite detector energy gap, the detector's response indeed diverges. However, the divergence is only logarithmic in the duration of wall's evolution. This adds to the evidence that, within first order perturbation theory, a localised matter system coupled to the field may not be as sensitive to the divergence in local expectation value of field observables such as the stress-energy tensor [40, 43, 44].

In Chapter 4, we turned our attention to the moving wall analysis. To ensure a well-defined early time state, we have restricted ourselves to a wall that follows an asymptotically inertial trajectory in the far past. When the spinor field is in a state corresponding to early time vacuum, we found that the wall radiates in such a way that the stress-energy tensor of the spinor field (4.1.11) is exactly equal to that of a massless scalar field at all times [1, 28, 48]. This implies, in particular, that an observer examining only the stress-energy tensor is unable to tell whether the radiation is made of fermions or bosons.

We then considered an observer who analyses the radiation using an Unruh-DeWitt detector. Specifically, we focused on a static observer and calculated the transition rate of the detector. Even though it is operationally difficult to be measured since an observer requires an ensemble of ensembles of detectors to do so, the transition rate has an intuitive physical interpretation. It quantifies how the transition probability of the detector would change when the detector continues to interact with the field at maximum coupling strength for an infinitesimal additional time. We found that the transition rate is finite at almost all times. It is divergent only when the detector-field interaction period coincides with the time taken for the field to be reflected back, backwards in time, to the observer. When compared to the corresponding result for a massless scalar field [49, 50], we found that the transition rate (4.2.11) indeed takes a different form. Hence,

an observer equipped with an Unruh-DeWitt detector will generically be able to distinguish fermions from bosons.

As an illustration, we then considered a wall trajectory for which a mirror reflecting a scalar field following the same trajectory is known to emit thermal radiation in the far future [49, 50]. For the wall reflecting a fermion field, we obtain an interesting result for the detector's late time transition rate: the detector clicks at a rate proportional to the Helmholtz free energy density of fermions, whose energy matches the detector energy gap ω, in a thermal bath at temperature $T = a/2\pi$. On one hand, this is to be contrasted with the expectation that the detector counts the number of particles, hence should contain a term proportional to the number density of thermal fermions with energy ω. On the other hand, the late time transition rate is to be compared with the corresponding result for a massless scalar field ϕ where the detector partially clicks at a rate proportional to the number density of bosons, with energy ω, in a thermal bath of the same temperature [49, 50]. The latter comparison shows that our second observer can indeed conclude that the radiation consists of fermions.

There are several limitations in our analysis that could be a source of ideas for future projects. First, we have only considered massless spinor fields in $1+1$ flat spacetimes. For a more realistic model of a Dirac field in 3+1 dimensions, it is important to consider massive fields. The problem of a motionless time-dependent spherical shell in $3+1$ Minkowski spacetime, for instance, can be reduced to the problem of a motionless time-dependent wall in $1+1$ half-Minkowski spacetime. However, even if the $3+1$ Dirac field is massless, separation of variables introduces an effective potential, which acts like a space-dependent mass term, to the $1+1$ problem. Furthermore, unlike a scalar field, there is no spherically symmetric mode which would reduce to a massless $1+1$ field. Second, the type of detector-field coupling we chose in the thesis is primarily for simplicity. At the moment, it is not known whether such a detector models any real world localised matter system. An investigation into other types of coupling, such as $v_\mu \overline{\psi}\gamma^\mu\psi$,

where v_μ is the detector's velocity, would be fruitful. Third, we have focused exclusively on the response of a static detector. It would be interesting to see how the detector's motion, inertial or otherwise, would change the results.

Fourth, specifically for the motionless evolving wall analysis, the boundary conditions we studied in this thesis is purely mathematical - except the no-wall and perhaps the MIT wall boundary conditions. It would be interesting to investigate the role of each wall parameter in real-world experiment. The correspondence to an idealised delta potential given in Section 3.1.2 could be a starting point for such an investigation.

Fifth, specifically for the moving wall analysis, only a wall trajectory that models a collapsing star has been considered in detail. Another interesting wall trajectory is one where the wall accelerates uniformly for a certain period of time. The similarity between the stress-energy tensor a scalar field and a spinor field implies that the wall analysed in this thesis also does not radiate when it is accelerating uniformly. For a scalar field, Davies and Fulling argued that a detector detects particle fluxes albeit the absence of any radiation [28]. However, Groove later made an analysis that resolves the discrepancy [65]. After identifying an approximation that led Davies and Fulling to their conclusion, he showed that a detector operating only in the region where the mirror accelerates uniformly indeed detects no particle. A calculation of the transition rate for our detector in a similar setting would thus complement Groove's work.

Finally, the scalar detectors that our results are compared against couple linearly either to the scalar field itself or its derivative. It would be interesting to consider a scalar detector that couples linearly to the scalar density $\phi^\dagger\phi$ of the scalar field. In particular, we see in Section 4.2.3 that the left-moving and right-moving components of the spinor field conspire in such a way that the late time transition rate of our detector is proportional to the Helmholtz free energy density of mode ω in a fermionic thermal bath. It would be interesting to see if a similar phenomenon occurs for the $\phi^\dagger\phi$ detector.

Appendix A

Supplement for Evolving Wall Analysis

A.1 Self-adjoint Extensions of the Dirac Operator on Disjoint Half-Lines

Consider the massless field Dirac operator $D = -i\alpha\partial_z$ acting on the Hilbert space $\mathcal{H} = \overleftarrow{\mathcal{H}} \oplus \vec{\mathcal{H}}$, where $\overleftarrow{\mathcal{H}} = L_2((-\infty, 0]) \oplus L_2((-\infty, 0])$ and $\vec{\mathcal{H}} = L_2([0, \infty)) \oplus L_2([0, \infty))$. We equip $\mathcal{H}$ with the inner product

$$(\phi_1, \phi_2) = \int_{-\infty}^{0} [\phi_1(z)]^\dagger \phi_2(z)\, \mathrm{d}z + \int_{0}^{\infty} [\phi_1(z)]^\dagger \phi_2(z)\, \mathrm{d}z\,, \tag{A.1.1}$$

where $\phi_1, \phi_2 \in \mathcal{H}$. Let the initial domain of D be

$$\mathcal{D}(D) = \{\phi \in \mathcal{H} \mid \partial_z \phi \in \mathcal{H}, \phi(0_-) = \phi(0_+) = 0\}, \tag{A.1.2}$$

where $\phi(0_-)$ and $\phi(0_+)$ are respectively the limiting values of the parts of $\phi(z)$ that lie in $\overleftarrow{\mathcal{H}}$ and $\vec{\mathcal{H}}$ as z approaches 0.

The fact that the limits in (A.1.2) exist so that we can impose the vanishing boundary condition at $z = 0$ can be seen as follows. For clarity, let the parts of

$\phi(z)$ that lie in $\overleftarrow{\mathcal{H}}$ and $\overrightarrow{\mathcal{H}}$ be denoted $\overleftarrow{\phi}(z)$ and $\overrightarrow{\phi}(z)$ respectively. Now, observe that the condition $\partial_z\phi \in \mathcal{H}$ for every $\phi \in \mathcal{D}(D)$ implies that $\partial_z\overleftarrow{\phi}_\pm \in L_2((-\infty, 0])$ and $\partial_z\overrightarrow{\phi}_\pm \in L_2([0, \infty))$, where, recall that, the subscripts $+$ and $-$ indicate the terms being the coefficient of the spinor basis U_+ and U_- respectively. It follows that for any $a \in (0, \infty)$ and $b \in (0, \infty)$, $\partial_z\overleftarrow{\phi}_\pm$ is square integrable in the closed interval $[-a, 0]$ and $\partial_z\overrightarrow{\phi}_\pm$ is square integrable in the closed interval $[0, b]$. Hence, $\partial_z\overleftarrow{\phi}_\pm$ and $\partial_z\overrightarrow{\phi}_\pm$ are integrable in these respective closed interval, which implies that the functions $\overleftarrow{\phi}_\pm$ and $\overrightarrow{\phi}_\pm$ are absolutely continuous, and in particular continuous, in these respective closed intervals. The continuity at $z = 0$, in the sense of a one-sided continuity, shows that the limits $\phi(0_-)$ and $\phi(0_+)$ exist.

In addition to implying the continuity of $\overleftarrow{\phi}_\pm$ and $\overrightarrow{\phi}_\pm$ that we've just stated, the conditions $\partial_z\overleftarrow{\phi}_\pm \in L_2((-\infty, 0])$ and $\partial_z\overrightarrow{\phi}_\pm \in L_2([0, \infty))$ also imply that

$$\lim_{z\to-\infty} \overleftarrow{\phi}_\pm(z) = \lim_{z\to\infty} \overrightarrow{\phi}_\pm(z) = 0 \qquad \forall\phi \in \mathcal{D}(D). \tag{A.1.3}$$

See, for instance, pages 85 – 86 of [66] for the proof.

Consider now the adjoint of D, denoted $D^\dagger$. The adjoint's domain $\mathcal{D}(D^\dagger)$ consists of $\psi \in \mathcal{H}$ such that there exists $D^\dagger\psi \in \mathcal{H}$ satisfying the condition [67]

$$(\psi, D\phi) = (D^\dagger\psi, \phi) \qquad \forall\phi \in \mathcal{D}(D). \tag{A.1.4}$$

Integrating the left hand side of (A.1.4) by parts, we obtain

$$(-i\alpha\partial_z\psi, \phi) = (D^\dagger\psi, \phi) \qquad \forall\phi \in \mathcal{D}(D), \tag{A.1.5}$$

where the boundary terms vanish due to the vanishing of $\phi \in \mathcal{D}(D)$ at infinity and at $z = 0$ on both sides. From (A.1.5), we have that $D^\dagger = -i\alpha\partial_z$ in $\mathcal{H}$ and

$$\mathcal{D}(D^\dagger) = \{\psi \in \mathcal{H} \mid \partial_z\psi \in \mathcal{H}\}. \tag{A.1.6}$$

As above, the condition $\partial_z\psi \in \mathcal{H}$ implies that, for every $\psi \in \mathcal{D}(D^\dagger)$, the limits $\psi(0_-)$ and $\psi(0_+)$ exist and $\psi(z)$ vanishes at infinity. However, note that there is no boundary condition imposed on $\psi \in \mathcal{D}(D^\dagger)$ at $z = 0$ on either side. Since $\mathcal{D}(D) \neq \mathcal{D}(D^\dagger)$, our initial operator $(D, \mathcal{D}(D))$ is clearly not self-adjoint.

To find self-adjoint extensions of $(D, \mathcal{D}(D))$, we need to expand $\mathcal{D}(D)$ and shrink $\mathcal{D}(D^\dagger)$ until the two coincide. To this aim, we relax the boundary condition in (A.1.2) so that elements of $\mathcal{D}(D)$ can be non-vanishing at $z = 0$. At the same time, we require that elements of $\mathcal{D}(D^\dagger)$ obey some boundary condition at $z = 0$. We denote the new domain of D and $D^\dagger$ with $\mathcal{D}'(D)$ and $\mathcal{D}'(D^\dagger)$ respectively. Remember that, by construction, $\phi \in \mathcal{D}'(D)$ on the negative real line lives in a different subspace than that on the positive real line. Therefore, $\phi \in \mathcal{D}'(D)$ need not have the same limit on both sides of $z = 0$. The same remark applies to $\psi \in \mathcal{D}'(D^\dagger)$.

To derive explicitly the boundary condition such that $\mathcal{D}'(D) = \mathcal{D}'(D^\dagger)$, hence characterising the self-adjoint extensions of our initial operator $(D, \mathcal{D}(D))$, consider the sesquilinear form

$$\begin{aligned} B(\psi, \phi) &:= i\left[(\psi, -i\alpha\partial_z\phi) - (-i\alpha\partial_z\psi, \phi)\right] \\ &= \psi^\dagger(0_-)\alpha\phi(0_-) - \psi^\dagger(0_+)\alpha\phi(0_+), \end{aligned} \tag{A.1.7}$$

where $\psi \in \mathcal{D}'(D^\dagger)$ and $\phi \in \mathcal{D}'(D)$. In the second line, we have used the properties (A.1.3) for $\phi \in \mathcal{D}'(D)$ and a similar properties for $\psi \in \mathcal{D}'(D^\dagger)$. Expanding ψ and ϕ in terms of the spinor basis $\{U_+, U_-\}$ allows us to write

$$B(\psi, \phi) = u^\dagger \begin{pmatrix} I & 0 \\ 0 & -I \end{pmatrix} v, \tag{A.1.8}$$

where I is the 2×2 identity matrix and

$$u := \begin{pmatrix} \psi_+(0_-) \\ \psi_-(0_+) \\ \psi_+(0_+) \\ \psi_-(0_-) \end{pmatrix}, \qquad v := \begin{pmatrix} \phi_+(0_-) \\ \phi_-(0_+) \\ \phi_+(0_+) \\ \phi_-(0_-) \end{pmatrix}. \tag{A.1.9}$$

By the lemma in Appendix A of [68], it follows that the self-adjoint extensions of our initial operator $(D, \mathcal{D}(D))$ are parametrised by the boundary condition

$$\begin{pmatrix} \psi_+(0_+) \\ \psi_-(0_-) \end{pmatrix} = U \begin{pmatrix} \psi_+(0_-) \\ \psi_-(0_+) \end{pmatrix}, \tag{A.1.10}$$

where U is a 2×2 unitary matrix, which we shall parametrise as

$$U = e^{i\varphi} \begin{pmatrix} e^{i\varphi_1} \cos\theta & ie^{i\varphi_2} \sin\theta \\ ie^{-i\varphi_2} \sin\theta & e^{-i\varphi_1} \cos\theta \end{pmatrix}, \tag{A.1.11}$$

where $(\varphi, \varphi_1, \varphi_2, \theta) \in \mathbb{R}^4$. Note that the arrangement of (A.1.10) and the choice of parametrisation (A.1.11) are so that $U = I$ corresponds to the essentially self-adjoint Dirac operator on the full real line $\mathbb{R}$. As noted in the main text, due to the way we parametrise U, there are more than one set of parameters $(\varphi, \varphi_1, \varphi_2, \theta)$ corresponding to the same unitary matrix U.

A.2 Correspondence to δ-potential

Integrating both sides of (3.1.13) over a small interval $[-\epsilon, \epsilon]$, where $\epsilon > 0$, and taking the limit $\epsilon \to 0$, we obtain

$$i\alpha(\psi(0_+) - \psi(0_-)) = (S(t)\beta + V(t)) \lim_{\epsilon \to 0_+} \int_{-\epsilon}^{\epsilon} \delta(z)\psi \, \mathrm{d}z \,, \tag{A.2.1}$$

where $\psi(0_\pm) \equiv \psi(t, 0_\pm)$. In arriving at (A.2.1), we have assumed that $\partial_t\psi$ on the left hand side of (3.1.13) is continuous and, in particular, does not behave like $\delta(z)$ at the origin. Instead of using (3.1.15) from the outset, let us begin here with a more general version, that is

$$\lim_{\epsilon\to 0_+}\int_{-\epsilon}^{\epsilon}\delta(z)\psi(z)\,\mathrm{d}z := h_-\psi(0_-) + h_+\psi(0_+), \tag{A.2.2}$$

where h_- and h_+ are real positive constants that add up to one. A definition analogous to (A.2.2) is used, for instance in [69], to describe an asymmetric δ-shell. In our case here, (A.2.2) describes a δ-potential wall that treats the right and left portions of the spacetime differently.

Substituting (A.2.2) into (A.2.1) and expanding $\psi(0_\pm)$ in the spinor basis $\{U_+, U_-\}$, the terms proportional to U_+ give

$$\begin{aligned}&(i - V(t)h_+)\psi_+(0_+)\\ &\quad = (i + V(t)h_-)\psi_+(0_-) + S(t)h_+\psi_-(0_+) + S(t)h_-\psi_-(0_-)\end{aligned} \tag{A.2.3}$$

while the terms proportional to U_- give

$$\begin{aligned}&(i - V(t)h_-)\psi_-(0_-)\\ &\quad = (i + V(t)h_+)\psi_-(0_+) + S(t)h_-\psi_+(0_-) + S(t)h_+\psi_+(0_+).\end{aligned} \tag{A.2.4}$$

To find the relation between $(S(t), V(t), h_-, h_+)$ and $(\varphi(t), \varphi_1(t), \varphi_2(t), \theta(t))$, we need to bring (A.2.3) – (A.2.4) into the form of (3.1.3). This can be done as follows. We multiply (A.2.3) with $(i - V(t)h_-)$ and eliminate $\psi_-(0_-)$ from the resulting equation using (A.2.4). After some rearrangement, we obtain

$$\begin{aligned}&(V(t)^2h_-h_+ - S(t)^2h_-h_+ - iV(t) - 1)\psi_+(0_+)\\ &\quad = (S(t)^2h_-^2 - V(t)^2h_-^2 - 1)\psi_+(0_-) + iS(t)\psi_-(0_+).\end{aligned} \tag{A.2.5}$$

Analogously, we multiply (A.2.4) with $(i - V(t)h_+)$ and eliminate $\psi_+(0_+)$ from the resulting equation using (A.2.3). After some rearrangement, we obtain

$$\begin{aligned}(V(t)^2 h_- h_+ - S(t)^2 h_- h_+ - iV(t) - 1)\psi_-(0_-) \\ = (S(t)^2 h_+^2 - V(t)^2 h_+^2 - 1)\psi_-(0_+) + iS(t)\psi_+(0_-).\end{aligned} \tag{A.2.6}$$

Now, notice that the factor $V(t)^2 h_- h_+ - S(t)^2 h_- h_+ - iV(t) - 1$ on the left hand side of (A.2.5) and (A.2.6) never vanishes. If $V(t) = 0$, then the remaining terms is always less than or equal to -1. If $V(t) \neq 0$, then the factor certainly does not vanish. Hence, we can divide both sides of (A.2.5) and (A.2.6) with the factor. Upon comparison with (3.1.3) and (3.1.4), we can make the identifications (suppressing the dependence on t in all parameters)

$$\frac{S^2 h_-^2 - V^2 h_-^2 - 1}{V^2 h_- h_+ - S^2 h_- h_+ - iV - 1} = e^{i(\varphi+\varphi_1)} \cos\theta, \tag{A.2.7}$$

$$\frac{S}{V^2 h_- h_+ - S^2 h_- h_+ - iV - 1} = e^{i(\varphi+\varphi_2)} \sin\theta, \tag{A.2.8}$$

$$\frac{S^2 h_+^2 - V^2 h_+^2 - 1}{V^2 h_- h_+ - S^2 h_- h_+ - iV - 1} = e^{i(\varphi-\varphi_1)} \cos\theta, \tag{A.2.9}$$

$$\frac{S}{V^2 h_- h_+ - S^2 h_- h_+ - iV - 1} = e^{i(\varphi-\varphi_2)} \sin\theta. \tag{A.2.10}$$

Since the left-hand side of (A.2.8) and (A.2.10) are identical, we have that $\varphi_2 = c_2\pi$, where $c_2 \in \mathbb{Z}$. The two constraints then reduce to a single one.

We now specialise to the case of a symmetric δ-potential where $h_- = h_+ = 1/2$. The first thing to note is that the left-hand side of (A.2.7) and (A.2.9) are now identical, implying that $\varphi_1 = c_1\pi$, where $c_1 \in \mathbb{Z}$. We are now left with

$$\frac{S^2 - V^2 - 4}{V^2 - S^2 - 4iV - 4} = (-1)^{c_1} e^{i\varphi} \cos\theta, \tag{A.2.11}$$

$$\frac{4S}{V^2 - S^2 - 4iV - 4} = (-1)^{c_2} e^{i\varphi} \sin\theta. \tag{A.2.12}$$

Using the fact that $\sin\theta$ and $\cos\theta$ never vanish simultaneously, we obtain (3.1.16) – (3.1.18) after separating the real and imaginary parts of the constraints (A.2.11) – (A.2.12).

The boundary conditions (3.1.10) used for wall appearance and disappearance correspond to $(-1)^{c_1} = 1$, $c_2 = n + 1$ and $\varphi = 2n\theta$. In order to solve the system of coupled hyperbolic equations obtained and express S and V in terms of n and θ, we analyse the following cases separately: $n = 0$ and $n \neq 0$; $\sin 2n\theta = 0$ and $\sin 2n\theta \neq 0$; $\cos\theta + \cos 2n\theta = 0$ and $\cos\theta + \cos 2n\theta \neq 0$. We found that $S(t)$ and $V(t)$ can eventually be written as in (3.1.19) – (3.1.20) for any value of n and θ. Whenever (3.1.19) – (3.1.20) diverges, $S(t)$ and $V(t)$ are undefined.

A.3 Total Energy of Creation and Demolition Process

For a wall creation, we may write $\theta(t_0 + x) = (\pi/2)f_\delta(x)$, where $f_\delta(x)$ is some smooth function satisfying $f_\delta(x) = 0$ for $x \leq 0$ and $f_\delta(x) = 1$ for $x \geq \delta$. To construct the family of functions $\{f_\delta(x)\}$ labelled by $\delta > 0$, we may consider compressing a given reference function $f_r(x)$ such that

$$f_\delta(x) = f_r(sx^a) \qquad \text{for } x > 0, \tag{A.3.1}$$

where s is the stretching factor and a is some positive real number. From the condition $f_\delta(\delta) = f_r(s\delta^a) = f_r(r)$, it follows that $s = r/\delta^a$ and

$$f'_\delta(x) = \frac{arx^{a-1}}{\delta^a} f'_r\left(\frac{rx^a}{\delta^a}\right). \tag{A.3.2}$$

Now, consider the integral part of (3.2.26). For generality, we substitute the exponent of the integrand with p here, where p is any non-negative integer. For

a wall creation described by the function $f_\delta(x)$ above, we have

$$\int_0^\delta [h_1'(t_0+x)]^p \,\mathrm{d}x = \left(\frac{\pi}{2}\right)^p \int_0^\delta [f_\delta'(x)]^p \,\mathrm{d}x$$
$$= \left(\frac{ar^{\frac{1}{a}}}{\delta}\right)^{p-1} \left(\frac{\pi}{2}\right)^p \int_0^r y^{\frac{(p-1)(a-1)}{a}} [f_r'(y)]^p \,\mathrm{d}y\,. \qquad \text{(A.3.3)}$$

To obtain the first equality, recall (3.1.11), from which we have $h_1'(t_0+x) = \theta'(t_0+x)$, and hence $h_1'(t_0+x) = (\pi/2) f_\delta'(x)$, for the interval $0 < x < \delta$. The second equality follows from the use of (A.3.2) and a change of integration variable $x \to y = rx^a/\delta^a$. For any $\delta > 0$, we know that the left-hand side is necessarily finite because $h_1'(t_0+x)$ is bounded. Since the pre-factor on the right-hand side is finite, the y-integral in the second line necessarily converges. More importantly, the y-integral is independent of δ. Writing the right-hand side of (A.3.3) as $K'\delta^{1-p}$, where K' is a δ-independent constant, it is clear how the left-hand side depends on δ. Substituting $p = 2$, it follows that, for (3.2.26), $\langle E \rangle = K\delta^{-1}$, where $K = (1+4n^2)(2\pi)^{-1}K'$.

A.4 Static MIT Wall Response Function

For a detector whose trajectory is parametrised by (3.3.1), a substitution of (3.3.5) into the response function (2.2.3) or (2.2.5) gives

$$F_{\text{MIT}}(\omega) = F_{\text{NW}}(\omega) + F^{(1)}_{\text{MIT}}(\omega) + F^{(2)}_{\text{MIT}}(\omega), \qquad \text{(A.4.1)}$$

where $F_{\text{NW}}(\omega)$, by virtue of being the contribution corresponding to the first term of (3.3.5), which is the no-wall point function, is given by (2.2.10) with

$(\Delta x)^2 = s^2$. The remaining two terms are given by

$$F^{(1)}_{\text{MIT}}(\omega) = \lim_{\epsilon\to 0_+} \frac{1}{\pi^2}\int_{-\infty}^{\infty} \mathrm{d}u\, \chi(u) \int_0^{\infty} \mathrm{d}s\, \chi(u-s)\, \mathrm{Re}\bigg\{ \frac{e^{-i\omega s}}{(s-i\epsilon)^2 - 4d^2}\bigg\}, \quad \text{(A.4.2)}$$

$$F^{(2)}_{\text{MIT}}(\omega) = \lim_{\epsilon\to 0_+} \frac{1}{\pi^2}\bigg| \int_{-\infty}^{\infty} \mathrm{d}\tau\, e^{-i\omega\tau} \chi(\tau) \frac{2d}{4d^2+\epsilon^2}\bigg|^2. \quad \text{(A.4.3)}$$

The first, second and third terms in (A.4.1) correspond to the first, second and third terms of (3.3.5) respectively.

Let us first analyse $F^{(1)}_{\text{MIT}}(\omega)$. Using the method of partial fractions, we can write $F^{(1)}_{\text{MIT}}(\omega)$ as a sum of two terms, $F^{(1)}_{\text{MIT,s}}(\omega)$ and $F^{(1)}_{\text{MIT,r}}(\omega)$, where

$$F^{(1)}_{\text{MIT,s}}(\omega) = \lim_{\epsilon\to 0_+} \frac{1}{4\pi^2 d}\int_{-\infty}^{\infty} \mathrm{d}u\, \chi(u) \int_0^{\infty} \mathrm{d}s\, \chi(u-s)\, \mathrm{Re}\bigg\{ \frac{e^{-i\omega s}}{s-2d-i\epsilon}\bigg\}, \quad \text{(A.4.4)}$$

$$F^{(1)}_{\text{MIT,r}}(\omega) = -\lim_{\epsilon\to 0_+} \frac{1}{4\pi^2 d}\int_{-\infty}^{\infty} \mathrm{d}u\, \chi(u) \int_0^{\infty} \mathrm{d}s\, \chi(u-s)\, \mathrm{Re}\bigg\{ \frac{e^{-i\omega s}}{s+2d-i\epsilon}\bigg\}. \quad \text{(A.4.5)}$$

The integrand of $F^{(1)}_{\text{MIT,s}}(\omega)$ contains a singularity at $s = 2d > 0$ when $\epsilon = 0$. After a change of variable $s \to r = s - 2d$, we may use the Sokhotsky formula (2.2.8) to find the limit $\epsilon \to 0_+$ of the inner integral. This gives us

$$F^{(1)}_{\text{MIT,s}}(\omega) = \frac{1}{4\pi^2 d}\mathrm{Re}\bigg\{ e^{-2i\omega d}\bigg[i\pi G(2d) + \int_0^{2d} \frac{\mathrm{d}r}{r}\Big(G(2d+r)e^{-i\omega r} - G(2d-r)e^{i\omega r}\Big) + \int_{2d}^{\infty} \frac{\mathrm{d}r}{r} G(2d+r)e^{-i\omega r}\bigg]\bigg\}, \quad \text{(A.4.6)}$$

where $G(y)$ is as given by (3.3.10). For $F^{(1)}_{\text{MIT,r}}(\omega)$, notice that the integrand is bounded from above and, due to the switching function, has a compact support. Hence, by dominated convergence theorem, we may set $\epsilon = 0$ under the double integral. After a change of variable $s \to r = s + 2d$, we obtain

$$F^{(1)}_{\text{MIT,r}}(\omega) = -\frac{1}{4\pi^2 d}\,\mathrm{Re}\bigg\{ e^{-2i\omega d}\int_{2d}^{\infty} G(2d-r)e^{i\omega r}\bigg\}. \quad \text{(A.4.7)}$$

Combining (A.4.6) and (A.4.7), we obtain (3.3.8).

Next, consider $F^{(2)}_{\text{MIT}}(\omega)$. From (A.4.3), we see that, similar to $F^{(1)}_{\text{MIT,r}}(\omega)$, the integrand is bounded from above and, due to the switching function, has a compact support. Hence, dominated convergence theorem implies that we may set $\epsilon = 0$ under the integral. The form given in (3.3.9) follows when we set $\epsilon = 0$ in the last term of (3.3.5) for a static detector and substituted it into (2.2.5).

Large Energy Gap Limit

The large energy gap limit of $F_{\text{NW}}(\omega)$ is readily available from [53], that is

$$F_{\text{NW}}(\omega) = -\frac{\omega\Theta(-\omega)}{\pi}\int_{-\infty}^{\infty}\mathrm{d}u\,[\chi(u)]^2 + O^{\infty}\big(|\omega|^{-1}\big). \tag{A.4.8}$$

To obtain large $|\omega|$ expression of $F^{(1)}_{\text{MIT}}(\omega)$, we start by writing (3.3.8) as

$$\begin{aligned} F^{(1)}_{\text{MIT}}(\omega) = \frac{1}{4\pi^2 d}\text{Re}\Bigg\{ e^{-2i\omega d}\Bigg[& 2i\pi G(2d)\Theta(-\omega) \\ & + \int_0^{\infty}\mathrm{d}r\cos\omega r\frac{G(2d+r)-G(2d-r)}{r} \\ & - i\int_0^{\infty}\mathrm{d}r\sin\omega r\frac{G(2d+r)+G(2d-r)-2G(2d)}{r}\Bigg]\Bigg\} \end{aligned} \tag{A.4.9}$$

by adding and subtracting $2G(2d)\sin\omega r/r$ under the r-integral and using the identity $\int_0^{\infty}(\sin\omega x/x)\,\mathrm{d}x = (\pi/2)\,\text{sgn}(\omega)$. The method of repeated integration by parts, integrating the trigonometric factor [70], then shows that the integral terms are $O^{\infty}(|\omega|^{-1})$.

The double integral in (3.3.9) is absolutely convergent, allowing us to reverse the order of integration [71]. Then, the large $|\omega|$ of $F^{(2)}_{\text{MIT}}(\omega)$ can be obtained by repeated integration by parts, integrating the trigonometric factor [70]. This gives $F^{(2)}_{\text{MIT}}(\omega) = O^{\infty}(|\omega|^{-1})$. Combining the results, we obtain (3.3.11).

A.5 General Evolving Wall Response Function

Implementing the procedure that leads to (3.3.5), but now using (3.2.12) and (3.2.13), we obtain, for $z, z' > 0$,

$$\begin{aligned}
&W^{(2,\bar{2})}_{\epsilon,\mathrm{GEW}}(u,v;u',v') \\
&\quad = \cos\left([\varphi(u)-\varphi(u')]+[\varphi_1(u)-\varphi_1(u')]\right) W^{(2,\bar{2})}_{\epsilon,\mathrm{NW}} \cos\theta(u)\cos\theta(u') \\
&\qquad + \cos\left([\varphi(u)-\varphi(u')]+[\varphi_2(u)-\varphi_2(u')]\right) W^{(2,\bar{2})}_{\epsilon,\mathrm{NW}} \sin\theta(u)\sin\theta(u') \\
&\qquad + \cos\left([\varphi(u)+\varphi(u')]+[\varphi_2(u)+\varphi_2(u')]\right) W^{(2,\bar{2})}_{\epsilon,\mathrm{MIT}_1} \sin\theta(u)\sin\theta(u') \\
&\qquad + 2\,\mathrm{Re}\Big\{ e^{i[\varphi(u)-\varphi(u')]+i[\varphi_2(u)-\varphi_2(u')]} W^{(2,\bar{2})}_{\epsilon,\mathrm{GEW}_1} \Big\} \sin\theta(u)\sin\theta(u') \\
&\qquad + 2\,\mathrm{Re}\Big\{ e^{-i[\varphi(u)+\varphi(u')]-i[\varphi_2(u)+\varphi_2(u')]} W^{(2,\bar{2})}_{\epsilon,\mathrm{GEW}_2} \Big\} \sin\theta(u)\sin\theta(u'), \qquad \text{(A.5.1)}
\end{aligned}$$

where $W^{(2,\bar{2})}_{\epsilon,\mathrm{NW}}$ is as given by (2.2.9),

$$W^{(2,\bar{2})}_{\epsilon,\mathrm{MIT}_1}(u,v;u',v') = \frac{1}{2\pi^2}\frac{1}{(u-v'-i\epsilon)(v-u'-i\epsilon)} \qquad \text{(A.5.2)}$$

is the second term in (3.3.5) and

$$W^{(2,\bar{2})}_{\epsilon,\mathrm{GEW}_1}(t,z;t',z') = \frac{1}{4\pi^2}\frac{1}{4zz'+2i\epsilon(z-z')+\epsilon^2} \qquad \text{(A.5.3)}$$

$$W^{(2,\bar{2})}_{\epsilon,\mathrm{GEW}_2}(t,z;t',z') = \frac{1}{4\pi^2}\frac{1}{4zz'+2i\epsilon(z+z')-\epsilon^2}. \qquad \text{(A.5.4)}$$

Recall that the two point function is given by the formula (3.3.2). The first three terms in (A.5.1) come from the first term of (3.3.2) while the last two terms in (A.5.1) come from the second term of (3.3.2).

Substituting (A.5.1) into (2.2.5) then gives

$$F_{\mathrm{GEW}}(\omega) = F^{(0)}_{\mathrm{GEW}}(\omega) + F^{(1)}_{\mathrm{GEW}}(\omega) + F^{(2)}_{\mathrm{GEW}}(\omega) \qquad \text{(A.5.5)}$$

where

$$F^{(0)}_{\mathrm{GEW}}(\omega) = \lim_{\epsilon\to 0_+} \frac{-1}{\pi^2}\int_{-\infty}^{\infty} \mathrm{d}u\,\chi(u)\int_0^{\infty}\mathrm{d}s\,\chi(u-s)\,\mathrm{Re}\Big\{\frac{e^{-i\omega s}}{(s-i\epsilon)^2}\Big\} f_0(u,s), \tag{A.5.6}$$

$$F^{(1)}_{\mathrm{GEW}}(\omega) = \lim_{\epsilon\to 0_+} \frac{1}{\pi^2}\int_{-\infty}^{\infty} \mathrm{d}u\,\chi(u)\int_0^{\infty}\mathrm{d}s\,\chi(u-s)\,\mathrm{Re}\Big\{\frac{e^{-i\omega s}}{(s-i\epsilon)^2-4d^2}\Big\} f_1(u,s), \tag{A.5.7}$$

$$F^{(2)}_{\mathrm{GEW}}(\omega) = \frac{1}{4\pi^2 d^2}\int_{-\infty}^{\infty} \mathrm{d}u\,\chi(u)\int_0^{\infty}\mathrm{d}s\,\chi(u-s)\cos(\omega s) f_2(u,s), \tag{A.5.8}$$

and

$$\begin{aligned} f_0(u,s) = {}& \cos\big([\varphi(u)-\varphi(u-s)]+[\varphi_1(u)-\varphi_1(u-s)]\big)\cos\theta(u)\cos\theta(u-s) \\ & + \cos\big([\varphi(u)-\varphi(u-s)]+[\varphi_2(u)-\varphi_2(u-s)]\big)\sin\theta(u)\sin\theta(u-s), \end{aligned} \tag{A.5.9}$$

$$f_1(u,s) = \cos\big([\varphi(u)+\varphi(u-s)]+[\varphi_2(u)+\varphi_2(u-s)]\big)\sin\theta(u)\sin\theta(u-s), \tag{A.5.10}$$

$$\begin{aligned} f_2(u,s) = {}& \big\{\cos([\varphi(u)-\varphi(u-s)]+[\varphi_2(u)-\varphi_2(u-s)]) \\ & + \cos([\varphi(u)+\varphi(u-s)]+[\varphi_2(u)+\varphi_2(u-s)])\big\}\sin\theta(u)\sin\theta(u-s). \end{aligned} \tag{A.5.11}$$

Note that $W^{(2,\bar{2})}_{\mathrm{GEW}_1}$ and $W^{(2,\bar{2})}_{\mathrm{GEW}_2}$ are bounded from above for a detector at rest. In arriving at (A.5.8), we have used that fact and the fact that χ has a compact support to use the dominated convergence theorem and bring the limit $\epsilon \to 0_+$ under the double integral of the response function.

To further simplify the expression, recall the two trigonometric identities

$$\cos(A \pm B) = \cos(A)\cos(B) \mp \sin(A)\sin(B), \tag{A.5.12}$$

$$\cos(A) + \cos(B) = 2\cos\left(\frac{A+B}{2}\right)\cos\left(\frac{A-B}{2}\right). \tag{A.5.13}$$

The first identity allows us to write (A.5.6) and (A.5.7) as

$$F^{(0)}_{\rm GEW}(\omega) = \sum_{j=1}^{4} \lim_{\epsilon\to 0_+} \frac{-1}{\pi^2} \int_{-\infty}^{\infty} \mathrm{d}u\, \chi_j(u) \int_0^{\infty} \mathrm{d}s\, \chi_j(u-s)\, \mathrm{Re}\Big\{ \frac{e^{-i\omega s}}{(s-i\epsilon)^2} \Big\}, \quad \text{(A.5.14)}$$

$$\begin{aligned} F^{(1)}_{\rm GEW}(\omega) = &\lim_{\epsilon\to 0_+} \frac{1}{\pi^2} \int_{-\infty}^{\infty} \mathrm{d}u\, \chi_3(u) \int_0^{\infty} \mathrm{d}s\, \chi_3(u-s)\, \mathrm{Re}\Big\{ \frac{e^{-i\omega s}}{(s-i\epsilon)^2 - 4d^2} \Big\} \\ &- \lim_{\epsilon\to 0_+} \frac{1}{\pi^2} \int_{-\infty}^{\infty} \mathrm{d}u\, \chi_4(u) \int_0^{\infty} \mathrm{d}s\, \chi_4(u-s)\, \mathrm{Re}\Big\{ \frac{e^{-i\omega s}}{(s-i\epsilon)^2 - 4d^2} \Big\}, \end{aligned} \quad \text{(A.5.15)}$$

where χ_j for $j = 1, 2, 3, 4$ are given by (3.3.19) – (3.3.22). The second identity, on the other hand, gives

$$F^{(2)}_{\rm GEW}(\omega) = \frac{1}{2\pi^2 d^2} \int_{-\infty}^{\infty} \mathrm{d}u\, \chi_3(u) \int_0^{\infty} \mathrm{d}s\, \chi_3(u-s) \cos(\omega s). \quad \text{(A.5.16)}$$

Each term in (A.5.14) is none other than the response of the detector in absence of wall, but with a modified switching function given by one of (3.3.19) - (3.3.22). Similarly, each term in (A.5.15) is simply $F^{(1)}_{\rm MIT}(\omega)$ with a modified switching function. Comparing (A.5.16) and (3.3.9), we notice a similar pattern. Since derivations of regulator-free expressions of $F_{\rm NW}(\omega)$ and $F^{(1)}_{\rm MIT}(\omega)$ rely only on the fact that χ is bounded and has compact support [53], similar results follow immediately. Together with the fact that

$$\sum_{j=1}^{4} [\chi_j(\tau)]^2 = [\chi(\tau)]^2 \quad \text{(A.5.17)}$$

for any functional form of $\varphi(\tau)$, $\varphi_1(\tau)$, $\varphi_2(\tau)$ and $\theta(\tau)$, we obtain (3.3.13) and (3.3.14).

A.6 Wall Creation Response Function

A.6.1 Large Energy Gap Limit for Smooth Wall Creation

Recall first that (3.3.23) is valid for a general evolving wall. Therefore, the large $|\omega|$ limit of $F_{\rm WC}(\omega)$ can easily be obtained by substituting (3.3.30) and (3.3.31) into (3.3.23).

To write the large $|\omega|$ limit of $F_{\rm WC}(\omega)$ in the form given by (3.3.32), we need the expressions for $\int_{-\infty}^{\infty} \mathrm{d}u\, \chi_3(u)\chi_3(u-2d)$ and $\int_{-\infty}^{\infty} \mathrm{d}u\, \chi_4(u)\chi_4(u-2d)$ where χ_3 and χ_4 are given respectively by (3.3.30) and (3.3.31). Since the expressions are slightly different for $2d < \delta$ and $2d \geq \delta$, let us consider the two cases in turn.

Consider first $2d < \delta$. Since $\chi_3(u-2d)$ is simply $\chi_3(u)$ that is shifted by $u = 2d$ to the right on a χ_3-to-u graph, $\chi_3(u)\chi_3(u-2d)$ vanishes for $u \leq t_0 + 2d$ when χ_3 is given by (3.3.30). Therefore, we have that

$$
\begin{aligned}
&\int_{-\infty}^{\infty} \mathrm{d}u\, \chi_3(u)\chi_3(u-2d) \\
&\quad = \int_{t_0+2d}^{t_0+\delta} \mathrm{d}u \cos(2nh_1(u)) \sin h_1(u)\chi(u) \\
&\qquad\qquad \times \cos(2nh_1(u-2d)) \sin h_1(u-2d)\chi(u-2d) \\
&\qquad + (-1)^n \int_{t_0+\delta}^{t_0+2d+\delta} \mathrm{d}u\, \chi(u) \cos(2nh_1(u-2d)) \sin h_1(u-2d)\chi(u-2d) \\
&\qquad + \int_{t_0+2d+\delta}^{\infty} \mathrm{d}u\, \chi(u)\chi(u-2d) \\
&\quad = \int_{t_0+2d}^{t_0+\delta} \mathrm{d}u \cos(2nh_1(u)) \sin h_1(u)\chi(u) \\
&\qquad\qquad \times \cos(2nh_1(u-2d)) \sin h_1(u-2d)\chi(u-2d) \\
&\qquad + (-1)^n \int_{t_0+\delta}^{t_0+2d+\delta} \mathrm{d}u\, \chi(u) \cos(2nh_1(u-2d)) \sin h_1(u-2d)\chi(u-2d) \\
&\qquad + \int_{t_0+2d}^{\infty} \mathrm{d}u\, \chi(u)\chi(u-2d) - \int_{t_0+2d}^{t_0+2d+\delta} \mathrm{d}u\, \chi(u)\chi(u-2d), \qquad \text{(A.6.1)}
\end{aligned}
$$

where we have added and subtracted $\int_{t_0+2d}^{t_0+2d+\delta} \mathrm{d}u\, \chi(u)\chi(u-2d)$ to obtain the second equality. By a similar observation, when χ_4 is given by (3.3.31), we have

$$\begin{aligned}
&\int_{-\infty}^{\infty} \mathrm{d}u\, \chi_4(u)\chi_4(u-2d) \\
&\quad = \int_{t_0+2d}^{t_0+\delta} \mathrm{d}u \sin(2nh_1(u)) \sin h_1(u)\chi(u) \\
&\qquad\qquad \times \sin(2nh_1(u-2d)) \sin h_1(u-2d)\chi(u-2d). \qquad \text{(A.6.2)}
\end{aligned}$$

Substituting (A.6.1) and (A.6.2) into (3.3.23), and recollecting terms, we obtain (3.3.32) with $\Delta F_{\mathrm{WC}}(\omega)$ given by

$$\begin{aligned}
\Delta F_{\mathrm{WC}}(\omega) = &\int_{t_0+2d}^{t_0+\delta} \mathrm{d}u \cos(2nh_1(u)) \sin h_1(u)\chi(u) \\
&\qquad \times \cos(2nh_1(u-2d)) \sin h_1(u-2d)\chi(u-2d) \\
&+ (-1)^n \int_{t_0+\delta}^{t_0+2d+\delta} \mathrm{d}u\, \chi(u) \cos(2nh_1(u-2d)) \sin h_1(u-2d)\chi(u-2d) \\
&- \int_{t_0+2d}^{t_0+2d+\delta} \mathrm{d}u\, \chi(u)\chi(u-2d) \\
&- \int_{t_0+2d}^{t_0+\delta} \mathrm{d}u \sin(2nh_1(u)) \sin h_1(u)\chi(u) \\
&\qquad \times \sin(2nh_1(u-2d)) \sin h_1(u-2d)\chi(u-2d). \qquad \text{(A.6.3)}
\end{aligned}$$

Since each integrand is bounded, each integral in (A.6.3), and hence $\Delta F_{\mathrm{WC}}(\omega)$, is $O(\delta)$. Note that the last term in (A.6.3) vanishes when $n = 0$.

Next, consider $2d \geq \delta$. By a similar observation as above, we obtain

$$\begin{aligned}
&\int_{-\infty}^{\infty} \mathrm{d}u\, \chi_3(u)\chi_3(u-2d) \\
&\quad = (-1)^n \int_{t_0+2d}^{t_0+2d+\delta} \mathrm{d}u\, \chi(u) \cos(2nh_1(u-2d)) \sin h_1(u-2d)\chi(u-2d) \\
&\qquad + \int_{t_0+2d}^{\infty} \mathrm{d}u\, \chi(u)\chi(u-2d) - \int_{t_0+2d}^{t_0+2d+\delta} \mathrm{d}u\, \chi(u)\chi(u-2d), \qquad \text{(A.6.4)}
\end{aligned}$$

and

$$\int_{-\infty}^{\infty} \mathrm{d}u\, \chi_4(u)\chi_4(u-2d) = 0, \tag{A.6.5}$$

where (A.6.5) follows from the fact that $\chi_4(u) \neq 0$ only for $t_0 < \tau < t_0 + \delta$. It follows that, when $2d \geq \delta$, $\Delta F_{\mathrm{WC}}(\omega)$ in (3.3.32) is given by

$$\begin{aligned}\Delta F_{\mathrm{WC}}(\omega) = (-1)^n \int_{t_0+2d}^{t_0+2d+\delta} \mathrm{d}u\, \chi(u) \cos(2nh_1(u-2d)) \sin h_1(u-2d)\chi(u-2d) \\ - \int_{t_0+2d}^{t_0+2d+\delta} \mathrm{d}u\, \chi(u)\chi(u-2d).\end{aligned} \tag{A.6.6}$$

A.6.2 Rapid Creation Limit at Finite Energy Gap

We start by analysing the wall creation version of (3.3.13) and (3.3.16), which are denoted by $F^{(0)}_{\mathrm{WC}}(\omega)$ and $\Delta F^{(0)}_{\mathrm{WC}}(\omega)$ respectively. The convergence of the latter relies on us performing the u-integral before the s-integral, but not the summation over $j = 1, ..., 4$. Therefore, we may do the latter first to obtain

$$\sum_{j=1}^{4} \chi_j(u)[\chi_j(u) - \chi_j(u-s)] = \chi(u)[\chi(u) - \chi(u-s)] + \chi(u)\chi(u-s)\hat{\chi}(u,s), \tag{A.6.7}$$

where

$$\hat{\chi}(u,s) := 1 - \cos(2n[\theta(u) - \theta(u-s)]) \cos(\theta(u) - \theta(u-s)). \tag{A.6.8}$$

This allows us to write

$$F^{(0)}_{\mathrm{WC}}(\omega) = F_{\mathrm{NW}}(\omega) + \frac{1}{\pi^2} \int_{-\infty}^{\infty} \mathrm{d}u\, \chi(u) \int_0^{\infty} \mathrm{d}s\, \chi(u-s) \cos(\omega s) \frac{\hat{\chi}(u,s)}{s^2} \tag{A.6.9}$$

where the interchange of integration order in the second term is justified by absolute convergence of the double integral [71], which in turn follows from bound-

edness of $\hat{\chi}(u,s)/s^2$ at $s=0$. For convenience, we shall denote the second term in (A.6.9) above as $\Delta F^{(0)}_{\rm RWC}(\omega)$.

From (3.1.11), we can deduce the values of the $\hat{\chi}(u,s)$ in different regions of us-plane and obtain

$$\Delta F^{(0)}_{\rm RWC}(\omega) = \frac{1}{\pi^2}\int_{t_0+\delta}^{\infty} {\rm d}u\,\chi(u)\int_{u-t_0}^{\infty} {\rm d}s\,\chi(u-s)\frac{\cos(\omega s)}{s^2} + O(\delta). \tag{A.6.10}$$

The term $O(\delta)$ contains all double integrals whose absolute values can be estimated to be of order δ. Adding and subtracting $\chi(u-s)/s^2$ under the s-integral, we have

$$\begin{aligned}\Delta F^{(0)}_{\rm RWC}(\omega) = &-\frac{1}{\pi^2}\int_{t_0+\delta}^{\infty} {\rm d}u\,\chi(u)\int_{u-t_0}^{\infty} {\rm d}s\,\chi(u-s)\frac{1-\cos(\omega s)}{s^2}\\ &+\frac{1}{\pi^2}\int_{t_0+\delta}^{\infty} {\rm d}u\,\chi(u)\int_{u-t_0}^{\infty} {\rm d}s\,\frac{\chi(u-s)}{s^2} + O(\delta).\end{aligned} \tag{A.6.11}$$

Now, we add and subtract a double integral similar to the first term but with the outer u-integral integrating from $u=t_0$ to $u=t_0+\delta$. One of them can be combined with the first term to make the outer u-integral starts from $u=t_0$ while the other term, since its integrand is bounded and has a compact support, can be included in the $O(\delta)$ term. Then, we can write $\Delta F^{(0)}_{\rm RWC}(\omega) = \Delta F^{(0)}_{\rm RWC,ind}(\omega) + \Delta F^{(0)}_{\rm RWC,dep}(\omega) + O(\delta)$, where

$$\Delta F^{(0)}_{\rm RWC,ind}(\omega) = \frac{1}{\pi^2}\int_{t_0+\delta}^{\infty} {\rm d}u\,\chi(u)\int_{u-t_0}^{\infty} {\rm d}s\,\frac{\chi(u-s)}{s^2}, \tag{A.6.12}$$

$$\Delta F^{(0)}_{\rm RWC,dep}(\omega) = -\frac{1}{\pi^2}\int_{0}^{\infty} {\rm d}s\,\frac{1-\cos(\omega s)}{s^2} f(s), \tag{A.6.13}$$

and $f(s)$ is as given in (3.3.37). The subscripts "ind" and "dep" refer to the fact that $\Delta F^{(0)}_{\rm RWC,ind}(\omega)$ and $\Delta F^{(0)}_{\rm RWC,dep}(\omega)$ are the ω-independent and ω-dependent part of $\Delta F^{(0)}_{\rm RWC}(\omega)$ respectively. To obtain $\Delta F^{(0)}_{\rm RWC,dep}(\omega)$ in the form given in (A.6.13), we have changed the order of integration and redefined the integration variable of the inner integral to obtain $f(s)$ that is manifestly odd in s.

By integration by parts, integrating $1/s^2$, we may write $\Delta F^{(0)}_{\mathrm{RWC,ind}}(\omega)$ as

$$\Delta F^{(0)}_{\mathrm{RWC,ind}}(\omega) = \frac{\chi(t_0)}{\pi^2}\int_{t_0+\delta}^{\infty} \mathrm{d}u\, \frac{\chi(u)}{u-t_0} - \frac{1}{\pi^2}\int_{t_0}^{\infty} \mathrm{d}u\, \chi(u) \int_{u-t_0}^{\infty} \mathrm{d}s\, \frac{\chi'(u-s)}{s} + \frac{1}{\pi^2}\int_{t_0}^{t_0+\delta} \mathrm{d}u\, \chi(u) \int_{u-t_0}^{\infty} \mathrm{d}s\, \frac{\chi'(u-s)}{s}. \tag{A.6.14}$$

Boundedness and smoothness of χ then implies that the last term is $O(\delta)$. To isolate the divergent part, we integrate the first term in (A.6.14) by parts to obtain a term proportional to $\ln\delta$, a finite integral term and an $O(\delta)$ integral. Collecting the result, we have

$$\Delta F^{(0)}_{\mathrm{RWC,ind}}(\omega) = -\frac{[\chi(t_0)]^2}{\pi^2}\ln\delta - \frac{\chi(t_0)}{\pi^2}\int_{t_0}^{\infty} \mathrm{d}u\, \chi'(u)\ln(u-t_0) - \frac{1}{\pi^2}\int_{t_0}^{\infty} \mathrm{d}u\, \chi(u) \int_{u-t_0}^{\infty} \mathrm{d}s\, \frac{\chi'(u-s)}{s} + O(\delta). \tag{A.6.15}$$

Next, we shift our attention to (A.6.13). Introducing a temporary cutoff in the lower limit of s-integral followed by addition and subtraction of $(\cos(\omega s)/s^2)sf'(0)$ under the integral, the term can be written as

$$\Delta F^{(0)}_{\mathrm{RWC,dep}}(\omega) = -\frac{1}{\pi^2}\lim_{\epsilon\to 0_+}\left\{\int_{\epsilon}^{\infty} \mathrm{d}s\, \frac{f(s)}{s^2} - \int_{\epsilon}^{\infty} \mathrm{d}s\, \frac{\cos(\omega s)}{s} f'(0) - \int_{\epsilon}^{\infty} \mathrm{d}s \cos(\omega s)\frac{f(s)-sf'(0)}{s^2}\right\}. \tag{A.6.16}$$

Integration by parts of the first term, integrating s^{-1}, gives

$$\int_{\epsilon}^{\infty} \mathrm{d}s\, \frac{f(s)}{s^2} = -f'(0)\ln\epsilon - \int_{\epsilon}^{\infty} \mathrm{d}s \left(\frac{sf'(s)-f(s)}{s^2}\right)\ln s + O(\epsilon), \tag{A.6.17}$$

where the first and last terms arise from the expansion of $f(\epsilon)/\epsilon$ around $\epsilon = 0$. Using small argument form of cosine integral $\mathrm{Ci}(|\omega|\epsilon)$ (see Eq. 6.6.6 of [72]), the second term in (A.6.16) yields a term that cancels $-f'(0)\ln\epsilon$ in (A.6.17). This

allows us to take the limit $\epsilon \to 0_+$ and obtain

$$\Delta F^{(0)}_{\mathrm{RWC,dep}}(\omega) = -\frac{[\chi(t_0)]^2}{\pi^2}(\gamma + \ln|\omega|) - \frac{1}{\pi^2}\int_0^\infty \mathrm{d}s\, \frac{f(s) - sf'(s)}{s^2}(s)\ln s + \frac{1}{\pi^2}\int_0^\infty \mathrm{d}s \cos(\omega s)\frac{f(s) - sf'(0)}{s^2}. \tag{A.6.18}$$

Combining (A.6.15) and (A.6.18) then gives $F^{(0)}_{\mathrm{WC}}(\omega) = -([\chi(t_0)]^2/\pi^2)\ln(|\omega|\delta) + F_{\mathrm{NW}}(\omega) + F^{(0)}_{\mathrm{RWC}}(\omega) + O(\delta)$.

Now, consider the wall creation version of (3.3.14) together with (3.3.17), which are denoted $F^{(1)}_{\mathrm{WC}}(\omega)$ and $\Delta F^{(1)}_{\mathrm{WC}}(\omega)$ respectively. Since we are taking the limit $\delta \to 0$, we may assume $\delta < 2d$ *a priori*. From (3.3.31), it follows that $G_4(2d + r) = 0$ for $r \geq 0$. Substituting this into (3.3.17) gives us terms whose upper bound of absolute value proportional to

$$\left|\int_{2d-\delta}^{2d} \mathrm{d}r\, \frac{G_4(2d - r)}{r}\right| = O(\delta). \tag{A.6.19}$$

Thus, terms containing G_4 contribute at most $O(\delta)$. From (3.3.30), we firstly obtain $G_3(2d) = H_1(2d) + O(\delta)$ where $H_1(y)$ is given by (3.3.38). Next, substituting (3.3.30) into (3.3.17) gives us the integrals in (3.3.35) plus double integrals which are $O(\delta)$. To show the latter, however, one needs to be careful not to do the outer r-integral term-by-term unless the inner u-integral is finite. Collecting the results, we get $F^{(1)}_{\mathrm{WC}}(\omega) = F^{(1)}_{\mathrm{RWC}}(\omega) + O(\delta)$.

Finally, consider the wall creation version of (3.3.15) denoted $F^{(2)}_{\mathrm{WC}}(\omega)$. Using (3.3.30), we obtain $F^{(2)}_{\mathrm{RWC}}(\omega)$ as given in (3.3.36) plus some remainder $O(\delta)$. The response function as presented in (3.3.33) then follows when we collect all $O(\delta)$ terms together.

Appendix B

Supplement for Moving Wall Analysis

In this appendix, we derive the late time transition rate (4.2.19).

B.1 Finite Switch-On Time (H_{int} or $H_{\text{int}}^{\text{no}}$)

We start by considering a detector that is switched on at a strictly finite τ_0. The detector may interact either via (2.2.1) or (2.2.13). For the latter, ignore the analysis of $\dot{F}^{(2)}_{\text{MW}}(\omega,\tau)$.

Consider first $\dot{F}^{(0)}_{\text{MW}}(\omega,\tau)$. Substituting the collapsing star trajectory (4.2.16) into (4.2.12) and letting $h(\tau)=(1+e^{a\tau})^{-1}$, we have

$$\begin{aligned}\dot{F}^{(0)}_{\text{MW}}(\omega,\tau) = -\frac{\omega}{\pi}\Theta(-\omega) + \frac{1}{\pi^2}\int_0^{\Delta\tau} \mathrm{d}s\cos(\omega s)\left(\frac{1}{s^2} - X_\tau(s)\right) \\ + \frac{1}{\pi^2}\int_{\Delta\tau}^{\infty}\mathrm{d}s\,\frac{\cos(\omega s)}{s^2},\end{aligned} \tag{B.1.1}$$

where

$$X_\tau(s) = \frac{a h(\tau) e^{\frac{as}{2}}}{s(1+h(\tau)(e^{as}-1))^{\frac{1}{2}}\ln(1+h(\tau)(e^{as}-1))}. \tag{B.1.2}$$

Adding and subtracting an integral that has an integrand identical to the second term of (B.1.1), including the factor π^{-2}, but integrates from $s = \Delta\tau$ to $s = \infty$, we obtain

$$\dot{F}^{(0)}_{\rm MW}(\omega,\tau) = -\frac{\omega}{\pi}\Theta(-\omega) + \frac{1}{\pi^2}\int_0^\infty \mathrm{d}s\cos(\omega s)\left(\frac{1}{s^2} - X_\tau(s)\right) + \frac{1}{\pi^2}\int_{\Delta\tau}^\infty \mathrm{d}s\cos(\omega s)X_\tau(s). \tag{B.1.3}$$

Focusing on $s > 0$ that we are concerned with, partially differentiating $X_\tau(s)$ with respect to τ or h shows that $X_\tau(s)$ for fixed s monotonically decreases as τ increases. The upper and lower bounds of $X_\tau(s)$ are thus given by $X_-(s)$ and $X_+(s)$ respectively where

$$X_-(s) = \lim_{\tau\to-\infty} X_\tau(s) = \frac{1}{s^2}, \tag{B.1.4}$$

$$X_+(s) = \lim_{\tau\to\infty} X_\tau(s) = \frac{a}{2s\sinh\left(\frac{as}{2}\right)}. \tag{B.1.5}$$

Consider the limit $\tau \to \infty$ of $\dot{F}^{(0)}_{\rm MW}(\omega,\tau)$. From the upper bound of $X_\tau(s)$, which is given by (B.1.4), it follows that the last term in (B.1.3) is $O(1/\Delta\tau)$. Adding and subtracting $X_+(s)$ under the first integral in (B.1.3), and using the fact that $\cos(\omega s)[X_+(s) - 1/s^2]$ is an even function of s, we have

$$\dot{F}^{(0)}_{\rm MW}(\omega,\tau) = -\frac{\omega}{\pi}\Theta(-\omega) + \frac{1}{2\pi^2}\int_{-\infty}^\infty \mathrm{d}s\cos(\omega s)\left(\frac{1}{s^2} - X_+(s)\right) - \frac{1}{\pi^2}\int_0^\infty \mathrm{d}s\cos(\omega s)\left(X_\tau(s) - X_+(s)\right) + O\left(\frac{1}{\Delta\tau}\right). \tag{B.1.6}$$

Since $X_\tau(s) - X_+(s) \to 0$ pointwise in a monotone manner for $s \geq 0$, the magnitude of the third term in (B.1.6) decreases as τ increases and eventually vanishes in the limit $\tau \to \infty$.

Deforming the integration contour of the second term in (B.1.6) to a contour C in the complex s plane along the real axis but with a dip into the lower

half-plane near $s = 0$,

$$\dot{F}^{(0)}_{\rm MW}(\omega,\tau) = -\frac{\omega}{\pi}\Theta(-\omega) + \frac{1}{2\pi^2}\int_C \mathrm{d}s\,\frac{\cos(\omega s)}{s^2} - \frac{a}{4\pi^2}\int_C \mathrm{d}s\,\frac{\cos(\omega s)}{s\sinh\left(\frac{as}{2}\right)} + o(1). \tag{B.1.7}$$

Writing $\cos(\omega s) = 1 - (1 - \cos(\omega s))$, the integral factor of the second term in (B.1.7) becomes a sum of two integrals, one with the integrand s^{-2} and while the other $(1-\cos(\omega s))s^{-2}$. Setting the dip to be an anticlockwise semicircle with radius $r > 0$, we find that the former vanishes. To calculate the latter, deform C back to being a contour on the real line, integrate the integral by parts and use the identity $\int_0^\infty \sin(ax)/x\,\mathrm{d}x = (\pi/2)\,\mathrm{sgn}(a)$. Collecting the results, we find that the first two terms of (B.1.7) combine to give $\omega/2\pi$.

To evaluate the third term of (B.1.7), consider the integral factor

$$I(\omega) = \int_C \mathrm{d}s\,\frac{\cos(\omega s)}{s\sinh\left(\frac{as}{2}\right)}. \tag{B.1.8}$$

While the integrand of $I(\omega)$ has a singularity at $s = 0$, the integrand of $\partial I/\partial\omega$, obtained by differentiating $I(\omega)$ with respect to ω under the integral, is regular on the real line. Deforming C in $\partial I/\partial\omega$ back to being a contour on the real line and using 3.981.1 of [73], we find that $\partial I/\partial\omega = -(2\pi/a)\tanh(\pi\omega/a)$. By integrating $\partial I/\partial\omega$ with respect to ω, it follows that

$$I(\omega) = -2\ln\left(\cosh\left(\frac{\pi\omega}{a}\right)\right) + I_0, \tag{B.1.9}$$

where I_0 is independent of ω. To determine the value of I_0, notice that it is the value of $I(\omega)$ when $\omega = 0$. Hence, consider $I(0)$ and deform C so that it is the large R limit $C_1 + C_2 + C_3$ where C_1 runs from $s = -R$ to $s = -R - i\pi/a$ along $\mathrm{Re}\{s\} = -R$, C_2 runs from $s = -R - i\pi/a$ to $s = R - i\pi/a$ along $\mathrm{Im}\{s\} = -\pi/a$ and C_3 runs from $s = R - i\pi/a$ to $s = R$ along $\mathrm{Re}\{s\} = R$. The contributions from C_1 and C_3 are both $O(1/(R\sinh(aR/2)))$ and hence vanish as

$R \to \infty$. Parametrising C_2 as $x - i\pi/a$ for $x \in (-\infty, \infty)$ and using the identity $\sinh(x - i\pi/2) = -i\cosh(x)$, we find that

$$I(0) = -\frac{a}{\pi}\int_{-\infty}^{\infty} \frac{\mathrm{d}x}{(1 + a^2x^2/\pi^2)(\cosh(ax/2))} + \frac{ia^2}{\pi^2}\int_{-\infty}^{\infty} \frac{x\,\mathrm{d}x}{(1 + a^2x^2/\pi^2)(\cosh(ax/2))}. \tag{B.1.10}$$

The imaginary part of (B.1.10) vanishes since the integrand is odd. The real part can be evaluated using 3.522.8 of [73] after a change of variable to $y = ax/\pi$, giving $I(0) = -2\ln 2$. Combining the results above, we find that, as $\tau \to \infty$,

$$\dot{F}^{(0)}_{\rm MW}(\omega, \tau) = \frac{a}{2\pi^2}\ln\Big(1 + e^{\frac{2\pi\omega}{a}}\Big) + o(1). \tag{B.1.11}$$

Let us now look at $\dot{F}^{(1)}_{\rm MW}(\omega, \tau)$. To keep the analysis neat, we shall not write $w'(\tau)$ and $\Delta t_{\rm ret}(\tau)$ explicitly. For reference, we note here that

$$w'(\tau) = \frac{1}{1 + e^{a\tau}}, \tag{B.1.12}$$

$$w''(\tau) = -\frac{aw'(\tau)}{1 + e^{-a\tau}}, \tag{B.1.13}$$

$$\Delta t_{\rm ret}(\tau) = \tau + 2d + \frac{1}{a}\ln\big(1 + e^{-a\tau}\big) \tag{B.1.14}$$

for the collapsing star trajectory (4.2.16). In the case where $\tau_0 \geq -2d$, we have $\Delta t_{\rm ret}(\tau) > \Delta\tau$ for all $\tau \in (\tau_0, \infty)$. This implies that we may set $\epsilon = 0$ under the integral of (4.2.13). Since $\Big|\cos(\omega s)\sqrt{w'(\tau)w'(\tau - s)}\Big| \leq 1$ and $s + \Delta t_{\rm ret}(\tau - s) \geq \Delta\tau$ in this case, it follows that

$$\Big|\dot{F}^{(1)}_{\rm MW}(\omega, \tau)\Big| \leq -\frac{1}{\pi^2\Delta\tau}\ln\bigg(1 - \frac{\Delta\tau}{\Delta t_{\rm ret}(\tau)}\bigg), \tag{B.1.15}$$

which is valid for any finite τ. Implementing L'Hôpital's rule to the right hand side of (B.1.15), it follows that $\dot{F}^{(1)}_{\rm MW}(\omega, \tau) = O(1/\Delta\tau)$ in the limit $\tau \to \infty$.

In the case of $-\infty < \tau_0 < -2d$, there exists τ_c such that $\Delta\tau = \Delta t_{\rm ret}(\tau)$ when $\tau = \tau_c$ and $\Delta\tau > \Delta t_{\rm ret}(\tau)$ when $\tau > \tau_c$. Since we are interested in the late time limit $\tau \to \infty$, the latter will eventually necessarily be satisfied. Starting at some τ such that $\Delta\tau > \Delta t_{\rm ret}(\tau)$, we integrate (4.2.13) by parts, integrating the factor $(s - \Delta t_{\rm ret}(\tau) - i\epsilon)^{-1}$ in the integrand, and take the limit $\epsilon \to 0_+$ to obtain

$$
\begin{aligned}
&\dot{F}^{(1)}_{\rm MW}(\omega,\tau) \\
&\quad = \frac{1}{\pi^2}\bigg(\frac{\cos(\omega\Delta\tau)\sqrt{w'(\tau)w'(\tau_0)}}{\Delta t_{\rm ret}(\tau) + w(\tau) - w(\tau_0)}\ln(\Delta\tau - \Delta t_{\rm ret}(\tau)) - \frac{w'(\tau)}{\Delta t_{\rm ret}(\tau)}\ln(\Delta t_{\rm ret}(\tau))\bigg) \\
&\qquad + \frac{1}{\pi^2}\sqrt{w'(\tau)}\bigg(\int_0^{\Delta\tau} \mathrm{d}s\,\mathrm{Re}\{q_1(\tau,s)\}\ln|s - \Delta t_{\rm ret}(\tau)| \\
&\qquad\qquad + \frac{1}{2}\int_0^{\Delta\tau} \mathrm{d}s\,\mathrm{Re}\{q_2(\tau,s)\}\ln|s - \Delta t_{\rm ret}(\tau)| \\
&\qquad\qquad + \omega\int_0^{\Delta\tau} \mathrm{d}s\,\mathrm{Re}\{q_3(\tau,s)\}\ln|s - \Delta t_{\rm ret}(\tau)|\bigg) \\
&\qquad - \frac{1}{\pi}\sqrt{w'(\tau)}\bigg(\int_0^{\Delta t_{\rm ret}(\tau)} \mathrm{d}s\,\mathrm{Re}\{iq_1(\tau,s)\} + \frac{1}{2}\int_0^{\Delta t_{\rm ret}(\tau)} \mathrm{d}s\,\mathrm{Re}\{iq_2(\tau,s)\} \\
&\qquad\qquad + \omega\int_0^{\Delta t_{\rm ret}(\tau)} \mathrm{d}s\,\mathrm{Re}\{iq_3(\tau,s)\}\bigg),
\end{aligned}
\tag{B.1.16}
$$

where

$$
q_1(\tau,s) = \frac{e^{-i\omega s}(w'(\tau-s))^{\frac{3}{2}}}{(s + \Delta t_{\rm ret}(\tau-s))^2}, \tag{B.1.17}
$$

$$
q_2(\tau,s) = \frac{e^{-i\omega s}}{s + \Delta t_{\rm ret}(\tau-s)}\frac{w''(\tau-s)}{\sqrt{w'(\tau-s)}}, \tag{B.1.18}
$$

$$
q_3(\tau,s) = \frac{ie^{-i\omega s}\sqrt{w'(\tau-s)}}{s + \Delta t_{\rm ret}(\tau-s)}. \tag{B.1.19}
$$

The boundary terms in (B.1.16) clearly vanish as $\tau \to \infty$. For the integral terms, observe that, using (B.1.12) – (B.1.14), we have

$$
|q_1(\tau,s)| = |iq_1(\tau,s)| \le \frac{1}{4d^2}, \tag{B.1.20}
$$

$$
|q_2(\tau,s)| = |iq_2(\tau,s)| \le \frac{a}{2d}, \tag{B.1.21}
$$

$$
|q_3(\tau,s)| = |iq_3(\tau,s)| \le \frac{1}{2d}, \tag{B.1.22}
$$

uniformly in τ for $s \geq 0$. Each of the first three integrals in (B.1.16) then is bounded in magnitude by a τ-independent constant times

$$\begin{aligned} J(\tau) &= \sqrt{w'(\tau)} \int_0^{\Delta\tau} \mathrm{d}s \, |\ln|s - \Delta t_{\rm ret}(\tau)|| \\ &= \sqrt{w'(\tau)}\big[4 - \Delta\tau + \Delta t_{\rm ret}(\tau) \ln \Delta t_{\rm ret}(\tau) \\ &\qquad + (\Delta\tau - \Delta t_{\rm ret}(\tau)) \ln(\Delta\tau - \Delta t_{\rm ret}(\tau))\big], \end{aligned} \tag{B.1.23}$$

while each of the last three integrals is bounded in magnitude by a τ-independent constant times

$$K(\tau) = \sqrt{w'(\tau)} \int_0^{\Delta t_{\rm ret}(\tau)} \mathrm{d}s = \sqrt{w'(\tau)} \Delta t_{\rm ret}(\tau). \tag{B.1.24}$$

As $\tau \to \infty$, both $J(\tau)$ and $K(\tau)$ are exponentially suppressed by the prefactor $\sqrt{w'(\tau)}$, implying that each integral term in (B.1.16) vanishes at late times. Combining all the results above, it follows that $\dot{F}^{(1)}_{\rm MW}(\omega, \tau)$ vanishes in the limit $\tau \to \infty$ for any finite τ_0.

Finally, consider $\dot{F}^{(2)}_{\rm MW}(\omega, \tau)$. With the change of variable $s \to r = s/\Delta\tau$, (4.2.14) reads

$$\dot{F}^{(2)}_{\rm MW}(\omega, \tau) = \frac{2\Delta\tau\sqrt{w'(\tau)}}{\pi^2 \Delta t_{\rm ret}(\tau)} \int_0^1 \mathrm{d}r \cos(\omega r \Delta\tau) \frac{\sqrt{w'(\tau - r\Delta\tau)}}{\Delta t_{\rm ret}(\tau - r\Delta\tau)}. \tag{B.1.25}$$

Since $w'(\tau - r\Delta\tau) \leq 1$ and $\Delta t_{\rm ret}(\tau - r\Delta\tau) \geq 2d$, it follows that the integral factor in (B.1.25) is bounded by a τ-independent constant. At late times, the factor $\Delta\tau/\Delta t_{\rm ret}(\tau)$ converges to unity while $w'(\tau)$ vanishes exponentially. Hence, $\dot{F}^{(2)}_{\rm MW}(\omega, \tau) = o(1)$ as $\tau \to \infty$.

Combining the results, we see that only $\dot{F}^{(0)}_{\rm MW}(\omega, \tau)$ has a non-vanishing contribution (B.1.11) to the transition rate at late times when τ_0 is strictly finite, regardless of which interaction Hamiltonian governs the detector-field interaction. The result (4.2.19) hence follows.

B.2 Asymptotically Early Switch-On Time ($H_{\rm int}^{\rm no}$)

Now, consider a detector interacting via (2.2.13) and is switched on in the asymptotic past. Using the fact that the last term in (4.2.12) is $O(1/\Delta\tau)$ as $\tau_0 \to -\infty$, it follows that $\dot{F}^{(0)}_{\rm MW}(\omega,\tau)$ is now given only by the first two terms of (B.1.3). Since the last term in (B.1.3) vanishes as $\tau \to \infty$ when τ_0 is finite, the late time limit of $\dot{F}^{(0)}_{\rm MW}(\omega,\tau)$ is again given by (B.1.11).

For $\dot{F}^{(1)}_{\rm MW}(\omega,\tau)$, we can always choose to split the integration interval of (4.2.13), which is now $[0,\infty)$, into $[0,\tau-\tau') \cup [\tau-\tau',\infty)$ where $\tau' < \tau$ is some arbitrary constant. Choosing $\tau' < -2d$, in particular, and start analysing at τ such that $\tau - \tau' > \Delta t_{\rm ret}(\tau)$, we may then use similar method as above to show that the contribution from the interval $[0,\tau-\tau')$ vanishes at late times. The contribution from the other interval $[\tau-\tau',\infty)$ is given by

$$\Delta\dot{F}^{(1)}_{\rm MW}(\omega,\tau) = \frac{1}{\pi^2}\int_{\tau-\tau'}^{\infty} {\rm d}s\, \frac{\cos(\omega s)\sqrt{w'(\tau)w'(\tau-s)}}{(s-\Delta t_{\rm ret}(\tau))(s+\Delta t_{\rm ret}(\tau-s))}, \tag{B.2.1}$$

where we have set $\epsilon = 0$ since the integrand has no singularity. From the inequality $\Delta t_{\rm ret}(\tau-s) \geq 2d$, it follows that $s + \Delta t_{\rm ret}(\tau-s) \geq s + 2d$. Together with $\left|\cos(\omega s)\sqrt{w'(\tau)w'(\tau-s)}\right| \leq 1$, we have

$$\left|\Delta\dot{F}^{(1)}_{\rm MW}(\omega,\tau)\right| \leq -\frac{1}{\pi^2(2d+\Delta t_{\rm ret}(\tau))}\ln\left(\frac{1-\frac{\Delta t_{\rm ret}(\tau)}{\tau-\tau'}}{1+\frac{2d}{\tau-\tau'}}\right), \tag{B.2.2}$$

which implies that $\Delta\dot{F}^{(1)}_{\rm MW}(\omega,\tau)$ vanishes as $\tau \to \infty$.

Combining the results, we see that (4.2.19) remains valid in the case of asymptotically early switch-on time when the detector interacts via the normally-ordered interaction Hamiltonian $H_{\rm int}^{\rm no}$ given by (2.2.13).

Bibliography

[1] N. D. Birrell and P. C. W. Davies. *Quantum Fields in Curved Space*. Cambridge Monographs on Mathematical Physics. Cambridge University Press, Cambridge, UK, 1984.

[2] S. A. Fulling. *Aspects of Quantum Field Theory in Curved Space-Time*. London Mathematical Society Student Texts. Cambridge University Press, Cambridge, UK, 1989.

[3] R. M. Wald. *Quantum Field Theory in Curved Space-Time and Black Hole Thermodynamics*. Chicago Lectures in Physics. University of Chicago Press, Chicago, IL, 1995.

[4] L. H. Ford. Quantum field theory in curved space-time. In *Particles and Fields: Proceedings of the 9th Jorge Andre Swieca Summer School, Campos do Jordao, Brazil, February 16-28, 1997*, pages 345–388, 1997. [arXiv: gr-qc/9707062].

[5] V. Mukhanov and S. Winitzki. *Introduction to Quantum Effects in Gravity*. Cambridge University Press, Cambridge, UK, 2007.

[6] L. E. Parker and D. Toms. *Quantum Field Theory in Curved Spacetime*. Cambridge Monographs on Mathematical Physics. Cambridge University Press, Cambridge, UK, 2009.

[7] L. Parker. Particle creation in expanding universes. *Phys. Rev. Lett.*, 21:562–564, 1968.

[8] L. Parker. Quantized fields and particle creation in expanding universes. 1. *Phys. Rev.*, 183:1057–1068, 1969.

[9] L. Parker. Quantized fields and particle creation in expanding universes. 2. *Phys. Rev.*, D3:346–356, 1971. [Erratum: Phys. Rev. D3:2546 (1971)].

[10] S. W. Hawking. Particle creation by black holes. *Commun. Math. Phys.*, 43:199–220, 1975.

[11] J. D. Bekenstein. Black holes and entropy. *Phys. Rev.*, D7:2333–2346, 1973.

[12] J. D. Bekenstein. Generalized second law of thermodynamics in black hole physics. *Phys. Rev.*, D9:3292–3300, 1974.

[13] S. W. Hawking. Breakdown of predictability in gravitational collapse. *Phys. Rev.*, D14:2460–2473, 1976.

[14] S. D. Mathur. The information paradox: A pedagogical introduction. *Class. Quant. Grav.*, 26:224001, 2009. [arXiv: 0909.1038 [hep-th]].

[15] W. G. Unruh. Notes on black hole evaporation. *Phys. Rev.*, D14:870, 1976.

[16] B. S. DeWitt. Quantum gravity: The new synthesis. In *General Relativity: An Einstein Centenary Survey*, pages 680–745. Cambridge University Press, Cambridge, UK, 1980.

[17] D. Hümmer, E. Martin-Martinez, and A. Kempf. Renormalized Unruh-DeWitt particle detector models for boson and fermion fields. *Phys. Rev.*, D93(2):024019, 2016. [arXiv:1506.02046v2 [quant-ph]].

[18] J. Louko and V. Toussaint. Unruh-DeWitt detector's response to fermions in flat spacetimes. *Phys. Rev.*, D94(6):064027, 2016. [arXiv:1608.01002v2 [gr-qc]].

[19] S. Takagi. Vacuum noise and stress induced by uniform accelerator: Hawking-Unruh effect in Rindler manifold of arbitrary dimensions. *Prog. Theor. Phys. Suppl.*, 88:1–142, 1986.

[20] H. B. G. Casimir. On the attraction between two perfectly conducting plates. *Kon. Ned. Akad. Wetensch. Proc.*, 51:793–795, 1948.

[21] M. J. Sparnaay. Measurements of attractive forces between flat plates. *Physica*, 24:751–764, 1958.

[22] S. K. Lamoreaux. Demonstration of the Casimir force in the 0.6 to 6 micrometers range. *Phys. Rev. Lett.*, 78:5–8, 1997. [Erratum: Phys. Rev. Lett.81,5475(1998)].

[23] U. Mohideen and A. Roy. Precision measurement of the Casimir force from 0.1 to 0.9 micrometers. *Phys. Rev. Lett.*, 81:4549–4552, 1998. [arXiv: physics/9805038].

[24] R. S. Decca, D. Lopez, E. Fischbach, G. L. Klimchitskaya, D. E. Krause, and V. M. Mostepanenko. Tests of new physics from precise measurements of the Casimir pressure between two gold-coated plates. *Phys. Rev.*, D75:077101, 2007. [arXiv: hep-ph/0703290].

[25] G. T. Moore. Quantum theory of the electromagnetic field in a variable-length onedimensional cavity. *Journal of Mathematical Physics*, 11(9):2679–2691, 1970.

[26] C. M. Wilson, G. Johansson, A. Pourkabirian, M. Simoen, J. R. Johansson, T. Duty, F. Nori, and P. Delsing. Observation of the dynamical Casimir effect in a superconducting circuit. *Nature*, 479(7373):376–379, 2011. [10.1038/nature10561].

[27] P. C. W. Davies and S. A. Fulling. Radiation from a moving mirror in two-dimensional space-time conformal anomaly. *Proc. Roy. Soc. Lond.*, A348:393–414, 1976.

[28] P. C. W. Davies and S. A. Fulling. Radiation from moving mirrors and from black holes. *Proc. Roy. Soc. Lond.*, A356:237–257, 1977.

[29] R. D. Carlitz and R. S. Willey. Reflections on moving mirrors. *Phys. Rev.*, D36:2327–2335, 1987.

[30] R. D. Carlitz and R. S. Willey. The lifetime of a black hole. *Phys. Rev.*, D36:2336, 1987.

[31] T. D. Chung and H. L. Verlinde. Dynamical moving mirrors and black holes. *Nucl. Phys.*, B418:305–336, 1994. [arXiv:hep-th/9311007].

[32] M. Hotta, M. Shino, and M. Yoshimura. Moving mirror model of Hawking evaporation. *Prog. Theor. Phys.*, 91:839–870, 1994. [arXiv:hep-th/9403139v2].

[33] R. Parentani. The recoils of a dynamical mirror and the decoherence of its fluxes. *Nucl. Phys.*, B465:175–214, 1996. [arXiv:hep-th/9509104].

[34] M. Weinstein. Moving mirrors, black holes, Hawking radiation and all that. *Nucl. Phys. Proc. Suppl.*, 108:68–73, 2002. [arXiv:gr-qc/0111027].

[35] H. Saida, T. Harada, and H. Maeda. Black hole evaporation in an expanding universe. *Class. Quant. Grav.*, 24:4711–4732, 2007. [arXiv:0705.4012v2 [gr-qc]].

[36] M. Hotta, J. Matsumoto, and K. Funo. Black hole firewalls require huge energy of measurement. *Phys. Rev.*, D89(12):124023, 2014. [arXiv:1306.5057v4 [quant-ph]].

[37] M. Hotta, R. Schtzhold, and W. G. Unruh. On the partner particles for moving mirror radiation and black hole evaporation. *Phys. Rev.*, D91(12):124060, 2015. [arXiv:1503.06109v3 [gr-qc]].

[38] P. Chen and D. Yeom. Entropy evolution of moving mirrors and the information loss problem. *Phys. Rev.*, D96(2):025016, 2017. [arXiv:1704.08613v2 [hep-th]].

[39] M. R. R. Good, P. R. Anderson, and C. R. Evans. Mirror reflections of a black hole. *Phys. Rev.*, D94(6):065010, 2016. [arXiv:1605.06635v2 [gr-qc]].

[40] E. G. Brown and J. Louko. Smooth and sharp creation of a Dirichlet wall in 1+1 quantum field theory: how singular is the sharp creation limit? *JHEP*, 08:061, 2015. [arXiv:1504.05269 [hep-th]].

[41] N. Obadia and R. Parentani. Notes on moving mirrors. *Phys. Rev.*, D64:044019, 2001. [arXiv:gr-qc/0103061].

[42] A. Almheiri, D. Marolf, J. Polchinski, and J. Sully. Black holes: complementarity or firewalls? *JHEP*, 02:062, 2013. [arXiv:1207.3123 [hep-th]].

[43] J. Louko. Unruh-DeWitt detector response across a Rindler firewall is finite. *JHEP*, 09:142, 2014. [arXiv:1407.6299 [hep-th]].

[44] E. Martin-Martinez and J. Louko. (1+1)D calculation provides evidence that quantum entanglement survives a firewall. *Phys. Rev. Lett.*, 115(3):031301, 2015. [arXiv:1502.07749 [quant-ph]].

[45] T. Harada, S. Kinoshita, and U. Miyamoto. Vacuum excitation by sudden appearance and disappearance of a Dirichlet wall in a cavity. *Phys. Rev.*, D94(2):025006, 2016. [arXiv:1601.01172 [hep-th]].

[46] M. G. Calkin, D. Kiang, and Y. Nogami. Nonlocal separable potential in the one-dimensional Dirac equation. *Phys. Rev.*, C38:1076–1077, 1988.

[47] A. Chodos, R. L. Jaffe, K. Johnson, C. B. Thorn, and V. F. Weisskopf. New extended model of hadrons. *Phys. Rev.*, D9:3471–3495, 1974.

[48] M. R. R. Good. *Quantized Scalar Fields Under the Influence of Moving Mirrors and Anisotropic Curved Spacetime*. PhD thesis, University of North Carolina, 2011.

[49] L. Hodgkinson. *Particle detectors in curved spacetime quantum field theory*. PhD thesis, University of Nottingham, October 2013. [arXiv:1309.7281v2 [gr-qc]].

[50] B. A. Juárez-Aubry and J. Louko. Onset and decay of the 1 + 1 Hawking-Unruh effect: what the derivative-coupling detector saw. *Class. Quant. Grav.*, 31(24):245007, 2014. [arXiv:1406.2574v3 [gr-qc]].

[51] N. Friis, A. R. Lee, D. E. Bruschi, and J. Louko. Kinematic entanglement degradation of fermionic cavity modes. *Phys. Rev.*, D85:025012, 2012. [arXiv:1110.6756v2 [quant-ph]].

[52] N. Friis, A. R. Lee, and J. Louko. Scalar, spinor, and photon fields under relativistic cavity motion. *Phys. Rev.*, D88(6):064028, 2013. [arXiv:1307.1631v2 [quant-ph]].

[53] A. Satz. Then again, how often does the Unruh-DeWitt detector click if we switch it carefully? *Class. Quant. Grav.*, 24:1719–1732, 2007. [arXiv:gr-qc/0611067v3].

[54] S. Schlicht. Considerations on the Unruh effect: causality and regularization. *Class. Quant. Grav.*, 21:4647–4660, 2004. [arXiv:gr-qc/0306022v2].

[55] J. Louko and A. Satz. How often does the Unruh-DeWitt detector click? Regularisation by a spatial profile. *Class. Quant. Grav.*, 23:6321–6344, 2006. [arXiv:gr-qc/0606067v3].

[56] P. Langlois. *Imprints of spacetime topology in the Hawking-Unruh effect.* PhD thesis, Nottingham U., 2005. [arXiv:gr-qc/0510127].

[57] B. Thaller. *The Dirac equation.* Texts and monographs in physics. Springer-Verlag Berlin Heidelberg, 1992.

[58] A. Chodos, R. L. Jaffe, K. Johnson, and C. B. Thorn. Baryon structure in the bag theory. *Phys. Rev.*, D10:2599, 1974.

[59] B. H. J. Mckellar and G. J. Stephenson. Relativistic quarks in one-dimensional periodic structures. *Phys. Rev.*, C35:2262–2271, 1987. [Erratum: Phys. Rev.C36,1648(1987)].

[60] M. G. Calkin, D. Kiang, and Y. Nogami. Proper treatment of the delta function potential in the onedimensional Dirac equation. *American Journal of Physics*, 55(8):737–739, 1987.

[61] L. J. Zhou, M. E. Carrington, G. Kunstatter, and J. Louko. Smooth and sharp creation of a pointlike source for a (3+1)-dimensional quantum field. *Phys. Rev.*, D95(8):085007, 2017. [arXiv:1610.08455 [hep-th]].

[62] J. Louko and A. Satz. Transition rate of the Unruh-DeWitt detector in curved spacetime. *Class. Quant. Grav.*, 25:055012, 2008. [arXiv:0710.5671v3 [gr-qc]].

[63] L. Hodgkinson and J. Louko. How often does the Unruh-DeWitt detector click beyond four dimensions? *J. Math. Phys.*, 53:082301, 2012. [arXiv:1109.4377v3 [gr-qc]].

[64] J. I. Kapusta and C. Gale. *Finite-Temperature Field Theory: Principles and Applications.* Cambridge University Press, Cambridge, UK, 2006.

[65] P. G. Grove. On the detection of particle and energy fluxes in two-dimensions. *Class. Quant. Grav.*, 3:793–800, 1986.

[66] R. D. Richtmyer. *Principles of Advanced Mathematical Physics Vol 1.* Springer Berlin Heidelberg, 1978.

[67] G. Bonneau, J. Faraut, and G. Valent. Self-adjoint extensions of operators and the teaching of quantum mechanics. *Am. J. Phys.*, 69:322, 2001. [arXiv:quant-ph/0103153].

[68] J. Louko. Near-Dirichlet quantum dynamics for a p^3-corrected particle on an interval. *Gen. Rel. Grav.*, 47(5):55, 2015. [arXiv:1404.5256 [hep-th]].

[69] J. Dittrich, P. Exner, and P. Šeba. Dirac operators with a spherically symmetric δ-shell interaction. *J. Math. Phys.*, 30:2875, 1989.

[70] R. Wong. *Asymptotic Approximations of Integrals.* Classics in Applied Mathematics. Society for Industrial and Applied Mathematics, 2001.

[71] E. R. Love. Changing the order of integration. *Journal of the Australian Mathematical Society*, 11(4):421–432, 1970.

[72] *NIST Digital Library of Mathematical Functions*. http://dlmf.nist.gov/, Release 1.0.13 of 2016-09-16. F. W. J. Olver, A. B. Olde Daalhuis, D. W. Lozier, B. I. Schneider, R. F. Boisvert, C. W. Clark, B. R. Miller and B. V. Saunders, eds.

[73] I. Gradshteyn, I. Ryzhik, D. Zwillinger, and V. Moll. *Table of Integrals, Series, and Products (Eighth Edition).* Academic Press, Boston, 2015.